Arnusorn Saengprajak

Efficiency of Demand Side Management Measures in Small Village Electrification Systems

kassel university press

This work has been accepted by the faculty of electrical engineering / computer science of the University of Kassel as a thesis for acquiring the academic degree of Doktor der Ingenieurwissenschaften (Dr.-Ing.).

Supervisor: Prof. Dr.-Ing. Jürgen Schmid
Co-Supervisor: Prof. Dr.-Ing. habil. Ingo Stadler

Defense day: 20th November 2006

Bibliographic information published by Deutsche Nationalbibliothek
Die Deutsche Nationalbibliothek lists this publication in the Deutsche Nationalbibliografie; detailed bibliographic data is available in the Internet at http://dnb.ddb.de

Zugl.: Kassel, Univ., Diss. 2006
ISBN: 978-3-89958-273-4
URN: urn:nbn:de:0002-2733

Printed by: Unidruckerei, University of Kassel
Printed in Germany

Acknowledgements

This dissertation could not have succeed without the support of Prof. Dr.-Ing. Jürgen Schmid who not only served as my supervisor but also encouraged and challenged me throughout my academic program. I am also grateful to Prof. Dr.-Ing. habil. Ingo Stadler for all the suggestions and guidance during the working period.

Moreover, I would like to thank Dipl.-Ing. Franz Kininger for backing me on my first arrival in Germany, Dipl.-Ing. Ingo Hahn for his assistance in the IEE-RE laboratory, and Dipl.-Ing. Thorsten Bülo for the really useful recommendation on both working and living in Kassel. Furthermore, I am extremely grateful to Ms. Claudia Erdt, who has assisted me on many occasions. Also, many thanks to all the staff in the Department of Efficient Energy Conversion, whom I may not have mentioned, for all their kind support.

Besides, I wish to thank my benefactors in Thailand, Assoc. Prof. Dej-Anan Komasathid, Assis. Prof. Teerapot Puttakitakaweewong and Aj. Prayoon Satarat, for all the best advice in my study direction. Many thank for the financial aid and scholarship from Mahasarakham University and the Royal Thai Government.

I would like to thank Dr.-Ing. Nipon Ketjoy and all the staff at SERT, Naresuan University, for all kinds of assistance when I carried out research in Thailand.

As for all Thai friends in Germany, Dr.-Ing Boonyang Planklang, Dipl.-Ing. Phongsuk Ampha, Mr. Saenboon Amorntipsakul, Mr. Amnoiy Ruengwaree, Mr. Patcharasak Alai and the others, I say thank you very much for the great and warm support during the time I was there.

Above all, I would like to thank my family for the encouragement they have given to me all the time.

Abstract

This report presents the application of demand side management (DSM) to a small village electrified by a PV-Diesel hybrid system (PVHS). The purpose of this work is to reduce the electrical energy demand during the evening period by changing the working patterns (characteristics) of the electrical appliances. This method is expected to stabilise the system operation, extend the system component lifetime and reduce the energy costs. The study focuses on the refrigerator because it is possible to operate this appliance only in the day time and turn it off in the evening and night time. The study on the storage capability of refrigerators has been done in the laboratory at the IEE-RE, University of Kassel. A variety of sizes of boxes of water (5 kg to 30 kg) have been used as loads inside the refrigerator and tested to determine the storage capability in each case. The study found that refrigerators can hold the temperature in the range of 0 °C to 10 °C (the ISO standard temperature for preserving food) for about 12 hours without powered operation.

The experimental result was applied to the simulation of the electrification in the Ban Phang Praratchatan village by the PV-Diesel hybrid system. The operation period of the refrigerator was limited to only day time, from 6 a.m. to 6 p.m. Consequently, the study found that the daily peak energy demand could be reduced by 8.4 percent. The depth of discharge (DOD) of the battery has been altered by the reduction of the peak energy demand in the evening, so that the life cycle of the battery could be increased by 8.7 percent. Moreover, the efficiencies of PV-Diesel hybrid system as described by the performance ratio, the solar fraction and the final yield of the system are increased by 2.6 percent, 2.78 percent and 2.55 percent, respectively. In addition, the specific cost of the energy of the battery is reduced by 9.37 percent, and the new specific cost of the whole system is 0.549 Euro/kWh, which is a 2.0 percent reduction. However, the DSM method has no significance on the diesel generator operation characteristics because the daily energy demand does not change under this method.

The study shows that the benefit of the DSM method on the PV-Diesel hybrid system in Ban Pang Praratchatan village mainly occurred on the battery bank, which is the second most expensive part in the PVHS. The DSM also helps to reduce the specific cost of the energy of the battery part, which tends to decrease that of the whole system.

Zusamenfassung

Diese Arbeit zeigt die Anwendung eines Lastmanagementsystems (engl. Demand-Side-Management (DSM)) am Beispiel der Elektrifizierung eines kleinen Dorfes durch ein PV-Diesel-Hybridsystem. Das Ziel des angewendeten Systems ist es, die Nachfrage nach elektrischer Energie in den Abendstunden zu verringern, indem die Charakteristik von Verbrauchern gezielt beeinflusst wird. Dies soll die Stabilität des Gesamtsystems erhöhen, die Lebensdauer der Komponenten verlängern und die Energiegestehungskosten verringern. Die Arbeiten konzentrieren sich auf die Betrachtung des Kühlschrankes, da der Kühlschrank es ermöglicht, nur am Tage betrieben, und am Abend ausgeschaltet zu werden. Die Untersuchungen zur thermischen Speicherkapazität des Kühlschrankes wurde im Labor des IEE-RE an der Universität Kassel durchgeführt. Verschiedene Grössen von Wasserbehältern (5 kg bis 30 kg) wurden als Lasten verwendet, für die im Anschluss jeweils die Speicherkapazität des Kühlschrankes ermittelt wurde. Dabei stellte sich heraus, dass die Innenraumtemperatur des Kühlschrankes zwischen 0 °C und 10 °C (ISO-Standardtemperatur für die Lagerung von Lebensmitteln) für 12 Stunden ohne Betrieb des Kühlschrankes gehalten werden konnte.

Diese experimentellen Ergebnisse wurden auf die Simulation der Elektrifizierung in dem Dorf Ban Phang Praratchatan mit einem PV-Diesel Hybridsystem angewendet. Der Kühlschrank wurde nur am Tage betrieben und in der Nacht (ab 18 Uhr) für 12 Stunden abgeschaltet. Der tägliche Spitzenlastbedarf betrug in diesem Fall nur noch 2,035 kW, was einer Verringerung um 8,41 % entspricht. Die Entladetiefe der Batterie veränderte sich aufgrund der Verringerung der abendlichen Maximallast um 8,7 %, woraus sich eine prognostizierte Lebensdauer der Batterie von 2,500 Zyklen ergibt. Die die Effizienz des PV-Diesel-Hybridsystems beschreibenden Parameter erhöhten sich um 2,6 % (performance ratio), 2,78 % (solar fraction) und um 2,55 % (final yield). Die spezifischen Kosten der aus der Batterie bezogene Energie konnten um 9,37 % gesenkt werden. Die spezifischen Kosten des Gesamtsystems betragen somit 0,549 Euro/kWh, was einer Reduktion um 2,0 % entspricht. Auf den Betrieb des Dieselgenerators hat das Lastmanagementsystem keinen signifikanten Einfluss, da der tägliche Energiebedarf des Systems mit von der beschriebenen Methode nicht verändert wird.

Die Untersuchung zeigt, dass der Nutzen des Einsatzes eines Lastmanagementsystems in dem PV-Diesel-Hybridsystem in Ban Pang Praratchatan in erster Linie in Bezug auf die Batteriebank zu sehen ist, welche die Komponente mit den zweithöchsten Investitionskosten darstellt. Mit Hilfe des Lastmamagements können die spezifischen Energiekosten der Batterie gesenkt werden, wodurch wiederum die spezifischen Kosten des Gesamtsystems verringert werden. Das Konzept des Lastmanagements in ländlichen Gebieten, die mit Hilfe von PV-Diesel-Hybridsystemen elektrifiziert werden, wird umso attraktiver, je grösser das Dorf ist, da dann auch grössere Batteriebänke in den Systemen eingesetzt werden.

Contents

List of Figures

List of Tables

Chapter 1

Introduction

Having been applied for use with the terrestrial applications since early 1970s [1], photovoltaic (PV) technology has been popularly used around the world. The survey for the retail prices of PV modules during the period between October 2000 to September 2005 in the European Union found that the price has continually reduced with the growth of PV demand, as illustrated in Fig.1.1. Additionally, the market survey on the global cell and module production in 2004 showed that the total number of the solar cell units which were produced all over the world in that period was 1,256 MW, which is an increase of 67 percent from the year 2003's output of 750 MW as shown in Fig.1.2. These statistics confirm that PV has of late become an appealing option for the generation of electricity for humankind. Various kinds of PV system technologies have been developed for use in many different applications. In rural areas, PV electrification system can resolve the economic problem of expanding the utility grids into rural villages. Moreover, utilization of this technology positively effects environmental conservation, especially by reducing the global warming crisis by saving on the use of fossil fuel in the diesel generator. Consequently, from the many reasons above, PV electrification system has turned out to be preferable to the conventional approaches in generating electricity in the rural areas.

PV electrification system plays an important role not only in many rural areas but also in several small urban communities which have high potential of acquiring solar energy [4]. No matter how attractive this system is, its operation cost has prohibited the PV utilization promotion. Hence, to be able to compete with the other types of the conventional electrification systems, PV projects need to be subsidized by governments. For example, in Japan, by April 30, three weeks after the start of the FY 2004 application period beginning on April 8, the New Energy Foundation (NEF) received 6,873 applications requesting for subsidies from the Japanese Residential PV Dissemination Program [5]. Anyhow, the PV technology is getting more popular use only in some countries because the creation of awareness by the government of each country in the utilization of sustainable energy is different.

The information above shows that the number of residential areas or villages which use the PV electrification system is increasing. In addition however, there are several kinds of the PV electrification system, the most suitable of which for the application in small community is the PV-diesel hybrid system [6, 7]. The benefits of replacing the stand alone PV system or the other conventional electrification systems with the PV-diesel hybrid system are the followings: reduction in the fuel supply, continuous and flexible supply to the load curve, ease of up-sizing the system, reduction in the operation and maintenance costs of the diesel generator, increased reliability, continuous operation and efficiency independent

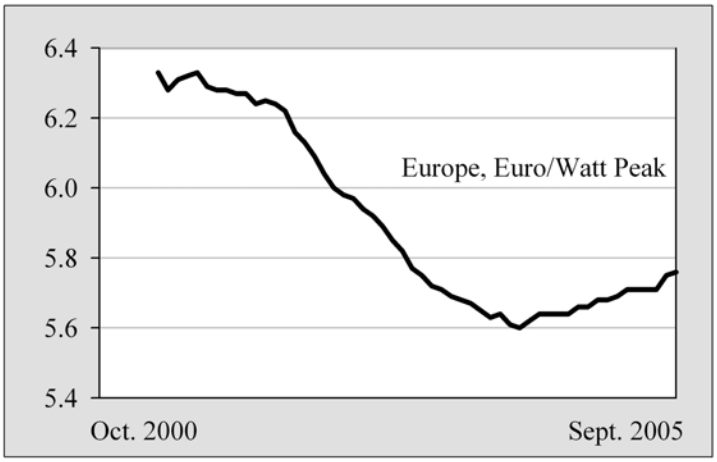

Figure 1.1: Photovoltaic module retail prices survey (Oct 2000 - Sept 2005) in Europe [2]

of the load curve as well as reduced pollution [8].

However, one important technical problem in the PV-Diesel hybrid system is the energy storage. Normally, lead-acid batteries are installed in such a system. It is often found that the real lifetime of this kind of battery will be shorter than the theoretical expectation [9, 10]. The replacements for the degraded batteries and the need for additional batteries, resulting from an increase in the energy consumption, causes the overall system cost to rise above the predicted level. Moreover, the demand for the battery in many systems causes not only economic problems but environment problems as well.

In order to reduce the battery use in the PV electrification system, other approaches of electrical energy storage, which do not base only on the battery, need to be studied. Moreover, in-depth study and research on the user side focusing on the household appliances can yield useful information for the demand side management activities, which can help to reduce the peak energy demand, which in turn results in the reduction of battery back-up on the generation side.

Although the refrigerator seems to be unsuitable for use in the PVHS due to its rather high demand for electrical power (see Fig. 1.3), it is still useful for preserving food and keeping vaccines in the village. However, a refrigerator can work as a secondary, passive and alternative energy storage device, it can be limited to operate only in the day time during which the deluge of electricity can be generated from the PV generator. Therefore, turning of the refrigerator in the evening period to save energy and reduction of the peak energy demand is possible.

This research aims to reduce the number of batteries used in the PV-diesel hybrid system by application of the DSM concepts on the user side. The first step of the research is implementation of an existing refrigerator, which could work as a secondary, passive and alternative energy storage device. The storage capacity of the refrigerator is determined by laboratory measurements. Further, the energy savings under the concept of indirect energy storage devices, as well as effects of the DSM on the PV-diesel hybrid system are investigated.

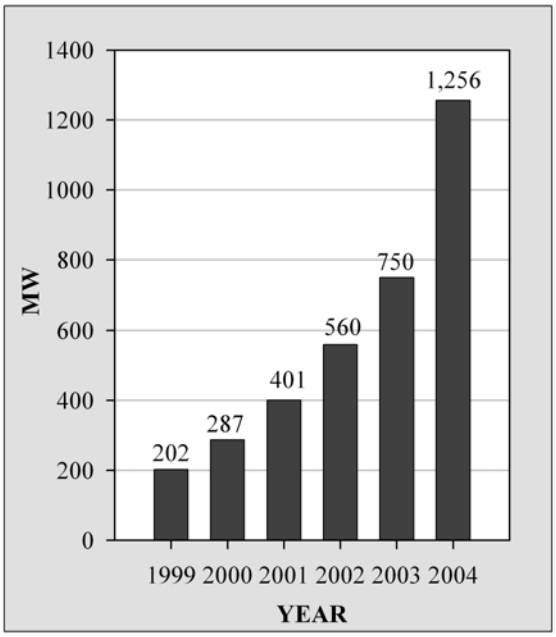

Figure 1.2: Global solar cell production 1999-2004 [3]

1.1 Review of small village electrification systems

In the last decade, the suitable villages for application of PV electrification system were located only in the rural areas because the operation and generation costs of this system are more worthwhile here compared to the other conventional system in many aspects. However, with the government support in many countries, and with the continued reduction of the PV component selling price, the PV system has of late become more suitable for many urban communities too. General domestic loads of any village consist of: lamps, televisions, radios, refrigerators, fans and sterio/tape players [8, 11, 12]. Figure 1.3 shows the typical energy consumed for each unit of electrical appliance in the small villages in the Northern part of Thailand.

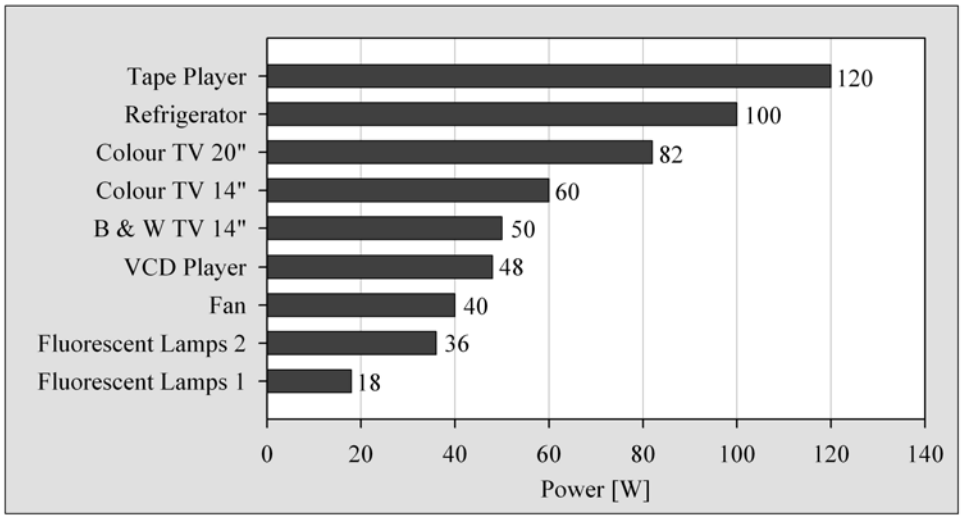

Figure 1.3: Typical electrical power consumption in small village, Thailand [13]

The conventional technology of electricity generation for small villages is the fossil fuel generator. With this technology, there are several weaknesses which can obviously be observed. Firstly, there is noise occurring from the operation process. Next, the environmental crisis, particularly the global warming problem, is contributed to by this technology. The last is the financial difficulty of the price of oil in the rural area where it is rather costly. The new approach for the electricity generation, the so called "PV-diesel hybrid system" is a combination of the PV technology and the diesel generator. This approach is applied to generate electricity instead of using only the diesel generator in the generation process because it provides more reduction on the economic cost. The comparative economics of the generation option as shown Figure 1.4, emphasizes that PV-hybrid system is highly suitable for small-medium sized communities. With the generation of electricity by the PV-diesel hybrid system, the specific fuel consumption can be reduced, similarly the operation hours of diesel engine. Consequently, by reducing the fuel consumption of the diesel system, the O&M costs of the whole system can be reduced as well. Moreover, the battery bank and total PV power installation may be significantly smaller than in a pure PV system. These two benefits are achieved without the reduction in the system reliability [8]. Generally, the appropriate size of a small village to be electrified by PV-hybrid system should be at least 100 resident families [15].

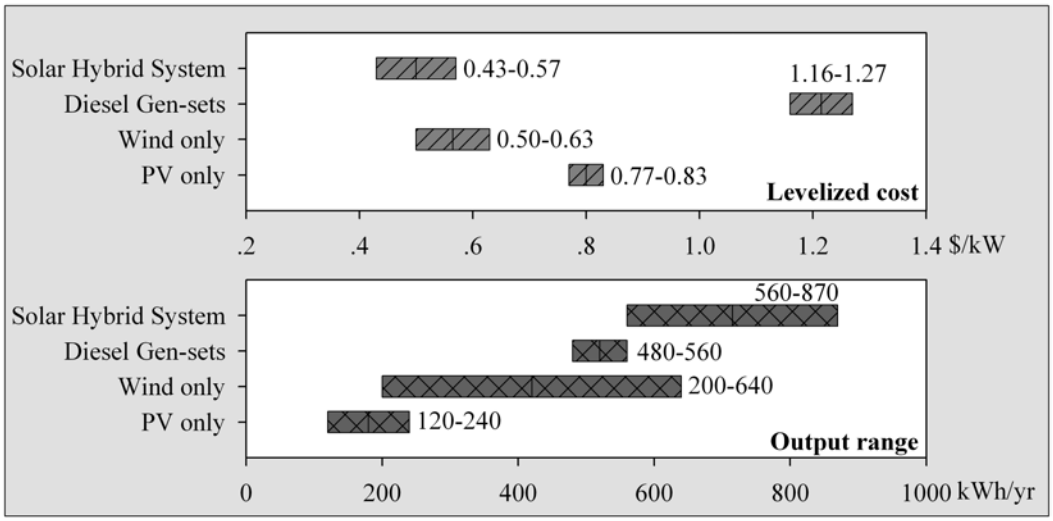

Figure 1.4: Comparative economics of different distributed generation options [14]

Although the PV-hybrid system seems to be superior to the pure diesel generator system, the PV generator in the hybrid system is not the major factor when the life time costs are considered. The costs of the energy storage and the remaining system components, including the planning and the installation costs, are dominant. The high storage costs are primarily from the commonly used lead-acid batteries. Every development which can extend the battery life time should be supported to accelerate the dissemination of PVs [16].

1.2 Formulation of problems

The PV/battery/diesel hybrid configuration has several advantages such as: the system load can be satisfied in the optimal way, diesel efficiency can be maximized, diesel maintenance can be minimized, and the capacity of diesel and battery can be reduced (while matching

the peak loads). However, the most profound problem after the installation of the system is the increase in energy demand in the village, as stated in section 6.1.4 (page 72). This resulted in the system failing and shorter battery life time than expected. In the case of the battery in the PV hybrid system, the literature infers that an optimum use of the battery storage in the PV-Hybrid system will minimize the cost of the power generation [17]. The use of the pure diesel system may result in higher frequency of the start/stop cycles of the diesel generator (frequent start-ups/stops promote wear). The use of the battery storage results in a considerable reduction of the generated diesel energy. However, focusing on the electricity generation cost, it can be concluded that the energy storage via electrochemical battery is the weakest part in PV electrification systems [10]. Normally, the lead-acid battery has a theoretical life time of about 6 years or more [9], but two-or-four-year life times are often found as well [10]. The replacement of batteries after degradation and the need for additional batteries due to the increase of energy consumption cause the overall cost of system to exceed the estimated figure. Moreover, the rise in the number of batteries needed in several systems causes both economic and environment problems.

With the Demand Side Management (DSM), the method used to control the energy demand on the user side, the fall of energy demand will take place. This situation leads to a significant decrease in the battery backup problem and overload situation of the generation system. With this method, the electrical appliances in the utility side must be investigated, and, this research has focused on the utilization of the load in a small village. In addition, the load which was applied by DSM concept is the refrigerator. Why refrigerator? This question can be clarified by the following reasons. Firstly, the refrigerator consumes rather high energy. This characteristic causes the energy demand rise especially in the evening and night time period. The other reason is that its capability in storing the consumed energy during the day in the form of low temperatures leads to the fact that the refrigerator can be used during the night with out powered operation, which results in benefits in the form of reduction in the daily peak energy demand.

In the research process, the first step is implementing DSM concepts on the existing refrigerator. In this stage, the refrigerator will work as a secondary and passive energy storage device by having the powered operation only in the day time during which plenty of electricity is generated from the PV generator. Accordingly, the cold storage capability of household refrigerator will be utilised. Furthermore, the feasibility study of energy savings under the concept of indirect energy storage devices will be carried out. In addition, the simulation of the lifetime extension of the battery and the calculation on the overall cost reduction of electricity generation after the DSM concept is applied to the PV-diesel hybrid system must be carried out.

1.3 Research objectives

As elaborated in the previous section, electrical appliances on the user side need to be investigated. Consequently, the battery lifetime, the system reliability and energy costs can be improved. The objective of this study is stated as follows:

1.3.1 Objectives

This research is aimed at studying the possibility of applying the DSM activity through the cold storage capability of a refrigerator to a small village which is electrified by the PV-diesel hybrid system. The objectives of this research are:

- Incorporating an existing refrigerator which is typicaly used in a small village in order to test its storage capability. This method should be useful for the DSM purpose. The test is based on the ISO test standard conditions for the refrigerator.
- Developing the simulation software to efficiently predict the refrigerator temperature. The software should be able to adjust the parameters which effect the refrigerator temperature. Accordingly, this tool could benefit the DSM planning.
- Exploring the outcome of utilizing the DSM with cold storage concept in the small village electrification by PV-Diesel hybrid system. This objective can be divided into several small parts such as to simulate the decrease of the energy demand when the DSM concept was applied to the village load, to estimate the extension of the battery lifetime, to forecast the cost reduction of the electrical generation, as well as to study how the system efficiency changes after the DSM application.

1.4 Research procedures

The research has been divided into the two parts. For the first part, investigating the household refrigerator is necessary. This was done in the Cooling Laboratory at IEE-RE, University of Kassel, in order to estimate the cold storage capability of refrigerators. The measurement results were used for comparison with the simulation results, to guarantee the accuracy of the simulation model and to establish the storage capability of refrigerator.

In the second part, the system simulation, the DSM concept through the cold storage capability data of refrigerator evaluated in the first step above was applied to the user side in the chosen village in order to study the possibilities of the reduction of the peak demand during the evening period and to determine the benefits of this activity. Accordingly, the main emphasis of this section is to define the village prototype to apply in the PV-diesel hybrid system. Ban-Phang Pha Ratchathan, a village located on the Northern part of Thailand, is a typical small village that was used as a model to test the hypothesis in this research. The village details will be described in section 6.1 (page 69).

1.5 Outline of the thesis

This thesis contains of seven Chapters. In **Chapter 1**, are an introduction and review of the small village electrification by PV technology. The problems in this kind of technology and as well as the research objectives are also provided in this chapter. In **Chapter 2**, the small village electrification technology is reviewed. The details of the different hybrid system topologies and the concept of modularization and standardization for the PNHS are reviewed. Moreover, the fundamental definitions and operation characteristics of PV modules, the battery, the diesel generator and the other components in PVHS are introduced. In addition, the mathematical models for each component including the economic

model are described in this chapter. In **Chapter 3**, the history of DSM in PV-hybrid system is reviewed. The DSM strategies and the concept of DSM via cold storage capability of refrigerator are also introduced. **Chapter 4** presents the heat transfer concept and mathematical model for estimating the refrigerator temperature. **Chapter 5** gives the details of the implementation result of the refrigerator obtained from experiments in the laboratory. This chapter also provides the simulation results of refrigerator under different operation conditions. The content of **Chapter 6** gives the case study results from the small village electrification where the DSM concept was applied to the utilization of electricity. The benefits of DSM on the extension of battery lifetime and the reduction of the energy cost are explained in this part too. At the end of the thesis in **Chapter 7**, the conclusions and the outlook of this research are provided.

Chapter 2

Small Village Electrification System

The most suitable electrification for the small village size is the Hybrid system [18]. The hybrid system is superior to the traditional diesel system in many aspects. For example, the hybrid system can reduce the fuel consumption and the operation and maintenance costs, while improving the quality of service [19, 20, 21]. Furthermore, the hybrid system is a renewable energy system that includes two or more different types of technologies which can produce the same type of energy, e.g. a wind turbine and a solar photovoltaic array are combined to meet a power demand[1]. In this research, PV-diesel hybrid system is the electrification system, which contains the PV generator as a primary generator and the diesel generator as a secondary generator, a storage system and a control/power electronics part.

The details in this part present the description of the different components in the PV-diesel hybrid system. The mathematical models for forecasting the climate conditions, as well as prediction of the operation of the PV-diesel hybrid system are also presented in this section. The aim of this part is to explain the complex component interaction in a PV-diesel hybrid system design. This chapter also takes note of the importance of component operation, load management and efficient use of any surplus energy on the operation of the PV-Diesel hybrid system.

2.1 Solar radiation data

The solar radiation data is very important in figuring out the amount of electricity generated by PV modules. The long term statistical data of solar radiation is also very important in deriving an equation to calculate the solar radiation data, and for use in the design of the PV electrification system. However, the solar radiation could be generated by the solar radiation model which is developed by basing on the meteorological data. The solar radiation models applied in this work are the followings:

[1]From: The Encyclopaedia of Alternative Energy and Sustainable Living

2.1.1 Extraterrestrial radiation on a horizontal surface and clearness index

Solar radiation at normal incidence received at the surface of the earth varies with the change of the extraterrestrial radiation. The calculation of the theoretically possible extraterrestrial radiation is necessary to obtain the ratio of the radiation level in the atmosphere. It is often necessary for the calculation of daily solar radiation to have the integrated daily extraterrestrial radiation on a horizontal surface (H_0) over the period from sunrise to sunset. The monthly mean daily extraterrestrial radiation, (H_0), is a useful quantity [22]. For latitudes in the range of +60 to -60, it can be calculated with Equation 2.1 using n for the mean day of the month in Table 2.2.

Month	Jan	Feb	Mar	Apr	May	Jun	July	Aug	Sep	Oct	Nov	Dec
Date	17	16	16	15	15	11	17	16	15	15	14	10
Day of year (n)	17	47	75	105	135	162	198	228	258	288	318	344

Table 2.1: Recommended Average Days for Months and Values of n

$$\bar{H_o} = \frac{24 \times 3,600}{\pi} G_{sc} \left(1 + 0.033\, cos\frac{360n}{365}\right) \times \left(cos\phi\, cos\sigma\, sin\omega_s + \frac{\pi\omega_s}{180}\, sin\phi\, sin\sigma\right) \quad (2.1)$$

Where

G_{sc} is the solar constant, 1,376 W/m^2
n is the day of the year
σ is the monthly mean solar declination, $Degrees$
ω_s is the sunset hour angle, $Degrees$
ϕ is the latitude of location, $Degrees$
$\bar{H}$ is the monthly mean daily total radiation on horizontal surface, $MJ/m^2.day$
$\bar{H_o}$ is the monthly mean daily extraterrestrial radiation on horizontal surface, $MJ/m^2.day$

Before reaching the surface of the earth, the radiation from the sun is attenuated by the atmosphere and the clouds. The ratio of solar radiation at the surface of the earth to extraterrestrial radiation is called the clearness index, thus the monthly average clearness index, $\bar{K_T}$, is defined as:

$$\bar{K_T} = \frac{\bar{H}}{\bar{H_o}} \quad (2.2)$$

Where $\bar{K_T}$ values depend on the location and the time of year considered; they are usually between 0.3 (for very overcast climates) and 0.8 (for very sunny locations).

2.1.2 Calculation of hourly global and diffuse irradiance

Solar radiation can be divided into two components: (1) beam or direct radiation, which is radiated from the sun to earth surface directly, (2) diffuse radiation, which is reflected and/or scattered by small matter in the atmosphere such as clouds or water drops, then to the earth surface [22, 23].

Monthly average daily diffuse radiation $\bar{H}_d$ is calculated from monthly average daily global radiation $\bar{H}$ using the equation 2.3.

$$\frac{\bar{H}_d}{\bar{H}} = 1.391 - 3.560\bar{K}_T + 4.189\bar{K}_T^2 - 2.137\bar{K}_T^3 \tag{2.3}$$

When the sunset hour angle for the average day of the month is less than 81.4, then:

$$\frac{\bar{H}_d}{\bar{H}} = 1.311 - 3.022\bar{K}_T + 3.427\bar{K}_T^2 - 1.821\bar{K}_T^3 \tag{2.4}$$

When the sunset hour angle is greater than 81.4 (the monthly average clearness index, K_T is calculated trough equation 2.2. Then, average daily radiation is then broken down into hourly values. This is done with the formula from Collares-Pereira and Rabl for global irradiance.

$$r_t = \frac{\bar{I}_t}{\bar{H}} = \frac{\pi}{24}\left(a + b\,cos\omega\right)\ \frac{cos\omega - cos\omega_s}{sin\omega_s - \frac{\pi\,\omega_s}{180}\,cos\omega s} \tag{2.5}$$

$$a = 0.409 + 0.5016sin\left(\omega_s - 60\right) \tag{2.6}$$

$$b = 0.6609 + 0.4767sin\left(\omega_s - 60\right) \tag{2.7}$$

where

r_t is the ratio of hourly total radiation to daily total radiation
$\bar{I}_t$ is the hourly mean total radiation on horizontal surface, $MJ/m^2.h$
ω is the hourly angle, $Degrees$

The formula from Liu and Jordan for diffuse irradiance:

$$r_d = \frac{\bar{I}_d}{\bar{H}_d} = \frac{\pi}{24}\frac{cos\omega - cos\omega_s}{sin\omega_s - \frac{\pi\,\omega_s}{180}\,cos\omega s} \tag{2.8}$$

where

r_d is ratio of hourly diffuses radiation to daily diffuse radiation
$\bar{I}_d$ is hourly mean diffuse radiation on horizontal surface, $MJ/m^2.h$

Correlation between hourly total, beam and diffuse radiation is:

$$\bar{I}_t = \bar{I}_b + \bar{I}_d \tag{2.9}$$

where

$\bar{I}_t$ is the hourly mean total radiation on horizontal surface, $MJ/m^2.h$
$\bar{I}_b$ is the hourly mean beam radiation on horizontal surface, $MJ/m^2.h$
$\bar{I}_d$ is the hourly mean diffuse radiation on horizontal surface, $MJ/m^2.h$

2.1.3 Radiation on a tilted surface and its estimation

Hourly radiation on a tilted surface is given by [22]:

$$\bar{I}_T = \bar{I}_b\,R_b + \bar{I}_d\left(\frac{1 + cos\beta}{2}\right) + \bar{I}_t\,\rho_g\left(\frac{1 - cos\beta}{2}\right) \tag{2.10}$$

where

I_T is the hourly mean diffuse radiation on tilted surface, $MJ/m^2.h$
β is the PV array tilted angle, $Degrees$
ρ_g is the ground albedo (0.2 for non-snow cover)

The ratio of the beam radiation on PV array that is fixed on the tilted surface to that on the horizontal surface can be determined by [22]:

$$R_b = \frac{cos\theta}{cos\theta_z} = \frac{\begin{array}{r}(sin\sigma\ sin\phi\ cos\beta \\ -sin\sigma\ cos\phi\ sin\beta\ cos\gamma + cos\sigma\ cos\phi\ cos\beta\ cos\omega \\ +cos\sigma\ sin\phi\ sin\beta\ cos\gamma\ cos\omega + cos\sigma\ sin\beta\ sin\gamma\ sin\omega)\end{array}}{cos\phi\ cos\sigma\ cos\omega + sin\phi\ sin\sigma} \tag{2.11}$$

2.2 Ambient temperature

The ambient temperature can be estimated by using the sinusoidal ambient temperature model which is based on the variation of maximum and minimum ambient temperatures in a day.

$$T_{amb}(t) = \frac{1}{2}\left[(T_{max} + T_{min}) + (T_{max} - T_{min})\ sin\left(\frac{2\pi}{24}t\right)\right] \tag{2.12}$$

where

$T_{amb}(t)$ is the ambient temperature at time, t
T_{max} is the maximum ambient temperature of the day
T_{min} is the minimum ambient temperature of the day
t = h-9
h is the considered time in unit of hour

2.3 Hybrid system configuration

The PV-Diesel hybrid system offers better reliability than a PV or diesel system alone because of a higher level of independence from climatic conditions as well as the redundancy built in the system by combining two generators. These two factors combined result in a higher system reliability. The efficiency of the PV-diesel hybrid system is also better than the generation system with only one of the generators. This is because the design of the hybrid system involves the optimization of both the generator operation and the full utilization of the energy produced by the generators. This allows the individual generators to be operated at their optimal or rated power and thereby raise the system efficiency. This is evident in the case of diesel engine generators which are operated at the rated capacity in hybrid systems leading to higher efficiency and lower specific fuel consumption. This system results in less environmental impacts, because of the optimization of the PV generator and secondary generators. Secondly the storage size, typically the size of the lead acid battery bank is also minimized in PV-Diesel hybrid systems leading to minimized environmental problems associated with the disposal and recycling of batteries. The PV-diesel hybrid system provides better economics in terms of distributed energy generation options as the storage requirements are low and investment costs are minimized [25]. The PV side, which is generally designed to take care of the worst period of the year, is now designed to meet

the load requirement during the best period resulting in considerable savings. As the specific fuel consumption of the hydrocarbon fuel generator is low, there is better economics on this front as well [18].

From the point of view of application, the PV-hybrid system has been classified into three configurations, i.e. series hybrid system topology, switched hybrid system topology and parallel hybrid system topology.

2.3.1 Series hybrid system configuration

Series hybrid system or DC bus configuration is the topology where the diesel generator, the PV generator and the storage are tied to the DC-bus [26]. Figure 2.1 shows the connection of diesel generator in series with the inverter to supply the AC load, so that the diesel generator cannot supply the load directly. The inverter converts the generated DC power from the different generators and the storage part to AC at the desired voltage and frequency and subsequently supplies to the load. The battery inverter should be adequate to cover the peak load, while the diesel generator capacity should be able to meet the peak load and charge the battery simultaneously [27]. The advantage of this topology is that the load is covered without power interruption in the event of operating the diesel generator or PV to charge the battery bank. The design principles of these systems are rather easy to implement. The serious disadvantages are associated with the overall conversion efficiency, limited control over the diesel alternator in case of incorporating the renewable sources. Furthermore, expanding the supply system by increasing a component capacity or adding further generators is very complicated owing to the limited nominal capacity of the DC/AC power conditioning units.

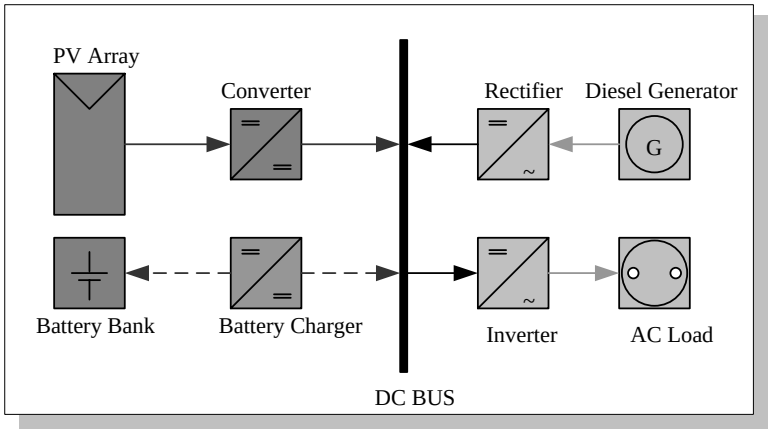

Figure 2.1: DC bus configuration

2.3.2 Switched hybrid system configuration

The switched hybrid system or DC-AC bus configuration is the topology where the battery bank can be charged by the diesel generator and the PV array. Figure 2.2 shows that the electricity can be supplied directly to the load by the diesel generator. If the diesel generator output power exceeds the load demand, the excess energy will be used to recharge the battery bank. During period of low electricity demand, the diesel generator is switched off and the load is supplied by the PV array, together with stored energy from the battery bank.

When comparing the overall conversion efficiency, the switched system is more efficient than the series system.

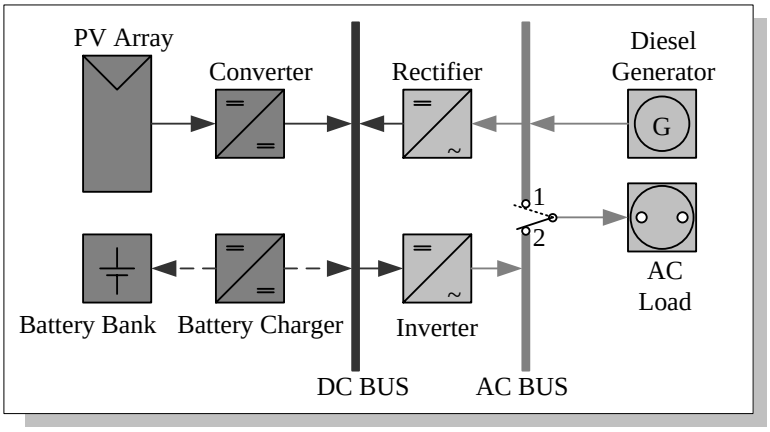

Figure 2.2: Switched hybrid system configuration

2.3.3 Parallel hybrid system configuration

Parallel hybrid system or AC bus configuration is the topology where all the system components are connected with the load via the AC power line, as shown in Fig. 2.3. This AC-side topology (or parallel topology) has a superior performance over the series configuration since the inverter can be synchronized with the generator so that both can supply the load simultaneously [28]. This offers some flexibility of the energy sources to meet the load. During high load conditions or peak times both the diesel and the battery are operated in parallel to cover the demand. Several advantages of this concept include higher overall efficiency, smaller sizes of the converters while keeping a high level of energy availability, and optimal operation of the diesel generator due to reduction of its operating time and maintenance. The development of advanced bi-directional converters that combine the functionality of inverter and rectifier simplifies the control and the load dispatch problem. The bi-directional battery converter can either share the load with the diesel generator or accept power from the diesel generator and operate as a battery. In this way, the expansion or modification of the hybrid system configurations can easily be carried out in order to cover the demand growth or change in demand behavior.

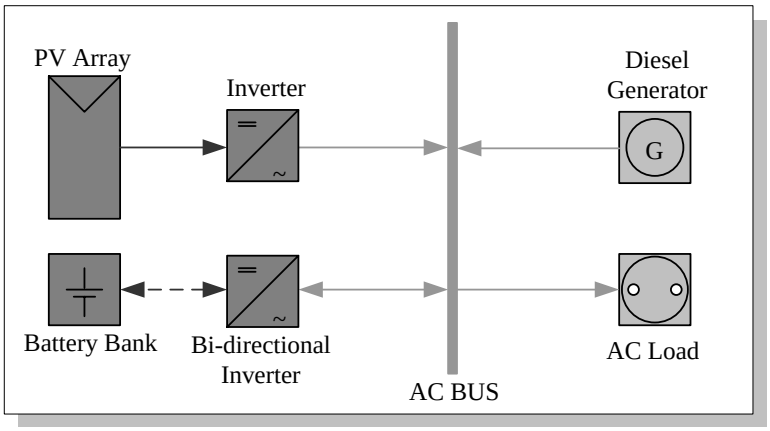

Figure 2.3: AC bus configuration

2.4 Load characteristics

The load profiles describe the variation of the electricity demand with time. The predicted Load profile is the important criterion for the selection of an adequate power supply system for the remote village. The demand for electricity in each area is different. With respect to the development of a hybrid system, it is possible to work out two main subcategories as follows:

- ***Remote electrification*** (night load profile or multi user profile), in this category the load profile is obtained for the remote settlements withlow power level (i.e. several households and schools). The most common appliances are lamps, television sets and refrigerators.
- ***Professional application*** (day load profile or single user profile), in this category the load profile is obtained for the high reliability professional applications (i.e. workshops, hospitals, restaurants and hotels) depending on the application, here are mostly appliances with high load demand.

The daily energy consumption and the annual energy growth should be estimated according to the load profile category to properly size the hybrid system to provide an adequate power supply system for the remote village. This is necessary in order to size both the generating plant and the user side in the distribution system. The sustainability of the system will not be guarantied if the capacity of the system is too small and leads to consumer dissatisfaction. Conversly, too large a capacity would mean additional investment costs and possibly too high tariffs.

The more reliable approach to assessing demand is to survey households in adjoining, already electrified areas or in a region with similar economic activities, demographic characteristics, etc. This would assess the average initial loads per household in these areas as well as their historical load growth.

2.5 Energy losses of PV-hybrid systems

A classification of all relevant energy losses in the stand-alone PV hybrid system is given as Capture losses and System losses [4]. Capture losses account for the part of the incident radiation energy that remains un-captured and which is therefore lost within a global energy balance. System losses define systematic energy losses that are due to the physical properties of the system components or the entire installation. Energy conversion losses or DC power line losses constitute important contributions to this category.

2.5.1 Capture losses

Capture or irradiation losses portray the fact that only part of the incoming irradiation is used for energy conversion. The losses are classified as follows:

- ***Shading losses:*** The losses due to shading correspond to the reduced energy received by a shaded module or array with respect to the un-shaded one under otherwise identical conditions. This direct irradiation losses can furthermore lead to mismatch

losses within the PV generator, caused by the non-uniform irradiation distribution over the entire array.

- ***Module orientation losses:*** Orientation losses constitute the irradiation losses caused by a module disposition different from that perpendicular to the incoming sun rays. The losses can be considerably reduced by using a tracking system that allows an automated adjustment of the module tilt angle with respect to the position of the sun.
- ***Spectral losses:*** With respect to airmass (AM) 1.5, the module characteristics as they are given by the manufacturer are determined at standard reference test conditions (STC), e.g. at a standard spectrum of AM 1.5. The deviation between the available irradiation spectrum and AM 1.5 causes the so-called spectral losses.
- ***Reflection losses:*** Reflection losses are irradiation losses at the surface of the PV module where some part of the incident sunlight is reflected and therefore a loss to the energy conversion is suffered.
- ***Surface soiling:*** Dirt on a module causes energy losses due to the fact that transmission of sunlight at the module surface is reduced by the dirt particles.

2.5.2 System losses

System losses cover all energy losses which occur during the conversion of incoming energy (solar irradiation, fossil fuel) into usable AC electricity. The losses can be classified as follows:

- ***Inverter and battery charger conversion losses:*** Inverter losses vary with the inverter DC/AC efficiency. Since the stand-alone inverters are powered by the local DC grid, the stand-by consumption is included in this category. The AC/DC efficiency of the battery charger is generally somewhat lower than the DC/AC inverter efficiency. Note that AC/DC losses are only one part of the overall losses generated during battery charging from the AC source; battery storage losses (see below) and subsequent DC/AC conversion losses occur before the initially provided energy can be consumed by an AC load.
- ***Battery storage losses:*** Storage losses comprise all energy losses within a battery. They are described by the charge and discharge efficiencies of the battery as well as the self-discharge characteristics.
- ***Auxiliary generator losses:*** The specific fuel consumption of the auxiliary generator depends on its operating mode. The corresponding generator efficiency defines the auxiliary generator losses with respect to a maximum efficiency.
- ***PV-battery mismatch losses:*** In many stand-alone PV hybrid systems the PV generator is directly wired to the storage battery. Hence, the operating point of the modules is defined by the actual battery voltage. PV-battery mismatch losses cause the difference between the actual operating voltage and the maximum power voltage V_{mpp}; the PV array does not function at its maximum power point corresponding to the given meteorological conditions.
- ***PV array mismatch losses:*** PV array mismatch losses are caused by the deviations of the I-V curves of interconnected PV modules from that of the PV array. As a result, the overall power output of the array is smaller than the sum of output powers

of all individual modules at a given operating point. PV array mismatch losses can be caused by different origins, which are: (a) the differences between I-V curves do exist even for modules of the same type, caused by small variations in the manufacturing process; (b) partial shading of the PV generator does not only create mismatch losses due to the spatial variation of the irradiation (see capture losses above) but also due to the resulting temperature differences, leading to deviations of the I-V curves; (d) differences in cable length and resistance of different strings or sub arrays may cause additional mismatch losses.

- ***Wiring losses:*** Wiring losses comprise all ohmic losses between system components. DC cable resistances, relays, switches or any other connections contribute to this energy loss. Blocking diodes in parallel strings of the PV generator also form part of the wiring losses. Due to the usually low AC currents compared to DC currents, AC wiring losses can generally be neglected.

2.6 Photovoltaic generator

As mention above, photovoltaic generator is the primary generator in the PV-Diesel hybrid system. It is used to convert the energy content of the sunlight directly into electricity and subsequently supply the loads. Photovoltaic generator consists of several photovoltaic modules from which electricity is produced by solar cells inside. The process of converting sunlight into electricity is called the "photovoltaic phenomenon". This phenomenon is described within this part. Moreover, the important functional detail of the solar cell, the PV module as well as the relevant characteristics of the PV power systems are presented.

2.6.1 Solar cell

A solar cell is a semiconductor device that can convert solar energy into DC electricity through the photovoltaic phenomenon. However, energy from solar cell is only available when enough irradiation is accessible. The solar cells are available in a wide range of power rating, up to 100 Wp. In some cases, cells are up to 300 Wp [29]. Solar cells are contained in a panel called the PV panel or PV module. Neighbouring module are interconnected in order to produce higher voltage/current to the loads. A solar cell is made up of at least two layers of semiconductor materials. One layer has a positive doping, the other is negatively doped. The description of photovoltaic phenomenon is; when light enters the cell, some of the photons of the light are absorbed by the semiconductor atoms, freeing electrons from the negative layer of the cell to flow through an external circuit and back into the positive layer. This flow of electrons constitutes an electric current. Figure 2.4 shows the solar cell construction and the photovoltaic effect.

When light is incident on a solar cell, free charge carriers are created due to the photovoltaic effect. This causes a current to flow through a connected load. The photocurrent, which is internally generated in a solar cell, is proportional to the radiation intensity. Figure 2.5 shows a typical equivalent circuit for a solar cell. The mathematical modeling of an ideal exposed solar cell leads to the following equation:

$$I_{PV} = I_{ph} - I_D = I_{ph} - I_0 \cdot \left(e^{\frac{qV}{kT}} - 1\right) \tag{2.13}$$

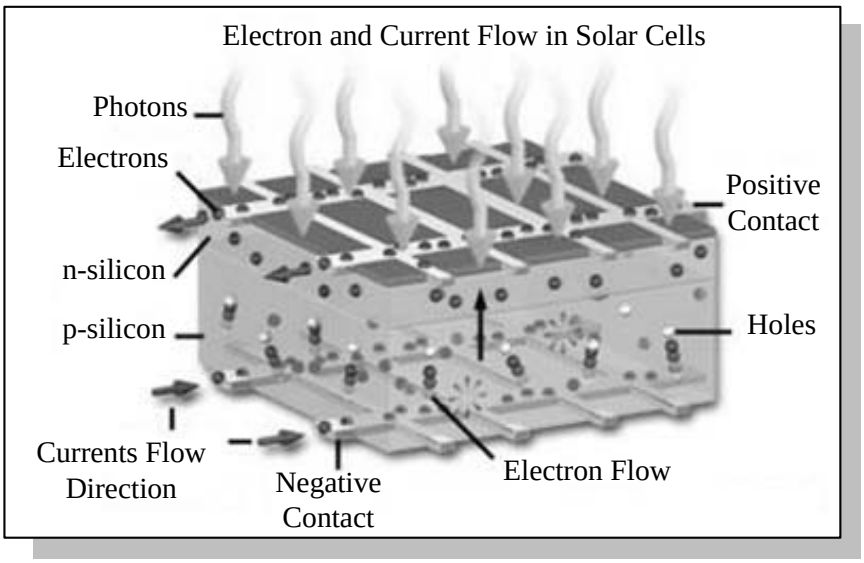

Figure 2.4: Photovoltaic effect [30]

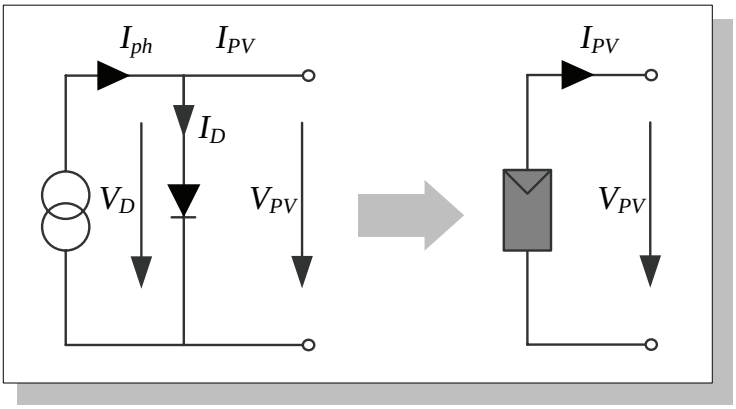

Figure 2.5: Equivalent circuit diagram for a solar cell

where

I_{PV}	is the current, A
I_{ph}	is the photocurrent, A
I_0	is the dark current, A
q	is the elementary charge, $e = 1.6x10^{-19}As$
V	is the output voltage, V
k	is the boltzmann constant, $8.65x10^{-5}eV/K$
T	is the diode temperature, K

When the terminals are short-circuited (load resistance equal zero), the output voltage and the voltage across the diode is zero. According to equation 2.13: since V = 0, no current I_D flows therefore the entire photocurrent I_{ph} generated from the radiation flows to the output. Thus the cell current has its maximum at this point with the value I_{cell} and refers to the so-called short-circuit current I_{sc}. For an infinitely large load resistance (open circuit), the output current is then zero ($I_{cell} = 0$) and thus the entire photocurrent flows through the internal diode. The open-circuit voltage V_{oc} can therefore be derived again from equation 2.13. The I-V characteristic of a solar cell showing I_{sc} and V_{oc} is shown in Figure 2.6. The typical value of the open-circuit voltage is located about 0.5 to 0.6 V for crystalline cells and 0.6 to 0.9 V for amorphous cells.

The power of a solar cell is the product of current and voltage (I.V), and is described by a curve such as shown in Figure 2.6. Although the current has its maximum at the short-circuit point, the voltage is zero and thus the power is also zero. The situation for current and voltage is reversed at the open-circuit point, so again the power here is zero. In between, there is one particular combination of current and voltage, for which the power reaches a maximum. The so-called maximum power point (MPP) represents the working point at which the solar cell can deliver maximum power for a given radiation intensity. It is situated near the bend of the I-V characteristic curve. The corresponding values of V_{MPP} and I_{MPP} can be estimated from Voc and Isc as follows [31]:

$$V_{MPP} \approx (0.75 - 0.9)V_{oc}$$
$$I_{MPP} \approx (0.85 - 0.95)I_{sc}$$

The maximum power rating is the power at the MPP. The rated current I_{mpp} and rated voltage V_{mpp} correspond to the MPP. The rated power is measured under Standard Test Conditions (STC), i.e. at an irradiation intensity of $I_{STC} = 1000W/m^2$, cell temperature $T_{cell} = 25^oC$ and air mass AM=1.5. It is quantified in units of peak Watts Wp. A maximum point power tracker (MPPT) may be necessary in order to operate at the optimum point on the I-V curve.

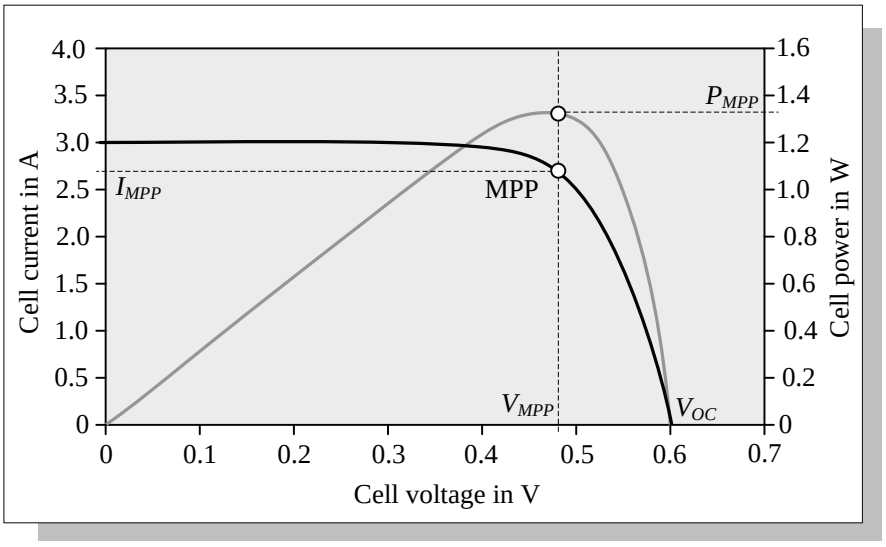

Figure 2.6: I-V and P-V characteristics of the solar cell showing the Maximum Power Point (MPP)

2.6.2 PV module

Each individual PV module contains cells which are connected in series, and in parallel combinations to obtain the desired voltage and current. For identical modules or cells connected in series the voltages are additive, converly when they are connected in parallel, the currents are additive. The PV plant usually consists of multiple connected modules. These modules are called arrays. The configuration of a module and an array is shown in Figure 2.7.

The PV plants have a relationship between specific voltage (V) and current (I), which is depicted in an I-V curve. The maximum power point (MPP) operation is where the maximum

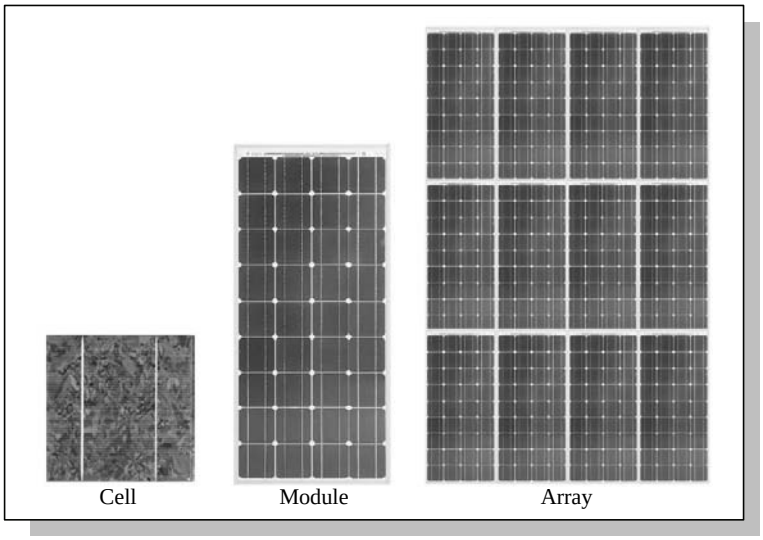

Figure 2.7: Typical configuration of solar cells in modules and arrays [32]

panel output power is obtained with given irradiation and temperature levels. Manufacturers typically provide I-V curve specifications at different irradiation levels (200 and 1000 W/m^2) by keeping other variables such as temperature and wind speed constant, as shown in Figure 2.8.

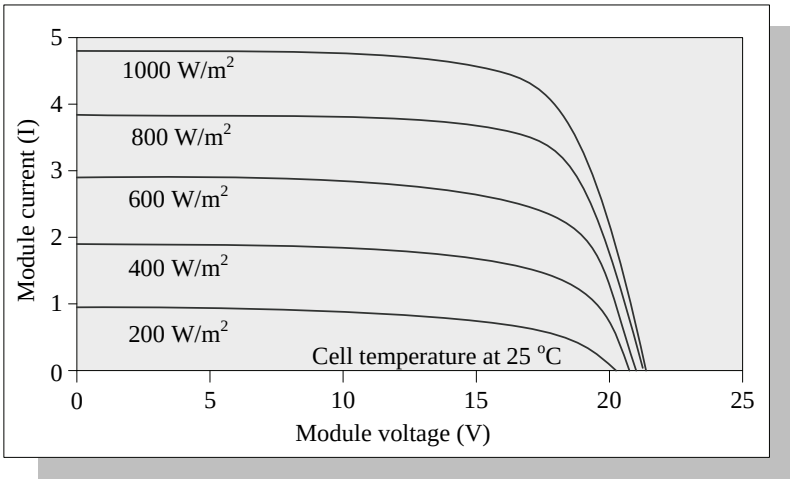

Figure 2.8: Influence of the irradiance E on the I-V characteristics of a solar cell [33]

At constant irradiation levels, the PV panel generates a roughly constant current, starting from the short circuit current (I_{SC}) to just before the current values near the open circuit voltage (V_{OC}). To account for the effect of panel temperature, I-V curves for different temperatures, keeping of the irradiation level constant, are also shown in Figure 2.9. These show that at constant irradiation the voltage is decreases as the temperature is rises.

The important parameters for the PV module are fill factor (FF), maximum power point (MPP) and efficiency of the module (η).

Fill factor: This parameter is used to measure the quality of a solar cell. It describes how closely the current-voltage characteristic curve approximates the ideal rectangular form. Fill factor is defined as:

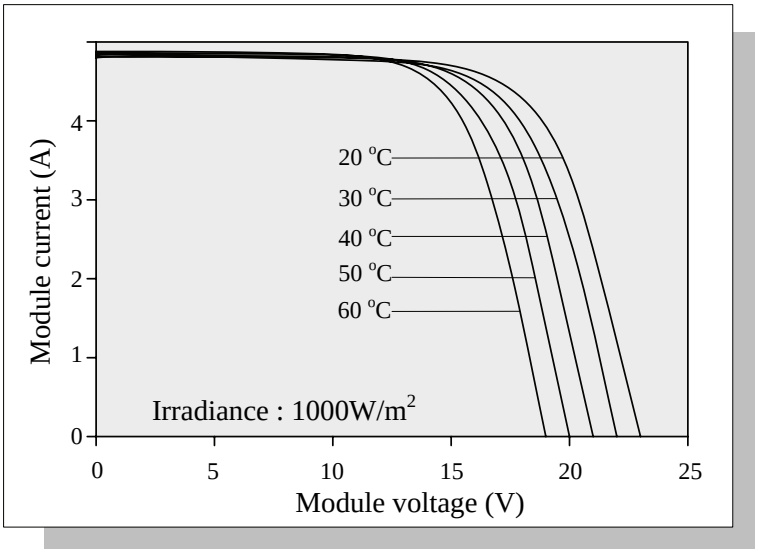

Figure 2.9: Temperature dependence of solar cell characteristics [33]

$$FF = \frac{V_{MPP} \cdot I_{MPP}}{V_{oc} \cdot I_{sc}} \tag{2.14}$$

The fill factor for crystalline solar cells is about 0.7 to 0.8. The maximum output power of the cell is then

$$P_{MPP} = V_{MPP} \cdot I_{MPP} = V_{oc} \cdot I_{sc} \cdot FF \tag{2.15}$$

Thus the efficiency of the solar cell, which refers to the ratio of the output electrical power to the input solar radiation (P_{in}), is defined by the following relation.

$$\eta = \frac{V_{OC} \cdot I_{sc} \cdot FF}{P_{in}} \tag{2.16}$$

Until now the highest obtained efficiency of the silicon solar cells with the irradiation of a solar spectrum at AM 1.5 is approximately 24 percent. The efficiency of silicon solar modules from line production for terrestrial applications is situated between 10 and 14 percent. However, the theoretical efficiency of the silicon solar module is approximately 26-27 percent.

More clearly, the PV cell is a semiconductor device that can convert solar energy into DC electricity through the photovoltaic effect. Cell types include monocrystalline silicon, polycrystalline silicon, amorphous silicon (a-Si), gallium arsenide (GaAs), copper indium diselenide (CuInSe2, CIS), cadmium telluride, or a combination of two materials in a tandem cell. At present, only silicon cells are available in large quantities in the market [34]. Figure 2.10 illustrates the various commercial large area module efficiencies and the best laboratory efficiencies obtained for various materials and technologies [35].

The energy productivity of the PV plant mainly depends on the solar irradiation behavior at the site of interest, such as radiation intensity (W/m^2), duration and yearly causes, as well as module orientation. PV module installation requires only a simple tilting structure for the surface area. It is only natural to try and maximize the PV output at or close to the hour of peak demand [36]. It is found that this can be done by changing the surface azimuth angle to an angle suitable for maximizing the PV generation at any prescribed hour of peak load. This orientation strategy is of course inherently linked to the fact that the overall energy generated during the day is less than that generated by a south-facing array.

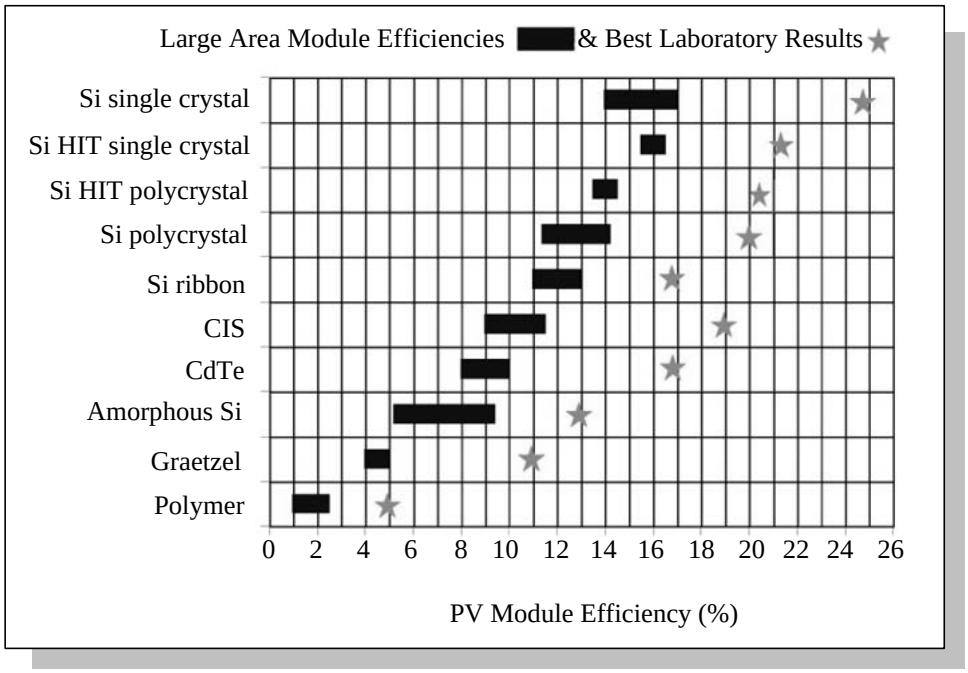

Figure 2.10: PV module efficiency (%)

2.6.3 Maximum Power Point Tracker (MPPT)

The position of the points of maximum power on the PV generator characteristic depends strongly on the irradiation and the cell temperature. In principle, a continuous tracking of the working point voltage (MPP tracking)is necessary for achieving of a maximum energy yield, as shown in Figure 2.6 (page 19). The additional energy gains, estimated by comparing at a given (correctly selected) voltage, are 3 to 5 percent above that without tracking. A tracking of the MPP is therefore only meaningful if components for energy processing, e.g. network inverters or DC/DC converter with the possibility of a working point adjustment are available and the tracking of the working point does not bring additional energy losses and only small addition costs.

2.6.4 Power conditioning

Power conditioning units are all those components in a system that contribute to the power handling (or power actuator), such as inverter, and bi-directional converter for the charge regulation of the battery. They are altogether of fundamental importance to the improvement of the energy performance. The power conditioning structure of modular systems comprises the power conditioning unit and its interfacing facility (hardware components) as well as its interactions (control and communication algorithms) for components adaptation and dynamic interactive effects.

The best possible yield from the irradiation intensity is given when the output power of the inverter unit is maximized and supplied to the load. The maximum power point (MPP) is particularly affected by the irradiation intensity and the temperature of the module. Fluctuations of these parameters, especially of the irradiation intensity, cause frequent current variations which are hard to smoothen. A further important operating function, which also depends on the power conditioning unit, is the maximum power point tracking (MPPT). At

the MPP an optimization process is carried out by the inverter to adjust the module output voltage and current in order to reach maximum output power. These parameters play an important role in maximizing the efficiency and reducing the use of the fossil fuel generator and the battery storage.

2.6.5 Mathematical model for Photovoltaic generators

A photovoltaic generator is the whole assembly of solar cells, connections, protection parts, supports and etc. This section presents the model focusing only on cell/module/array. Steps in calculation of PV module current, under standard conditions are presented below [37, 38]:

$$P^{C}_{max,0} = \frac{P^{M}_{max,0}}{(N_{SM} \times N_{PM})} \tag{2.17}$$

$$V^{C}_{OC,0} = \frac{V^{M}_{OC,0}}{N_{SM}} \tag{2.18}$$

$$I^{C}_{SC,0} = \frac{I^{M}_{SC,0}}{N_{PM}} \tag{2.19}$$

$$V^{C}_{t,0} = \frac{mkT^{C}_{0}}{e} \tag{2.20}$$

$$V_{OC,0} = \frac{V^{C}_{OC,0}}{V^{C}_{t,0}} \tag{2.21}$$

where

$P^{C}_{max,0}$ is the maximum power for the cell
$P^{M}_{max,0}$ is the maximum power to the module
$V^{C}_{OC,0}$ is the open circuit voltage for the cell
$V^{M}_{OC,0}$ is the open circuit voltage for the module
$I^{C}_{SC,0}$ is the short circuit current for the cell
$I^{M}_{SC,0}$ is the short circuit current for the module
N_{SM} is the number of cells in series
N_{PM} is the number of cells in parallel
$V^{C}_{t,0}$ is the thermal voltage in the semicaonductor of a single solar cell at STC
m is the idealising factor
k is the Boltzmann's constant, $k = 1.381 \times 10^{-23}$, J/K
T^{C}_{0} is the cell temperature at standard condition $(25^{o}C)$
e is the electron charge $(e = 1.602 \times 10^{-19}C)$
$V_{OC,0}$ is the open circuit voltage

One important parameter is fill factor, its defined as:

$$FF = \frac{(V_{OC,0} - ln\,(V_{OC,0} + 0.72))}{(V_{OC,0} + 1)} \tag{2.22}$$

$$FF_{0} = \frac{P^{C}_{max,0}}{\left(V^{C}_{OC,0} \times I^{C}_{SC,0}\right)} \tag{2.23}$$

$$r_{S} = 1 - \frac{FF}{FF_{0}} \tag{2.24}$$

$$R_S^C = \frac{r_S \times V_{OC,0}^C}{I_{SC,0}^C} \tag{2.25}$$

Where

FF	is the fill factor
FF_0	is the fill factor at standard condition
r_S	is the series resistance
R_S^C	is the equivalent serial resistance of the cell

Cell parameters for the operating conditions are:

$$C_1 = \frac{I_{SC,0}^C}{G_{a,0}} \tag{2.26}$$

$$I_{SC}^C = C_1 \cdot G_a \tag{2.27}$$

$$T^C = T_a + C_2 \cdot G_a \tag{2.28}$$

$$V_{OC}^C = V_{OC,0}^C + C_3 \left(T^C - T_0^C\right) \tag{2.29}$$

$$V_t^C = \frac{mk\left(273 + T^C\right)}{e} \tag{2.30}$$

where

C_1	is the constant, Am^2/W
C_2	is the constant, $C_2 = 0.03Cm^2/W$
C_3	is the constant, usually considered to be $C_3 = -2.3mV/^oC$
$G_{a,0}$	is the irradiation, W/m^2
G_a	is the ambient irradiation, w/m^2
V_t^C	is the thermal voltage in the semiconductor of a single solar cell at the operating conditions
T_a	is the ambient temperature, ^oC
T^C	is the working temperature of the cell

Module current for operating conditions

$$I^M = N_{PM} \cdot I_{SC}^C \left[1 - exp\left(\frac{V^M - N_{SM} \cdot V_{OC}^C + I^M \cdot R_S^C \cdot \frac{N_{SM}}{N_{PM}}}{N_{SM} \cdot V_t^C}\right)\right] \tag{2.31}$$

where

I_{SC}^C	is the short circuit current for the cell at the operating conditions
V_{OC}^C	is the open circuit voltage for the cell at the operating conditions
I^M	is the total generated current by the module
V^M	is the applied voltage at the module's terminal

Norminal conditions	**Standard Condition**
Radiation: $G_{a,ref} = 800W/m^2$	Irradiation: $G_{a,ref} = 1000W/m^2$
Ambient temperature: $T_{a,ref} = 20^oC$	Cell temperature: $T_0^C = 25^0C$

Table 2.2: Nominal and stand conditions n

Array current for operating conditions

$$I^A = \sum_{i=1}^{M_P} I_i \tag{2.32}$$

or

$$I^A = M_P \cdot I^M \tag{2.33}$$

where:

I_i is the current from module i, A
I^A is the total current of the array, A
M_P is the number of modules in parallel

Power generated by PV array

$$P^A = I^A \cdot V^A \tag{2.34}$$

where

P^A is the power generated by PV array
I^A is the total generated current by the PV array
V^A is the applied voltage at the PV array

Note: In order to clearly specify where each element belongs (cell or module),the parameters in the mathematical model use the following notation: the parameters with superscript *M* refer to the PV module, while the parameters with superscript *C* refer to the solar cell.

2.7 Diesel generators

Fossil fuels generators consist of an engine that drives an electric generator. Besides Otto and diesel-motors, gas turbines are very reliable units for large scale applications. However, the most common engines used in supplying small and medium loads are diesel generators. In this section some performance characteristics related to the diesel engine operation in power generation applications are presented.

2.7.1 The diesel generator and the RE system

The diesel generator has the benefit of strengthening the reliability of the RE system [21]. The utilization of diesel generator is dependent on the fraction of renewable energy in the total energy consumption. The application of diesel generator in the hybrid system can be considered as:

- ***High renewable energy penetration system:*** In this case, the generator is used mainly as a backup unit and will not necessarily be started every day.
- ***Low renewable energy penetration system:*** The genset is the main generator and runs many hours every day. Fuel consumption and maintenance should be optimized to decrease the energy cost.
- ***Medium renewable energy penetration system:*** The generator usually runs from time to time.

Even in high renewable energy penetration systems, the fuel generator might be needed to temporarily increase the overall electrical power of the system in order to run some occasional big loads. In this case, parallel operation of the genset with the battery inverter is required to allow the adding of the power of all controllable power units. The characteristics of the demand, the possibility to operate in parallel with battery inverter, and the penetration level of renewable energy are used to determine the size of the standby generator.

2.7.2 Technical characteristics

Normally the rotation speed of 60 Hz generators is at either 3600 rpm or 1800 rpm. Corresponding speeds for 50 Hz generator are 3000 rpm and 1500 rpm. The 3600 rpm units are 2-pole generators, which are convenient for use in light duty (less than 400 hours/year) applications. The 1800 rpm units are 4-pole generators, which are recommended when more than 400 hours of operation per year are anticipated [39]. Diesel generators are the most common electricity producers in a large number of small and decentralized power systems throughout the world and especially in developing countries [40]. However, using diesel in these locations can often be very expensive due to the additional transportation costs involved. The important performance factors from the point of view of system technology are [41]:

- *The engine performance over its operating range*
- *The engine fuel consumption within this operating range and the cost of the required fuel*
- *The engine noise and air pollutant emissions within this operating range*
- *The initial cost of the engine and its installation*
- *The reliability of the engine, its maintenance requirements and how these affect the energy availability and operating costs*

These factors control the total engine operating costs, which usually is the primary consideration of the user. The nominal lifetime of the diesel generator depends on the size of the engine. Diesel generators are available in sizes ranging from kilowatts to some megawatts. Compared to renewable energy converters, fossil fueled generators have low investment costs and produce power on demand. Disadvantages of conventional generator operation include fuel dependence, transport and storage costs of fuel, high maintenance costs and exposure to fumes and noise.

2.7.3 Fuel consumption and efficiency

The fuel consumption of a diesel engine generally depends on the machine type and construction characteristics. Its efficiency varies from 20 to 37 percent at high load levels [41]. Fuel efficiency drops drastically at low load levels. Diesel fuel consumption is a function of the engine load and the revolution; therefore, it is always represented by a two-dimensional field. Constant speed engines are usually used for electricity production, which makes the fuel consumption only dependent on the loading ratio of the engine [42]. Figure 2.11 (a) shows typical fuel consumption for an 80 kW generator as a function of the loading ratio [43].

In electricity generation, a back-up generator is characterized by its efficiency η_D and its consumption in relation to the produced electrical energy as follows:

$$\eta_D = \frac{P_{E_G}}{Q_{LV} \cdot m_f} \tag{2.35}$$

where

P_{E_G} is the generated electrical energy, kW
m_f is the rate of fuel consumption, l/h
Q_{LV} is the low heat value of the fuel, kWh/l

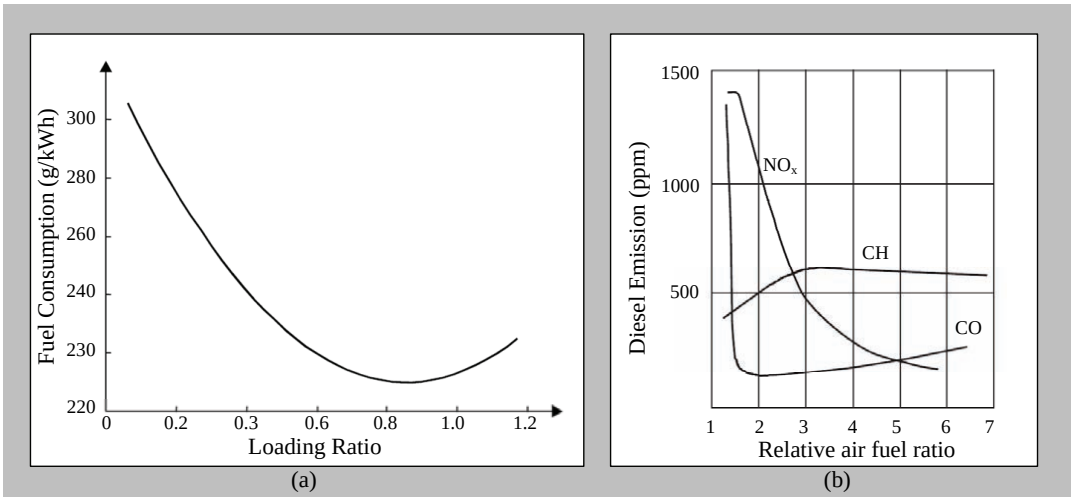

Figure 2.11: (a) Fuel consumption of the diesel engine for an 80 kW generator, (b) the emissions from the diesel generator at different relative air fuel ratios

2.7.4 Operating lifetime of the diesel generator

According to the manufacturer information, if the diesel generator is used with regular maintenance and for the intended purpose (back-up, continuous and etc), its operating lifetime depends on the unit size. The operations between 20,000 to 100,000 operating hours are expected until complete overhaul is required. For an aggregate size up to 100 kW an operating lifetime of 30,000 hours is expected, and for bigger aggregate sizes between 500 kW to 1 MW, the expected operating hours are between 40,000 to 100,000 [44].

Some factors which have negative effects on the engine operating lifetime are listed as follows:

- ***Partial load conditions:*** low load operation (i.e. $< 40\ percent$ of the nominal load) of a diesel engine may lead to increased corrosive wear due to the presence of sulfur in the diesel fuel, degrading the engine performance as well as causing operational problems, consequently, lower lifetime and high operating costs.

- ***Start/Stop frequency:*** the start/stop frequency has not only negative effects on the diesel maintenance but also a failure to start-up the machine can occur at each starting time [45]. Hence, the system reliability and the energy availability are strongly affected if the diesel generator is not used properly.

- ***Cold-or warm-starting:*** the cold-or warm-starting as well as quick loading of the engine greatly influences the engine wear. Cold-starting accelerates the wear because the lubrication films on the piston assembly, crankshaft bearing, and other connecting points have drained away during standstill. Also at the cold-starting, the lubricant has a high viscosity which results in low mechanical efficiency.

- ***Regular maintenance:*** neglected maintenance of the equipment, especially ignoring the changing of the lubrication oil and oil-filters as recommended in the operation manual can strongly reduce the engine lifetime. Contaminating the lubrication oil with fuel and fuel additives changes the chemical properties of the oil. Therefore, its viscosity continuously decreases during the operation of the engine.

2.7.5 Emissions generation

Emmisions of Hydrocarbons (HC) and nitrogen oxides (NO_x) from diesel engines vary widely with the operating conditions. The diesel engine works under full load conditions with *relative air/fuel ratio*, λ[2] between 1.2 and 1.8 and in idling condition between 5 and 10. Figure 2.11 (b) shows the effect of variation in value of λ on the diesel emissions. Operating the diesel at small λ (i.e. in high load levels) leads to high temperature which causes a high level of NO_x. Development of HC is strongly dependent on the oxygen content of the fuel mixture. Carbon monoxide develops in small concentration if there is enough oxygen in the mixture and the fuel is well distributed inside the combustion chamber. Accordingly, engine idling and low load operation produces significantly higher HC emissions than operating the engine at or near full load. Also, overloading the engine will result in augmentation of the hydrocarbons. Moreover, hydrocarbon emissions have been shown to be sensitive to oil and coolant temperature: when these temperatures were increased from 40^o to 90 ^oC, HC emissions decreased by 30 percent, which indicates the undesirable effect of cold starting on the produced emissions.

2.7.6 Mathematical model for the diesel generator

Conventional generators normally have diesel engines which are directly coupled to generators. The frequency of the AC power is maintained by a governor on one of the engines. The governor adjusts the flow of fuel to the engine to keep the engine and generator speed essentially constant. The grid frequency is directly related to the speed of the generator, and is, therefore, maintained at the desired level. The diesel generator model uses the net load energy demand to calculate energy supplied by the diesel generator for a basic case and additional system configurations. The energy flow model of the diesel generator as used in computer program is [23, 46]:

Energy generated by diesel generator

$$E_{Diesel} = DieselCap \times \eta_{Diesel} \tag{2.36}$$

where:

E_{Diesel}	is the energy generated by diesel generator, kWh
$DieselCap$	is the diesel generator capacity, kWh
η_{Diesel}	is the diesel generator efficiency (20-40), $\%$

2.8 Lead-acid batteries

Electrical energy can be produced by the different conversion methods. It is possible to convert solar energy directly to electrical energy via PV modules. But since the sun does not shine all around the clock, then it is necessary to store the electrical energy. This is done in accumulators, also called batteries, from which electrical power can be drawn at any time of the day.

[2] λ is the relative air/fuel ratio

2.8.1 Principal types of batteries

There are several different types of battery chemistry including liquid lead-acid, nickel-iron (NiFe), nickel-cadmium (NiCd), alkaline, and gel-cell. Batteries are either sealed or vented. Simply, there are only two principal types of batteries: starting and deep-cycle.

- ***Starting batteries*** are designed for high cranking power, but not for deep cycling. Used as energy storage, they will not last long in a deep cycle application. Starting batteries use lots of thin plates to maximize the surface area of the battery. This allows very high starting current but causes the plates to warp when the battery is cycled. This type of battery is not recommended for the storage of energy in hybrid system. However, they are recommended as starting battery for the back-up generator.
- ***Deep cycle batteries*** are the type of battery best suited for use with inverters. The physical dimension of the plates is thicker and the active material that holds the charge is denser to increase cycle life. The deep cycle type of battery is designed to have the majority of their capacity used before being recharged. They are available in many sizes and in either non-sealed or sealed types.

The open (also called vented) lead acid batteries are the most commonly available and cheapest batteries used today for PV systems [47]. Lead acid battery is an electrochemical battery that uses lead and lead oxide for electrodes and sulfuric acid for the electrolyte. The next subsection is describes this type of battery.

2.8.2 The lead-acid battery

The lead-acid battery, invented in 1859 by French physicist Gaston Planté, is the most commonly used as the rechargeable battery today[3]. It also represents the oldest design with one of the worst energy-to-weight ratios, although the power-to-weight ratio can be quite good. Also, the energy-to-volume ratio is good compared to other types of batteries. It is cheap and can supply high surge currents needed in starter motors.

Lead-acid batteries consist of six cells of 2 V nominal voltage. Each cell contains (in the charged state) electrodes of lead metal (Pb) and lead (IV) oxide (PbO_2) in an electrolyte of about 37 percent w/w[4] sulfuric acid (H_2SO_4). Modern designs have gellified electrolytes. In the discharged state both electrodes turn into lead (II) sulfate and the electrolyte turns into water. (This is why discharged lead-acid batteries can freeze.) The chemical reactions are (charged to discharged):

- ***Anode (oxidation):***

$$Pb_{(s)} + SO^{2-}_{4(aq)} \leftrightarrow PbSO_{4(s)} + 2e^- \tag{2.37}$$

- ***Cathode (reduction):***

$$PbO_{2(s)} + SO^{2-}_{4(aq)} + 4H^+ + 2e^- \leftrightarrow PbSO_{4(s)} + 2H_2O_l \tag{2.38}$$

[3]Wikipedia, The Free Encyclopedia:http://en.wikipedia.org/wiki/Lead-acid_battery

[4]w/w is "'weight by weight", e.g. 2percent w/w means that the mass of the substance is 2 percent of the total mass of the solution or mixture.

2.8.3 The battery capacity

Capacity is the measure of the amount of current that can be stored and withdrawn from a battery. The unit for capacity is ampere-hours (Ah). It is practical to use an approximate value of the capacity of a battery called the nominal capacity. The nominal capacity of a battery is a measure given by the manufacturer for the capacity guaranteed to be reached when a new battery is discharged according to a standardized test procedure.

For the starting, lighting, and ignition (SLI) batteries, the battery is discharged 20 hours with a constant current down to a predetermined cut-off voltage. This current is called I_{20} and the corresponding capacity value is denoted C_{20}.

Nominal discharge current refers to the value related to the nominal capacity value. If the nominal current is related to the C_{20} capacity, then the corresponding current is named I_{20}. If the nominal capacity value of a battery is divided by 20, then the average discharge current I_{20} can be taken out of the battery for 20 hours [31].

Unfortunately, the capacity of a battery is not a constant quantity, but depends on the amount of discharge current. The manufacturers therefore give the rated capacities of their batteries always with reference to a certain discharge current. The so-called rated battery capacity refers to the capacity of the battery under given standard conditions: it is common practice to define the rated capacity at 20 ^oC by discharging the battery with a rated battery current (I_{10}). Some battery manufacturers indicate the 100-hour discharge capacity for batteries intended for PV applications. When comparing such capacity, it should be remembered that, for a given battery, the 100-hour capacity is always at least 30 percent higher than the 10-hour capacity [48].

2.8.4 The depth of discharge (DOD)

Depth of discharge is the opposite of state of charge, (100 percent minus state of charge in percent). A fully discharged battery has reached 100 percent depth of discharge. Maximum 80 percent depth of discharge is recommended to give a reasonable lifetime of a lead acid battery. A maximum 50 percent design DOD is recommended in a PV system due to the often very slow and irregular recharge.

In practice, harmful deep discharge is to be avoided: the consumers will be compulsorily disconnected from battery as soon as the discharge voltage threshold is reached, i.e. with the help of a so-called deep discharge protection (DDP). This threshold is basically given in the data sheets by the manufacturer for different discharge currents. Preferably, the value of this threshold should depend on the discharge current. Figure 2.12 shows the relation between the discharge current and the voltage during discharge for the lead-acid battery. At constant discharge current, the terminal voltage of thebattery varies inversely with time.

2.8.5 The state of charge (SOC)

One important parameter that defines the energy content of the battery is the state of charge (SOC). This parameter indicates how much charge is available in the battery with reference to its capacity. This definition includes a degree of ambiguity, because the capacity here can carry different values, either the nominal capacity, or the actual capacity.

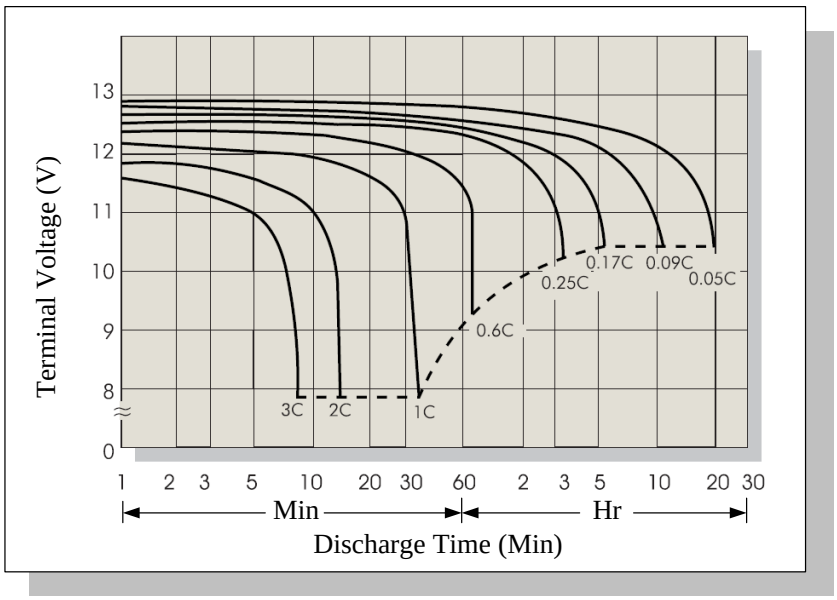

Figure 2.12: Discharge characteristic curves [49]

When a battery is fully charged to the nominal capacity, the state of charge is 100 percent. A fully discharged battery has 0 percent state of charge. In normal operation a battery should not be discharged below 20 percent state of charge to avoid effects that will dramatically shorten the lifetime of the battery. A PV system should not be designed for a daily discharge below 50 percent SOC.

The ability to determine the battery state of charge in a system at any time is very important from the point of view of the system operation. Knowing the state of charge continuously makes the system energy management possible. In addition, for a stand-alone photovoltaic system, the required battery capacity can be more accurately determined, which implies higher reliability of the energy supply and lower system cost [48].

2.8.6 Temperature effects on the battery capacity

The nominal capacity is normally measured at 20^oC of battery temperature, with a constant current discharge, down to a certain fixed cut off voltage of the battery. In cold climates the usable capacity may be significantly reduced, as low temperatures will slow down the chemical reactions in the battery. This will result in a useable capacity at, for example, minus 10^oC battery temperature of only 60 percent of the nominal one at 20^oC. The capacity is still there if the battery is warmed to 20^oC, but at low temperature one can not utilize the full amount.

When possible the battery should therefore be placed indoors or otherwise sheltered from low temperatures by insulation or perhaps even placed in the ground if any other heat sources are not available. Seasonal storage containers with phase change materials with water as the main storage component have been shown to work well.

In warm climates the opposite effect on capacity does not occur at battery temperatures above 20^oC. In this case the battery should be placed in such a way as to avoid high temperatures. Already a 10^oC temperature rise above 20^oC will double the corrosion velocity of the electrodes and reduce the battery lifetime significantly as shown in Figure 2.13.

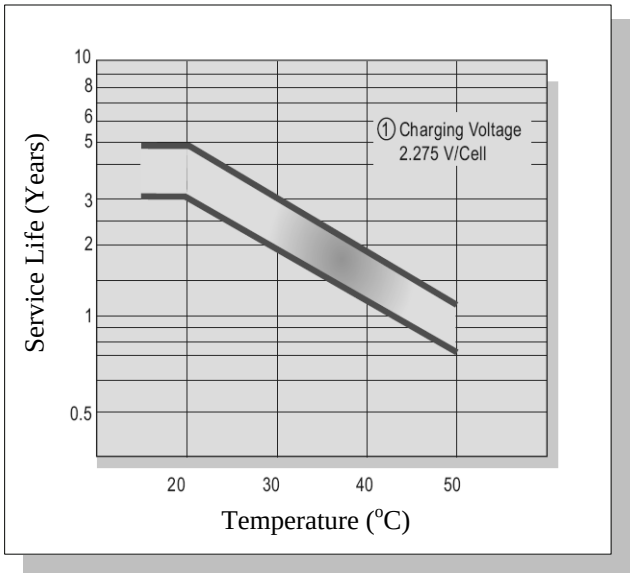

Figure 2.13: Temperature effect on trickle service life of battery [49]

2.8.7 Cycle life of lead-acid batteries

The cycle life refers to a capability of the battery to withstand a certain number of charge or discharge cycles of given depth of discharge (DOD). Since the lifetime of the battery also depends on the average depth of discharge during cycling (expressed in percentage (%) of rated capacity), the cycling capability may be more conveniently expressed by multiplying this average depth of discharge by the battery lifetime expressed in number of cycles. The result is called the nominal cycling capability, which is expressed as the number of equivalent 100 percent nominal capacity cycles. The starter battery typically has a low cycling capability of less than 100 nominal cycles, which means that it is able to withstand for example 500 cycles of maximum 20 percent depth of discharge. The battery appropriate for PV application requires a good cycling capability of at least 500 nominal cycles, which means that it should be able to withstand for example 1000 cycles of 50 percent depth of discharge. Fig. 2.14 shows the cycle life as a function of DOD. Life cycles of battery is varies inversely with DOD of battery.

2.8.8 Requirements for solar batteries

Typical requirements for the battery to be used in long term storage are:

- ***Specific kWh-cost:*** Usually it refers to a sum of investment and operation costs of the battery divided by the stored kWh (kWh_{Σ}) during its whole life. This cost is thus influenced by the battery lifetime.
- ***Lifetime:*** The lifetime of the battery should be long, especially in order to keep the specific kWh-cost and the installation cost low, particularly in remote areas.
- ***The overall efficiency (η_{Σ}):*** should be as high as possible, to be able to pass the biggest proportion of the energy in the battery, which is generated by the PV generator on to the consumers.
- ***Self-discharge:*** The battery discharges itself even without load connected. This ef-

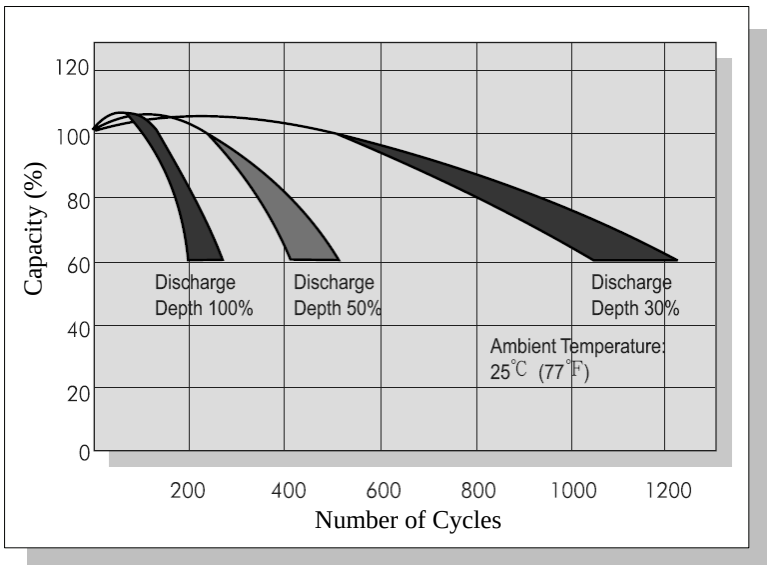

Figure 2.14: Cycle life as a function of deep of discharge [49]

fect is caused by secondary reactions at it electrodes and proceeds faster with higher temperature or older battery. Thermodynamic instability of the active materials and electrolytes as well as internal- and external short-circuits lead to capacity losses, which are defined as self-discharge. This loss should be small, particularly in relation to annual storage.

- ***Maintenance cost:*** The maintenance, e.g. water refilling in case of lead-acid batteries, should be kept as low as possible.
- ***Easy installation and operation:*** Since batteries are driven, often also from non-experts, easy installation and operation are therefore desirable.
- ***Power:*** In special cases battery must be highly loadable for a short time, e.g. at the start of diesel generators or in case of momentary power extension of PV systems.

2.8.9 Mathematical model for lead-acid batteries

An important element of a PV system is the battery. The battery is necessary in such a system because of the fluctuating nature of the output delivered by the PV arrays. Thus, during the hours of sunshine, the PV system is directly feeding the load, the excess electrical energy being stored in the battery. During the night, or during a period of low solar irradiation, energy is supplied to the load from the battery. The steps of the battery model are presented as followed [24]:

Minimum energy left in the battery

$$E_{BattMin} = (1 - DOD_{max}) \times BattCap \tag{2.39}$$

where:

$E_{BattMin}$	is the minimum energy left the battery, kWh
DOD_{max}	is the maximum depth of discharge of battery
$BattCap$	is the battery capacity, kWh

Maximum discharge energy of battery

$$E_{MaxDis} = (E_{Batt} - E_{BattMin}) \times (\eta_{Batt} \times \eta_{BattInv}) \tag{2.40}$$

where:

E_{MaxDis} is the maximum discharge energy of battery, kWh
E_{Batt} is the energy of battery, kWh
η_{Batt} is the battery efficiency, $\%$
$\eta_{BattInv}$ is the battery inverter efficiency, $\%$

Discharge energy of battery

$$E_{BattDis} = |E_{Load} - E_{Inv}| \tag{2.41}$$

where:

$E_{BattDis}$ is the discharge energy of battery, kWh
E_{Load} is the required energy for load, kWh

Energy used for charge the battery

$$E_{ChgBatt} = (E_{Line} \times \eta_{BattInv}) \times \eta_{Batt} \tag{2.42}$$

where:

$E_{ChgBatt}$ is the energy used for charge battery, kWh
E_{Line} is the energy in line after supplied to load, kWh

Energy of battery after charge

$$E_{BattNew(C)} = E_{BattOld(C)} + E_{ChgBatt} \tag{2.43}$$

where:

$E_{BattNew(C)}$ is the energy of battery after charge, kWh
$E_{BattOld(C)}$ is the energy of battery before charge, kWh

Energy of battery after discharge

$$E_{BattNew(D)} = E_{BattOld(D)} - \left(\frac{E_{BattDis}}{\eta_{BattInv} \times \eta_{Batt}} \right) \tag{2.44}$$

where:

$E_{BattNew(D)}$ is the energy of battery after discharge, kWh
$E_{BattOld(D)}$ is the energy of battery before discharge, kWh

Battery state of charge

$$SOC = \frac{E_{Batt}}{BattCap} \tag{2.45}$$

where:

SOC is the battery state of charge, $\%$
E_{Batt} is the energy of battery, kWh
$BattCap$ is the battery capacity, kWh

Surplus Energy in battery bank is defined by the equation below;

$$E_{Surplus} = E_{Batt} - BattCap \tag{2.46}$$

where:

$E_{Surplus}$ is the surplus energy, kWh
E_{Batt} is the energy of battery, kWh
$BattCap$ is the battery capacity, kWh

2.9 Charge controllers

Batteries represent a substantial cost factor, for example in case of a typical island house of about 15 to 20 percent of initial investments, which can rise to over 50 percent, if one considers the necessity for repeated replacement of the battery over the lifetime of the total system. Therefore it is aimed to achieve, by suitable charging and supervision strategies, as long life of the battery as possible under given operating conditions. Experiences from a great deal of systems show that with the presently used techniques, the obtained life of 2 to 4 years is clearly shorter than the expected values of 5 to 8 years. The determination of the causes responsible and the derived, and hence the development of new concepts and system components are thus important assignments in the future. In the following, basic principles of common charge regulators are described. The theme is limited thereby to charge regulators for the lead acid batteries used in larger systems [3].

2.9.1 Mathematical model for charge controllers

This section presents the modeling of the controller of a PV system. The charge controller is used to manage the energy flow to PV system, batteries and loads by collecting information on the battery voltage and knowing the maximum and minimum values acceptance for the battery voltage. The modeling of the controller is presented below [23, 46]:

$$E_{out} = E_{in} \cdot \eta_{Chg} \tag{2.47}$$

where:

E_{out} energy output from charge controller, kWh
E_{in} energy input to charge controller, kWh
η_{Chg} efficiency of charge controller

2.10 Inverter

As many small consumers are suitable for operation directly with DC voltage, then it is proper to directly connect the PV generators as well as batteries which basically deliver direct current (DC) or direct-currentvoltage to the load. However, most commercial devices need an alternating current (AC) voltage. Therefore, the power-conditioning elements, which are commonly called inverters because they invert the polarity of the source in the rhythm of the AC frequency, are often applied in PV systems. Also in grid-connected systems inverters are basically necessary for the conversion of DC power into grid-compatible AC power.

Since production cost of PV electricity is several times higher than conventional electric energy, conversion efficiency becomes predominant for the economics of the total PV system. Consequently, extremely high efficiency not only in the nominal power range but also

under partial load condition is a requirement for PV inverters in grid-connected as well as in stand-alone systems.

PV-Hybrid system consists mainly of the following components: the PV generator, the inverter, battery, battery inverter and generator. Additionally the system contains a supervisory control unit, which is in charge of the energy management. For the stand alone application, the output waveform of inverters becomes important. The deviation from the ideal sinusoidal voltage is normally described as total harmonic distortion (THD). For high-quality power supply, the THD of the output voltage should be less than 5 percent, which corresponds with the quality of the public grid [8]. A second and very important element for stand-alone applications, the ability to provide and to absorb reactive power, should be mentioned. Typical loads requesting reactive power are electric motors. In some inverter designs handling of reactive power is limited depending on the load type. In this case, the acceptable power factor is defined. The maximum power of the inverter is given in Kilo-Volt-Amperes (kVA) instead of Kilo-Watts (kW). The energy of the reactive power, which is to be absorbed and afterwards re-injected to the load, is normally stored in capacitors of appropriate sizes. Inverter efficiency is generally low at low power level and good (80 -90 percent) at high power levels depending on the inverter type, as shown in Figure 2.15.

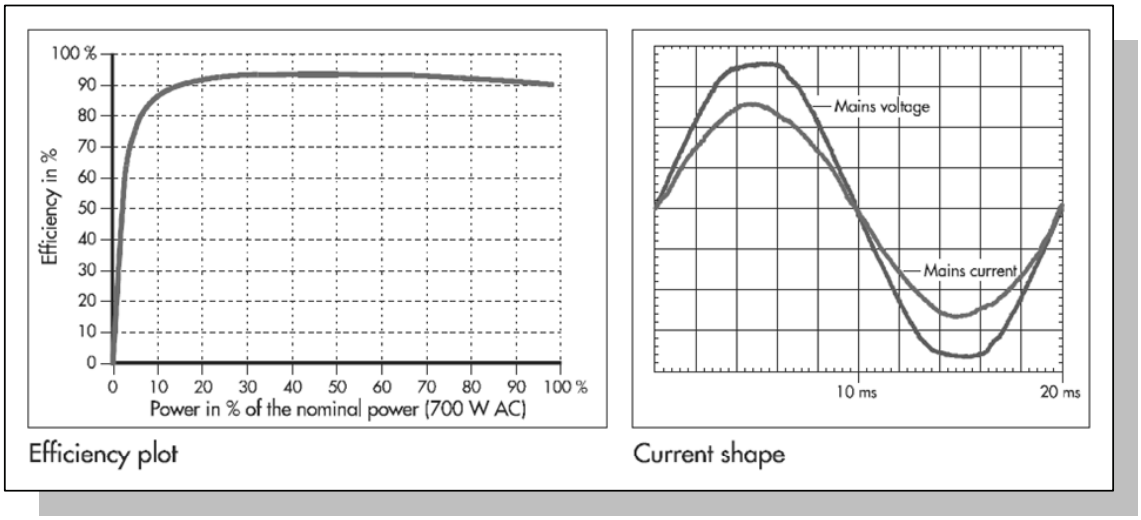

Figure 2.15: Typical efficiency curve and current and voltage from the inverter. Source: SMA,SWR 700

The actual power fed into the grid can be estimated by multiplying the actual power of the PV generator with the actual efficiency of the inverter. Important is the energy produced by the system after a certain period of time, e.g. after one year of operation. In this case the mean efficiency of the inverter taken into account for all load conditions throughout the year becomes important. As a first step, the inverter must allow the PV generator to operate continuously at the maximum power point (MPP) according to the maximum power point tracking (MPPT) as described in section 2.3.3. However, simulation has shown that for grid-connected PV systems constant voltage operation leads to losses of between only 1 and 2 percent when properly adjusted.

2.10.1 Mathematical model for inverters

The PV arrays produce DC power and therefore when the PV system contains an AC load, a DC/AC conversion is required. This is the reason why this section presents the inverter model. The inverter is characterized by a power dependent efficiency (η_{Inv}). The role of the inverter is to keep the voltage on the AC side constant at the rated voltage 230 V and to convert the input power into the output power with the best possible efficiency. The inverter model is [23, 46]:

$$E_{Inv} = E_{Array} \times \eta_{Inv} \tag{2.48}$$

where:

E_{Inv} is the energy output from inverter, kWh
E_{Array} is the energy generated by PV array, kWh
η_{Inv} is the inverter efficiency, $\%$

2.11 Economic model for PV-hybrid systems

The basis of most engineering decisions is economics. Designing and building a device or system that functions properly is only part of the engineer's task. The device or system must, in addition, be economic, which means that the investment must show an adequate return.

The economic model is based on the use of conventional life cycle costing economics. This includes yearly cash flows, the present value of system costs, incomes and levelized annual costs. In addition, the analysis has been designed to allow for a side-by-side comparison of the economics of a hybrid power system with those of a diesel-only powered system and grid extension.

2.11.1 Total capital cost

As detailed below, the cash flow analysis produces year-by-year detailed figures for project incomes and disbursements. The disbursements are separated into the following categories: installed capital costs/annuity payments, fuel costs, operation and maintenance expenses, and equipment replacement costs.

Installed Capital Cost is the initial venture capital for a PV system including equipment costs, installation expenses, tariffs, shipping costs, and possibly the cost of extending a distribution network from the PV power system to the consumer loads. While every effort has been made to identify the major capital costs, the model uses a balance of system term, $C_{Cap,BOS}$, in order to account for any capital costs which are unique to the user's application. Therefore the system installed capital cost, $C_{Cap,tot}$ is given by [46, 50, 51]:

$$\begin{aligned} C_{Cap,tot} = C_{Cap,PV} + C_{Cap,Inv} + C_{Cap,Diesel} + C_{Cap,Batt} \\ + C_{Cap,BOS} + C_{Cap,Inst} + C_{Cap,Oth} \end{aligned} \tag{2.49}$$

where:

$$C_{Cap,Inst} = C_{Ist,PV} + C_{Inst,Batt} + C_{Inst,Inv} + C_{Inst,BattInv} + C_{Inst,Diesel} \tag{2.50}$$

$$C_{Cap,Inv} = C_{Cap,Inv} + C_{Cap,BattInv} + C_{Cap,Chg} \tag{2.51}$$

$$C_{Cap,Oth} = C_{Ship} + C_{Oth} \tag{2.52}$$

where

$C_{Cap,tot}$ is the total capital cost of the system, currency
$C_{Cap,PV}$ is the capital cost of PV array, currency
$C_{Cap,Inv}$ is the capital cost of inverter, currency
$C_{Cap,BattInv}$ is the capital cost of battery inverter, currency
$C_{Cap,Chg}$ is the capital cost of charge controller, currency
$C_{Cap,Diesel}$ is the capital cost diesel generator, currency
$C_{Cap,Batt}$ is the capital cost of battery storage, currency
$C_{Cap,BOS}$ is the capital cost of BOS system, currency
$C_{Cap,Inst}$ is the installation cost, currency
$C_{Ist,PV}$ is the installation cost of PV, currency
$C_{Ist,Batt}$ is the installation cost of battery, currency
$C_{Ist,Inv}$ is the installation cost of inverter, currency
$C_{Ist,Diesel}$ is the installation cost of diesel generator, currency
$C_{Cap,Oth}$ is the capital cost of other, currency
C_{Ship} is the shipping cost, currency
C_{Oth} is the other costs, currency

2.11.2 Annual cost

These consist of regular maintenance costs, fuel cost (diesel generator) over the years. The actual data of annual maintenance and fuel cost on systems installed is difference for each location. Therefore the system annual cost, $C_{ann,tot}$ is given by [46, 51]:

$$C_{ann,tot} = C_{ann,PV} + C_{ann,Batt} + C_{ann,Inv} + C_{ann,Diesel} + C_{ann,Sys} + C_{ann,Fuel} + C_{ann,Oth} \quad (2.53)$$

where

$$C_{ann,Fuel} = C_{Fuel/L} \times FuelConsumption \times Hr_{Diesel} \quad (2.54)$$

$$C_{ann,Inv} = C_{ann,Inv} + C_{ann,BattInv} + C_{ann,Chg} \quad (2.55)$$

where

$C_{ann,tot}$ is the total annual cost of the system
$C_{ann,PV}$ is the annual cost of PV
$C_{ann,Batt}$ is the annual cost of Battery
$C_{ann,BattInv}$ is the annual cost of battery inverter
$C_{ann,Chg}$ is the annual cost of charge controller
$C_{ann,Inv}$ is the annual cost of inverter
$C_{ann,Diesel}$ is the annual cost of diesel
$C_{ann,Sys}$ is the annual cost of system
$C_{ann,Fuel}$ is the annual cost of fuel
$C_{Fuel/L}$ is the cost of fuel per liter
$FuelConsump$ is the diesel engine fuel consumption rate
Hr_{Diesel} is the hour operation of the diesel generator

2.11.3 Replacement cost

Replacement costs are slightly more complex in that they involve regular cash payments but are not truly annual. The main components of the system have to replace during the life time of the system. In order to convert replacements costs into annual ones therefore the replacement annual cost (C_{Repl}) equation is given by [46, 51]:

$$C_{Repl,Diesel} = C_{OH} \times (PWF, i, n) \tag{2.56}$$
$$C_{Repl,Batt} = C_{Batt} \times (PWF, i, n) \tag{2.57}$$
$$C_{Repl,Inv} = (C_{Inv} + C_{BattInv} + C_{Chg}) \times (PWF, i, n) \tag{2.58}$$
$$C_{Repl,Oth} = C_{Oth} \times (PWF, i, n) \tag{2.59}$$
$$\tag{2.60}$$

where

$C_{Repl,Diesel}$	is the yearly replacement cost of diesel generator
C_{OH}	is the overhaul cost of diesel generator
$C_{Repl,Batt}$	is the yearly replacement cost of battery
C_{Batt}	is the replacement cost of battery
$C_{Repl,Inv}$	is the yearly replacement cost of inverter
C_{Inv}	is the replacement cost of inverter
$C_{BattInv}$	is the replacement cost of battery inverter
C_{Chg}	is the replacement cost of charge controller
$C_{Repl,Oth}$	is the yearly replacement cost of ohters
C_{Oth}	is the replacement cost of ohters

and

$$PWF = F \cdot \left[\frac{1}{(1+i)^n}\right] \tag{2.61}$$
$$i = \frac{i_f - f}{1+f} \tag{2.62}$$

where

PWF	is the present-worth factor,
F	is the future money, $Currency$,
n	is the component lifetime, $Year$,
i	is the actual interest rate, $\%$ per year,
i_f	is the interest rate, $\%$ per year
f	is the inflation rate, $\%$ per year.

2.11.4 Present value of the annualized cost and salvage value

The series-present-worth factor (SPWF) translates the value of a series of uniform amounts C into the present worth. The present worth of the series can be found by applying the PWF to each of the C amounts given by [46, 51]:

$$C_{ann,PW} = (C_{ann,tot} \times (SPWF, i, n)) \tag{2.63}$$
$$SPWF = A \cdot \left[\frac{(1+i)^n - 1}{i\,(1+i)^n}\right] \tag{2.64}$$
$$C_{Sal,PW} = C_{Sal} \times (PWF, i, n) \tag{2.65}$$

where

$C_{ann,PW}$ is the annual present worth value
$C_{ann,tot}$ is the total annual value
A is the annual money (Currency)
n is the system lifetime (Years)
$C_{Sal,PW}$ is the salvage present worth value
C_{sal} is the salvage value

2.11.5 Life cycle cost (LCC)

The methodology used to define the LCC is a multi-step process, as presented above. This process requires sets of data from fielded systems and the development of a sophisticated database tool for analysis of the data. LCC determine which power supply systems can be cost-competitive with other energy options [46, 51], as shown in eq. 2.66

$$LCC = C_{Cap,tot} + C_{ann,PW} + C_{Repl,PW} + C_{Sal,PW} \tag{2.66}$$

where

$C_{Cap,tot}$ is the total capital cost,
$C_{ann,PW}$ is the annual present worth value,
$C_{Repl,PW}$ is the replacement present worth value
$C_{Sal,PW}$ is the salvage present worth value

2.11.6 Net present value (NPV)

In the economic model, the net present value of the project is determined from summing up the annual cost, replacement cost and the initial capital expenses, as given by [46, 50, 51].

$$NPV = (-C_{Cap,tot}) + C_{ann,PW} + C_{Repl,PW} \tag{2.67}$$

2.11.7 Levelized cost of energy (COE)

Another levelized calculation concerns the cost of energy, COE. The total levelized cost of energy is given by [46, 51]:

$$COE = \frac{LCC}{E_{Prod} \times SysLife} \tag{2.68}$$

where E_{Prod} is energy that system generated in one year (kWh/y) and $SysLife$ is system lifetime (years)

Chapter 3

Demand Side Management in PV-Hybrid Systems

3.1 Definition of demand-side management

Energy demand management is often referred to also as demand side management (DSM). DSM usually implies actions that influence the quantity of energy consumed by users. It can also include actions targeting reduction of peak demand during periods when energy supply systems are constrained. Peak demand management does not necessarily decrease total energy consumption but could be expected to reduce the need for investments in networks and/or power plants [52].

3.2 The history of demand side management in the power sector

The use of DSM in the power sector has evolved significantly over the past 20 years. In the 1970s, during concerns over fossil-fuel shortages and prices, many governments in North America and Europe delivered DSM programs directly to consumers. During the 1980s, power utilities in North America began to design and deliver DSM programs themselves [53]. Early mass-market programs were gradually replaced by more targeted programs designed to defer new generating capacity or manage peak demand. Many state and provincial governments in North America also developed regulatory systems that required an Integrated Resource Planning (IRP) approach to capacity expansion and tariff setting. This required DSM programs to be considered on an equal footing with supply options. The 1980s and early 1990s also saw the development of private sector energy service companies in North America and Europe. In the United States these companies were used to deliver DSM programs for utilities through DSM bidding processes. There are now fewer incentives for utilities to invest in DSM and large energy users have had access to lower priced power supplies. At the same time, however, national governments and multinational banks are recognizing the value of DSM in meeting environmental and development goals. Forty Major DSM initiatives are underway in India, Brazil, Thailand, China, and several other countries, involving both utilities and government agencies. New innovative methods of regulating utilities to make DSM programs that are in the public interest, viable to consumers and utilities are being studied in North America and Europe.

In renewable energy (RE) electrification sector, DSM have a benefit to strengthen the RE system [54]. DSM has been used in areas in which RE electrification system is supplied to the utilities, but there still are problems on the reliability of system during operation. DSM has been used to smooth out the daily peaks and fill valleys in the load curve to make the most efficient use of energy resources [55]. As the characteristic of PV system is to generate electricity only during day time, it is necessary for the RE system to have an energy back up system, such as battery bank, but which carries with it the environmental problems of disposal after use. In small village electrification, there is a variety of loads, whose number rises after the system is installed, and tend to occur over peak period resulting in possible system shutdown. The DSM concept has been applied to RE electrification system in order to reduce the peak energy demand and also to have an arrangement where household appliance operation can to be matched to the high potential production period of electrical energy produced from PV during the day. This could curb the short fall problem. The concept of DSM for this study is described below.

3.3 DSM strategies

The goal of demand-side management is to smooth out the daily peaks and valleys in electric demand to make the most efficient use of energy resources and to defer the need to develop new power plants. This may entail shifting energy use to off-peak hours, reducing energy requirements overall or even increasing demand for energy during off-peak hours. All DSM strategies have the goal of maximizing efficiency to avoid or postpone the construction of new generating plants. There are four basics of DSM strategies as describes below [56, 57].

3.3.1 Peak clipping

The peak clipping is strategy which seeks to reduce energy consumption at the time of the daily peak (about 7 p.m.). DSM programs which reduce peak load are generally performed by the utility or customer controls on appliances such as air conditioning or water heating. Timers for water heaters are a good example of this. Figure 3.1 shows typical diagram of this concept.

3.3.2 Valley filling

The goal of valley filling is to build up off-peak loads in order to smooth out the load and improve the economic efficiency of the utility, as shown in Figure 3.1. An example of valley filling is charging electric vehicles at night when the utility is not required to generate as much power as during the day.

3.3.3 Load shifting

The load shifting is a strategy which could be accomplished through measures such as thermal storage. Thermal energy storage enables a customer to use electricity to make ice or chilled water late at night when overall electricity consumption is low. The ice or chilled

water is then used to cool the building by day when overall electricity consumption is high. The concept of this strategy is shown in Figure 3.1.

3.3.4 Conservation

Conservation is the best known strategy which involves reducing the entire energy load, as shown in Figure 3.1. There are many DSM technologies and measures which are used by utilities to implement the four strategies. These include energy efficient appliances, time-of-use rates, interruptible rates, and many other measures which are currently under study by many DSM research institutes.

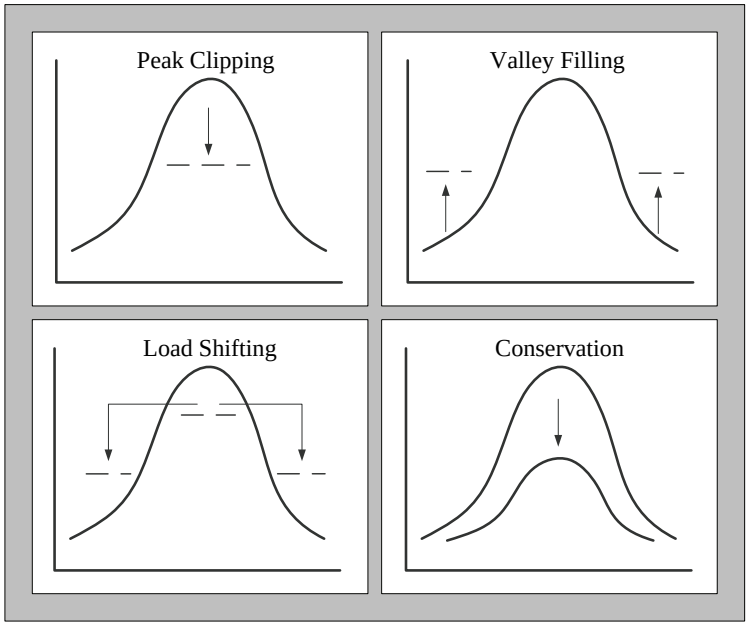

Figure 3.1: Diagram of typical DSM activities

3.4 DSM via the cold storage concept for cooling appliances

In small communities which are electrified by PV-hybrid mini grid systems, an increase in the energy consumption can cause problems in the supply reliability. An increase of the energy consumption causes the PVHS to demand more battery storage, which inturn translates into an increase in the energy price and environmental problems. This work deals with how to apply the DSM concept to small village electrification system. Reference to section 1.1 (page 3), there are several kinds of loads in RE electrification system for the small village. One interesting kind of load in such a system is the cooling appliance which consumes of high electrical energy for cooling down the chamber temperature. Although this kind of appliance is not appropriate for the PV electrification system, it is necessary for the villager for the health care clinic and food preservation purposes.

However, a good efficiency and high energy storage capability of the refrigerator enables the DSM to have a high possibility of application to this kind of cooling appliance. Two types of DSM strategies have been considered for use in this work, i.e. the peak clipping

and the load shifting strategies. The DSM concept is applied to RE electrification system via the cold storage concept. In this concept the refrigerator is turned off for a while during the peak period situation to reduce the high electrical energy consumption in such a duration. This is the so called “peak clipping strategy”. It mean that the condition of how long the refrigerator is to be turned off is already predicted. On the other hand, the refrigerator can be deeply cooled down during on the day, during which there is a lot of electricity from PV, in order to store thermal energy for the night. This working characteristic is called “the load shifting strategy”. Under these DSM activities, information should be obtained to show that the system has higher reliability and higher stability in the supply of electricity to users. Figure 3.2 shows the basic concept of DSM in this study.

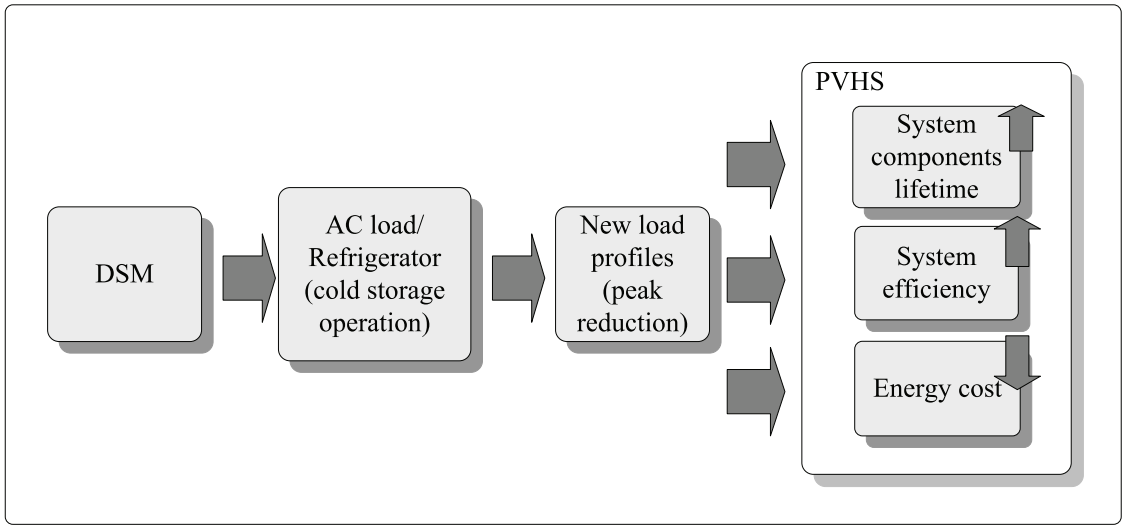

Figure 3.2: Demand side management via the cold storage concept for PV-hybrid system

Chapter 4

Refrigerator Model

In order to simulate the behavior of a cooling appliance under real time operation, the simulation model of a cooling appliance, i.e. a household refrigerator, was developed using the $Labview$ program. This chapter presents the description of refrigerator, the basic concept of heat transfer in the refrigerator and the numerical modeling of the refrigerator. The details are as follows.

4.1 The refrigeration process

The study is focused on the vapor-compression refrigeration process. This process is generally used for refrigeration propose, especially, in the household sector. The general refrigerator components are described below:

4.1.1 Refrigerator components

Usually the refrigerator temperature range is around 0 - 8 °C, when cabinet temperature is increased due to the heat transferred through refrigerator walls. Then, the compressor is operated in order to lower the cabinet temperature. Figure 4.1 shows the components of the basic refrigeration system. The operation of refrigerator is related to all components in the refrigerator, which consists of [58]:

- **Compressor** is a device in which work is done on a gas to raise its pressure. Generally there are two types of compressor, i.e. reciprocating compressor and screw compressor. The compressor for this study is screw compressor.
- **Condenser**, in a condenser, heat is removed to condense the vapor into liquid.
- **Evaporator**, Direct expansion evaporator is contained in refrigerator in this study. The purpose of evaporator is to remove heat from inside refrigerator.
- **Expansion device**, is used to reduce the pressure in the refrigeration system.

4.1.2 Vapor-compression refrigeration cycle

In the vapour-compression refrigerator, liquid refrigerators are used which are alternately evaporated and condensed. Using a liquid refrigerant, the Carnot cycle can be closely

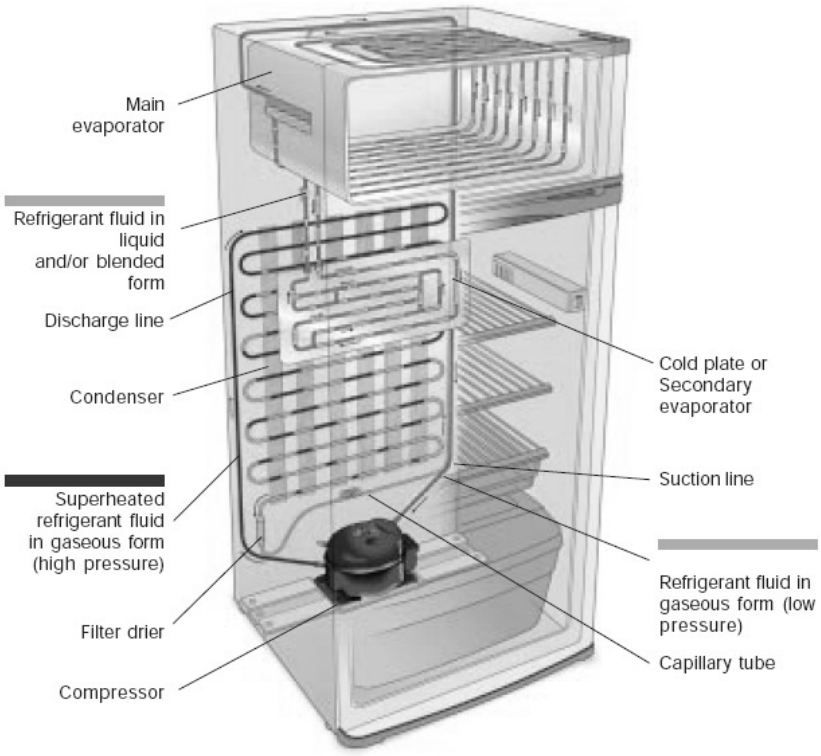

Figure 4.1: Components of basic refrigeration system [59]

approximated. Figure 4.2 shows refrigeration function on a two-phase systems. That during the evaporation of a liquid at constant pressure the temperature remains constant.

A wet low-pressure, low temperature refrigerant enters the evaporator at 4 in which it is evaporated to a nearly dry state at 1. This evaporation process produces the cooling effect. The refrigerant then enters a compressor, in which it is compressed, theoretically isentropically, to 2. As illustrated, the refrigerant would then be dry saturated at a higher pressure and temperature. The refrigerant then passes through a condenser at constant pressure and temperature and is condensed to liquid at 3. The refrigerant then passes through an expander (Throttle Valve) in which it is expanded, theoretically isentropically, back to its original low-pressures, low-temperature, wet state at 4. The throttling process 3-4 moves the cycle away from the Carnot cycle but the refrigerator has now become a more simple and practical arrangement.

In small refrigeration plant, such as in the domestic refrigerator, the evaporator is suspended directly in the cold chamber and the condenser is suspended in the surrounding atmospheric air. Also in small refrigeration plant, the throttling process may be accomplished by using a short length of capillary tubing. This produces a fixed low temperature in the evaporator. The control of the cold chamber temperature is obtained by using a thermostat in the cold chamber. When the required temperature is reached in the cold chamber, controls connected to the thermostat switch off the motor driving the compressor. The temperature in the cold chamber then slowly rises and the thermostat controls then, at the set temperature, switch on the motor and the process is then repeated. If a throttle valve is fitted, then there is a control on the evaporator temperature.

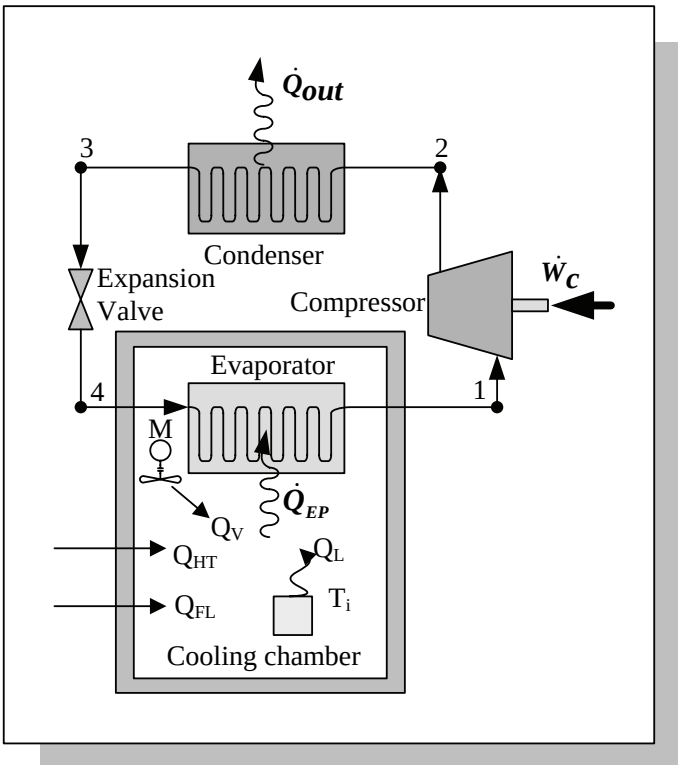

Figure 4.2: Vapor-compression refrigeration system

4.1.3 Energy balance in refrigeration systems

In reference to Figure 4.1, the temperature in the cooling chamber is increases with time. Factors contributing to the rise in the refrigerator temperature are the heat from product storage inside, the heat transfer at the wall, the heat transfer when the door is opened and the heat generated from ventilator in the chamber. When the temperature in cooling chamber raises to the set point of the thermostat, the compressor operates in order to cool down the chamber temperature. In this case, the heat is removed from the chamber via the heat exchanger, also called the "evaporator". The relationship between the energy input to the refrigeration cycle and the heat removal from the cooling chamber can described by the first law of thermodynamics, as shown in equation 4.1.

$$\oint W = \oint Q \tag{4.1}$$

or, $Nett\ work = Heat\ received - Heat\ rejected$. Then, the energy balance of the system as shown in Fig. 4.2 can be expressed as in equation 4.2.

$$Q_{out} = Q_{EP} + W \tag{4.2}$$

Where W is the net mechanical work of motor applied to the compressor. The ratio of transferred heat Q_{EP} to the needed work W in the motor is defined as the coefficient of performance (COP) in equation 4.3:

$$COP = \frac{Q_{EP}}{W} = \frac{T_i}{T_o - T_i} \tag{4.3}$$

And the electrical power supply to the compressor motor is defined as:

$$W = \eta M \cdot P_{el} \tag{4.4}$$

The efficiency of the electrical motor ηM can be considered between 0.75 and 0.85 [60]. Then equation 4.3 is rearranged as:

$$Q_{EP} = \eta M \cdot P_{el} \cdot \frac{T_i}{T_0 - T_i} \tag{4.5}$$

when the cooling chamber is considered as a system, heat stored in cooling chamber (Q_{in}) is defined as:

$$Q_{in} = Q_L + Q_{HT} + Q_{FL} + Q_V - Q_{EP} \tag{4.6}$$

where

Q_L	is the heat generated by the product stored, kW
Q_{HT}	is the heat transfer from the chambers wall, kW
Q_{FL}	is the heat transfer from the air when open the door, kW
Q_V	is the heat generated from the ventilator, kW
Q_{EP}	is the electrical power supply to motor, kW

4.2 The heat transfer concept

The operation of the cooling appliance does not stay in a steady state as ambient conditions and other conditions in the cooling appliance constantly change. In order to account for the transient behavior, the heat transfer and energy storage in the walls in each of the sides of the cooling appliance have to be modeled. This section describes the finite difference heat transfer model for the unsteady state conditions, as it does the conditions of the refrigerator operation.

4.2.1 Heat transfer in composite walls

The cooling appliances wall usually is a composite wall. Figure 4.3 shows the cross section of a commonly used composite wall. In practice, there are the temperature differences between a surfaces and its surroundings. Therefore, the heat transfer in the composite wall can include conduction, radiation and convection.

The quantity of heat transfer into refrigerator is depended on the difference between the internal ambient temperature and the external ambient temperature, the thickness of the wall layers, the thermal properties of the wall materials and the convection heat transfer coefficient of fluid in the internal and external surroundings. The heat transfer in the wall is unsteady state conduction because the ambient temperatures in both sides of the wall are not constant. This results in a non-constant amount of energy storage in the wall. The modeling method used to model the heat transfer in this investigation is the numerical finite-difference method.

4.2.2 The numerical finite-difference model

The finite-difference model divides the wall into nodes and the temporal heat transfer process is divided into discrete time steps. As mention that the heat transfer process in refrigerator or other types of cooling appliances is the unsteady state type and that it depends only on the distance in one direction. The mathematical model described here is only for two

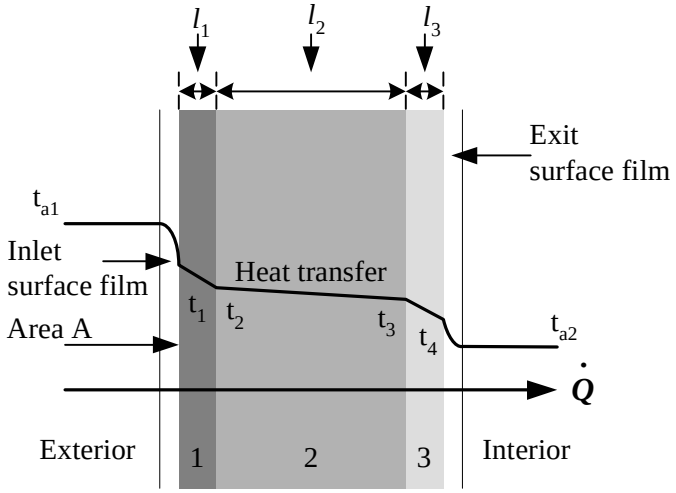

Figure 4.3: Heat transfer in composite walls

dimensions, i.e. (t, x), and the walls have no heat generated inside ($\dot{q} = 0$). The energy balance is performed for every node to calculate the node temperatures and heat flow at every time step. The energy balance for interior and exterior nodes are described below.

4.2.3 Energy balance for interior nodes

An energy balance equation gained from an explicit method is called "forward difference energy transfer equation" for the interior nodes. Figure 4.4 shows the change of an internal energy of node m per time step, in x direction. Energy transfer must equal to the heat flow into node m, from nodes $m - 1$ and $m + 1$. Equation 4.7 shows the energy balance for a node between two other interior nodes.

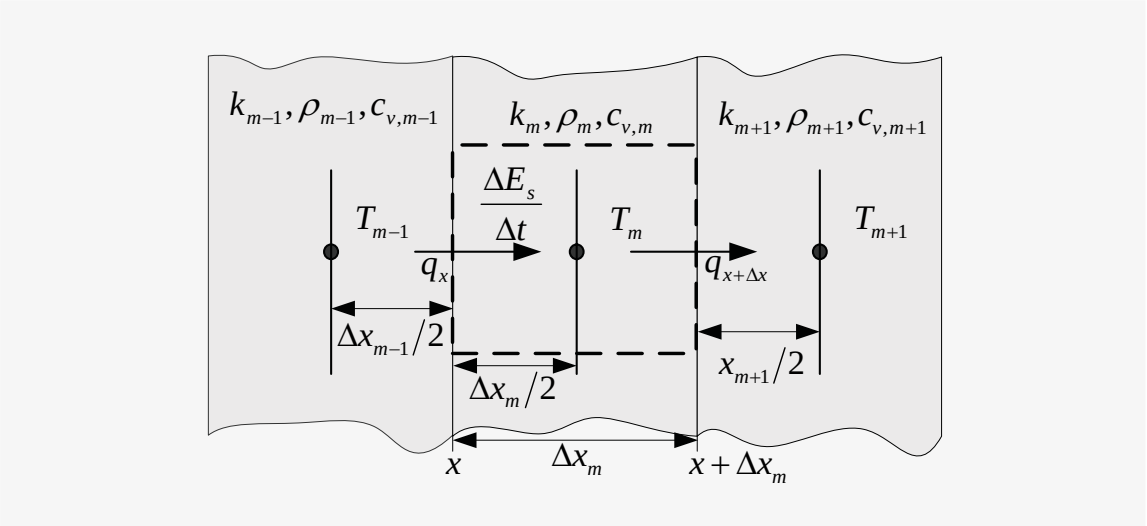

Figure 4.4: Finite difference model for interior nodes

$$q_x = q_{x+\Delta x} + \frac{\Delta E_s}{\Delta t} \tag{4.7}$$

or, when the walls have the same properties and $\Delta x_m = \Delta x_{m+1} = \Delta x_{m-1}$, then equation

4.7 is rearranged as:

$$-kA\frac{T_m^\tau - T_{m-1}^\tau}{\Delta x} = -kA\frac{T_{m+1}^\tau - T_m^\tau}{\Delta x} + \rho A\,\Delta x\,c_v\frac{T_m^{\tau+1} - T_m^\tau}{\Delta t} \tag{4.8}$$

The solution for $T_m^{\tau+1}$ is:

$$T_m^{\tau+1} = \frac{\alpha\Delta t}{\Delta x^2}\left(T_{m-1}^\tau + T_{m+1}^\tau\right) + \left(1 - 2\frac{\alpha\Delta t}{\Delta x^2}\right)T^\tau m \tag{4.9}$$

where $\alpha = k/\rho c_v$. To maintain stability, the coefficients associated with the T_m^τ term for each nodal equation must be equal to or greater than zero. Therefore:

$$1 - 2\frac{\alpha\Delta t}{\Delta x^2} \geq 0 \quad or \quad \frac{\alpha\Delta t}{\Delta x^2} \leq \frac{1}{2}$$

Setting $\alpha\Delta t/\Delta x^2 = \frac{1}{2}$, Eq. 4.9 becomes:

$$T_m^{\tau+1} = \frac{1}{2}\left(T_{m+1}^\tau + T_{m-1}^\tau\right) \tag{4.10}$$

and Δt is given by

$$\Delta t = \frac{1}{2}\frac{\Delta x^2}{\alpha} \tag{4.11}$$

4.2.4 Energy balance for exterior nodes

The nodes of each exterior sub-volume lie on the system boundary, these exterior sub-volumes are smaller in size than the interior sub-volumes. Refer to the exterior node $m = M$ as shown in Fig. 4.5, the heat transfer equation for this case is:

$$q_x = q_s + \frac{\Delta E_s}{\Delta t} \tag{4.12}$$

or

$$-k_M A\frac{T_M^\tau - T_{M-1}^\tau}{\Delta x} = h_i A\left(T_M^\tau - T_a^\tau\right) + \frac{\rho_M A\Delta x c_{v,M}}{2}\left(\frac{T_M^{\tau+1} - T_M^\tau}{\Delta t}\right) \tag{4.13}$$

where $q_s = h(T_M^\tau - T_a^\tau)$ is a term of convection heat transfer and h is the convection heat transfer coefficient. For the cooling appliance analysis such as in this research, T_a = T_i at $m = M$ and T_a = T_0 at $m = 1$. If $m = M$, the solution for $T_M^{\tau+1}$ in this case is:

$$T_M^{\tau+1} = \left[1 - \frac{2\alpha_M\Delta t}{\Delta x^2} + B_{i,i}\right]T_M^\tau + \left(\frac{2\alpha_M\Delta t}{\Delta x^2}T_{M-1}^\tau\right) - B_{i,i}T_i^\tau \tag{4.14}$$

If $m = 1$, the solution for $T_{m,m=1}^{\tau+1}$ is:

$$T_{m,m=1}^{\tau+1} = \left[1 + \frac{2\alpha_m\Delta t}{\Delta x^2} + B_{i,o}\right]T_m^\tau - \left(\frac{2\alpha_m\Delta t}{\Delta x^2}T_{m+1}^\tau\right) - B_{i,o}T_o^\tau \tag{4.15}$$

where, $B_i = Biot\ number = h\Delta x/k$.

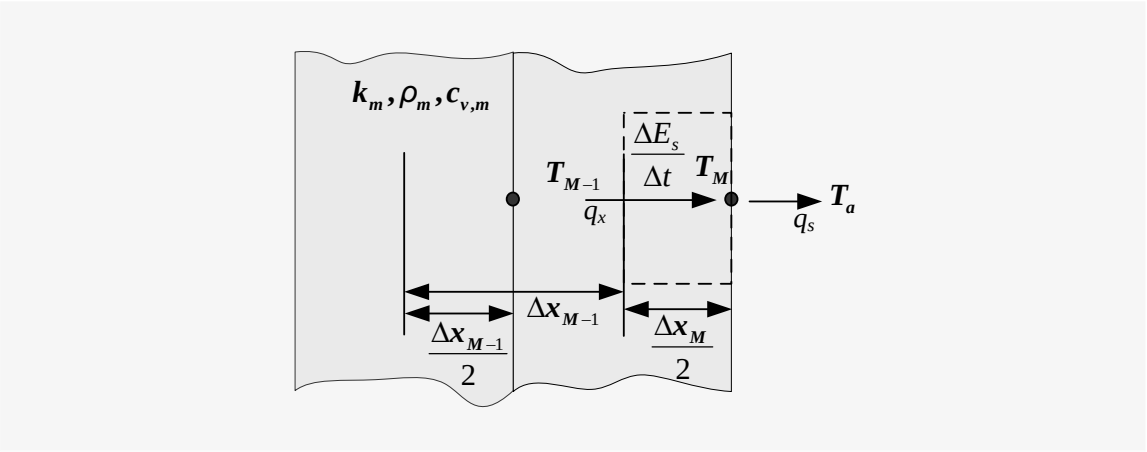

Figure 4.5: Finite difference model for exterior nodes

4.2.5 Predicted heat transfer from the surface

In order to determine the rate of heat transfer from the surface $x = M$ at time t, equation 4.13 has been modified. The solution for the surface heat transfer is:

$$q_s = h_i A \left(T_M^\tau - T_i^\tau\right) = -k_M A \frac{T_M^\tau - T_{M-1}^\tau}{\Delta x} - \rho_M A \frac{\Delta x}{2} c_{v,M} \left(\frac{T_M^{\tau+1} - T_M^\tau}{\Delta t}\right) \tag{4.16}$$

4.3 The refrigerator model

The product modeling of the refrigerator is related to the heat transfer in and out of the refrigerator, as well as to the characteristics of each component in therefrigerator. This section describes the product modeling of the refrigerator. The behavior of heat transfer in the refrigerator is described in this section. The finite element method has been used to analyze the heat transfer in the refrigerator. The working characteristics of each component have been studied and combined in the model in order to realize the operation of refrigerator. The derived refrigerator model has been combined with the refrigeration model, which related the terms of electrical energy input to refrigeration system, and the heat transfer model, i.e. the mechanism of increasing of temperature in the chamber. The model shows how to combine the effect of heat introduced in the chamber due to effects of many factors, both inside and outside refrigerator, also the amount of electrical energy input, which isneed for the compressor in order to bring down the temperature to the desired level, as shown in Eq. 4.6:

$$Q_{in} = Q_L + Q_{HT} + Q_{FL} + Q_V - Q_{EP}$$

To analyse heat loss from the product, the lumped capacitance method has been applied to this case [61]. Then, the equation of Q_L is defined as:

$$Q_L = -hA_p \left(T_P^\tau - T_i^\tau\right) = m_p c_p \frac{T_p^{\tau+1} - T_p^\tau}{\Delta t} \tag{4.17}$$

or rearranging to obtain the new temperature of product as:

$$T_p^{\tau+1} = exp\left[-\left(\frac{hA_s}{mc_p}\right)\Delta t\right]\left(T_p^{\tau} - T_i^{\tau}\right) + T_i^{\tau} \tag{4.18}$$

where t_s is an observation time interval, T_p is the product temperature. The term of heat transfer from the wall is defined as:

$$Q_{HT} = Q_{s,sides} + Q_{s,front} + Q_{s,back} + Q_{s,top} \tag{4.19}$$

Here, the front and back side are the same sizes, and the outside temperature, T_o, on each side is the same. The details of how to define Q_s are show in equation 4.16. The heat transfer by the air when the door of the chamber is opened is defined as:

$$Q_{FL} = \dot{m}_{FL} \cdot c_{p,FL} \cdot (T_o - T_i) \tag{4.20}$$

where $\dot{m}_{FL}$ and $c_{p,FL}$ are mass flow rate and thermal capacity of air, respectively. If the door is closed, this term of heat will be zero. And, the heat generated from the ventilator inside the chamber is defined as:

$$Q_V = \eta_{v,M} \cdot P_M \tag{4.21}$$

where $\eta_{v,M}$ and P_M are the efficiency of the ventilator motor and the electrical power supply to the ventilator, respectively. The refrigerators tested in the research had no ventilators inside, hence Q_V = 0. In case of Q_{EP}, it has been described in equation 4.5. When the heat in the chamber is increased, the chamber temperature (T_i), is also increased. The new value of T_i is defined as:

$$T_i^{\tau+1} = T_i^{\tau} + \frac{Q_{in} \cdot \Delta t}{m_a \cdot c_{v,a}} \tag{4.22}$$

where m_a and $c_{v,a}$ is mass of air and thermal capacity of air inside chamber, respectively.

4.4 Control of cooling appliances

The conventional control strategy is shown in Fig. 4.6. The compressor is started when the cooling chamber temperature T_i is higher than the allowed maximum temperature $T_{i,max}$ and is switch off when T_i is lower than the minimum temperature $T_{i,min}$.

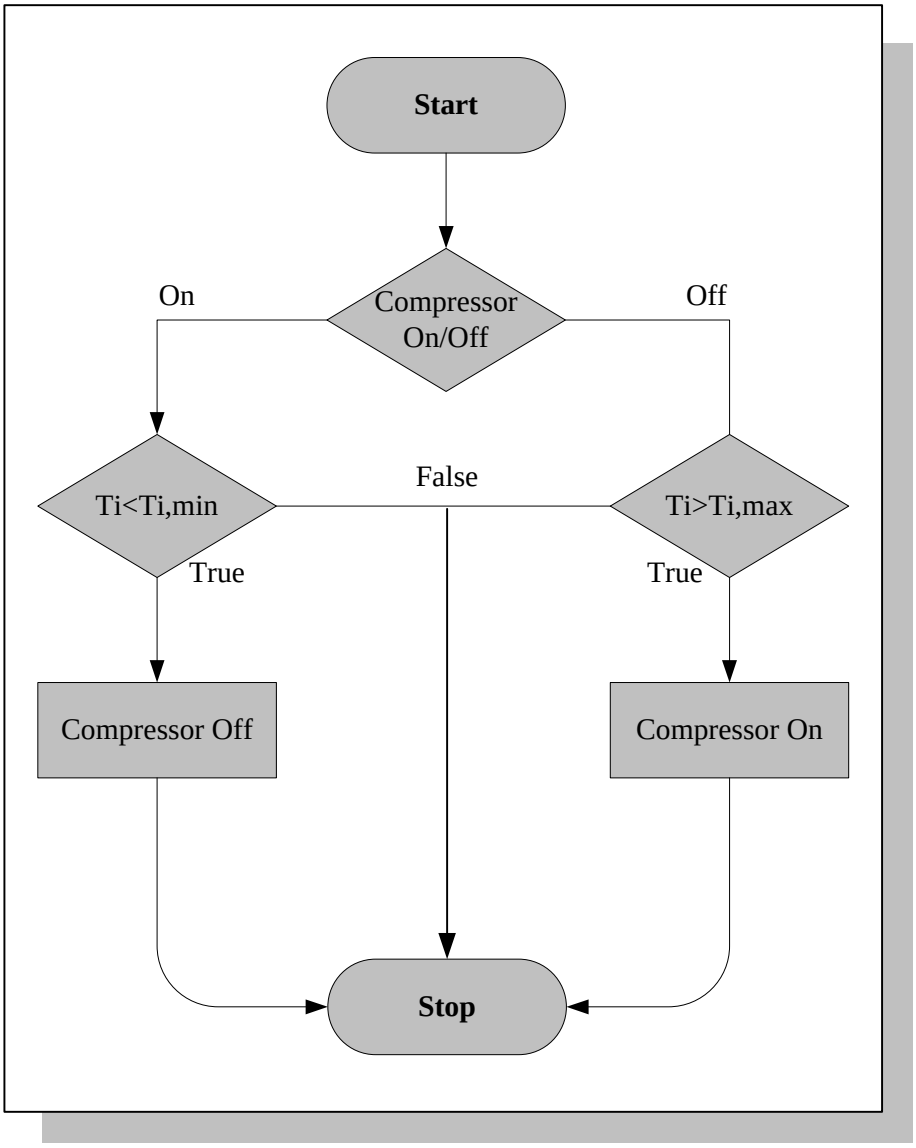

Figure 4.6: Conventional control of the cooling chamber temperature

Chapter 5

Refrigerator Measurement and Simulation Results

This chapter deals with the subject of the implementation of a household refrigerator. The experimental descriptions of refrigerator, which based on the ISO standard, and the experimental results of the cold storage capability of refrigerators are describes below.

5.1 Measurement and implementation of the test-refrigerator

As stated in section 3.4, page 43, the refrigerator offers the ability to do cold storage within itself.This can be exploited to benefit the DSM activity in small village electrification. The duration that it can keep temperatures in the range that the ISO standard specifies for food preservation, after the refrigerator is tuned off, is the subject of research in this part. This section describes the method used to establish the storage capability of a refrigerator that is typically used in the small village. The technical details of the refrigerators used in the experiments are as follows.

5.1.1 General description of refrigerators

The refrigerators which were involved in the laboratory measurements are the compact refrigerator type. It is a common type of refrigerator that has been popularly used in the small villages that electrify by RE systems. Both old and the new refrigerator models were experimented with in the Laboratory at the IEE-RE, University of Kassel. The old refrigerator model is the BBC KT 1403. Its capacity is 140 liters. The refrigerant R12 is used in this refrigerator. The voltage supply is 220 V, 50 Hz. The rated power consumption is 120 W. The new refrigerator model is Privileg Oeko Energiesparer. Its compressor model is HL 60RSA, from the Electrolux Company. The voltage supply of the refrigerator is 220-240 V, 50 Hz. The refrigerant in this refrigerator is R 600a. General descriptions of refrigerators are shown in Table 5.1.

Table 5.1 shows that the height, width and depth of the old refrigerator model is 80, 60 and 55 cm, respectively. The old refrigerator model has a freezing compartment inside. The height, width and depth of the new refrigerator model is 80 cm, 60 cm and 60 cm, respectively. The new refrigerator model has no freezing compartment inside. The difference in

	Old Type	New Type
Capacity (Liters)	140	150
Dimension (w/h/d, Centimeters)	60/80/55	60/80/60
Refrigerant	R134a	R600a
Rated power consumption (Watts)	120	80
Electrical Input	220-240 V/50 Hz.	220-240 V/50 Hz.

Table 5.1: Characteristics of refrigerators applied in tests in the laboratory

size between the new and the old refrigerator model is small. However, the thickness of the walls of both refrigerators is the same.

To simplify the analysis, the thickness as well as the type of materials contained inside each wall are assumed to be the same. The heat transfer at the bottom of refrigerator was assumed to be zero, which meant that there was no heat transferred at the bottom of refrigerator.

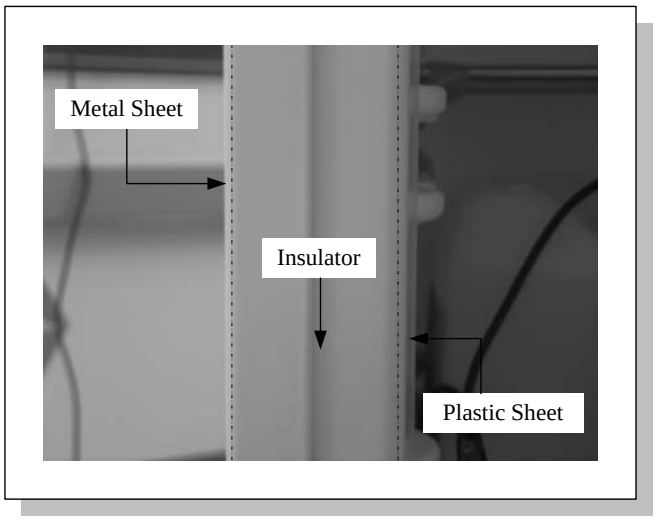

Figure 5.1: Components of the refrigerator wall

Figure 5.1 shows components of refrigerator wall constituting three layers inside the wall. The exterior layer is the steel sheet. The thickness of this layer is 2 mm. The properties of the steel sheet are: k = 54 $W/m \cdot K$, ρ = 8,073 kg/m^3, c_p = 0.435 $kJ/kg\,^oC$ [62]. The middle layer is an insulating board. The thickness is 50 mm. The physical properties of this layer are: k = 0.026 $W/m \cdot K$, ρ = 70.0 kg/m^3, c_p = 1.045 kJ/kg^oC. The interior wall is the plastic sheet. The thickness is 2 mm, and physical properties are: k = 0.04 $W/m \cdot K$, ρ = 16.0 kg/m^3, c_p = 1.210 $kJ/kg\,^oC$ [61].

5.1.2 The experiment conditions

The refrigerators were set up inside a room in which the room temperature can be controlled and kept at desire values. In Figure 5.2 is a picture of this kind of room. The important parameters for the experiment were the ambient temperature, the outside and inside surface temperature of the refrigerator walls, the chamber temperature and the product temperature. Boxes of water which were stored in refrigerator represented the products stored inside refrigerator.

Parameters	ISO
Ambient temperature (^oC)	25
Relative humidity (%)	45-47
Fresh-food temperature (^oC)	0-10
Energy measurement period (hr)	24
Load (kg of water)	8/16/24

Table 5.2: The ISO test parameters for the refrigerator measurements [63]

Figure 5.2: Climate chamber for refrigerator measurements

The product is divided into three samples to realize the operation of refrigerator. In the first case, amount of product inside refrigerator is 8 kg of water. For the second and the third case, amount of product is assigned to be 16 kg and 24 kg of water respectively. Figure 5.3 shows the refrigerator measurement. The temperature sensors were laid down in different positions in the refrigerator to measure the temperature at each point. Table 5.2 shows general descriptions of the test conditions in this study.

5.1.3 The HP 75000 series B data logger

This subsection describes the HP 75000 series B data logger which was used in the measurements herein. Figure 5.4 shows the HP 75000 series B VXI-bus series with a mainframe HP E1301A. The front view of the equipment shows that the front part contains the display screen, keyboard section, which could be used for self-sufficient programming, and the $3\frac{1}{2}$ in. floppy disk drive section, which is not built-in in this equipment.

The measurement technique is shown in Fig. 5.5. The voltage signals from the temperature sensors are sent to the HP E1334A multiplexer, which is connected to a circuit analyzer HP E1326B which functions as a multi-channel scanning multi-meter. For counting of the impulses produced by the electric meters, a counter/totalizer HP E1332A was used.

The Agilent E1332A 4-Channel Counter/Totalizer is a B-size, 1-slot, register-based VXI device. It provides seven counter functions: frequency (up to 4 MHz), period average,

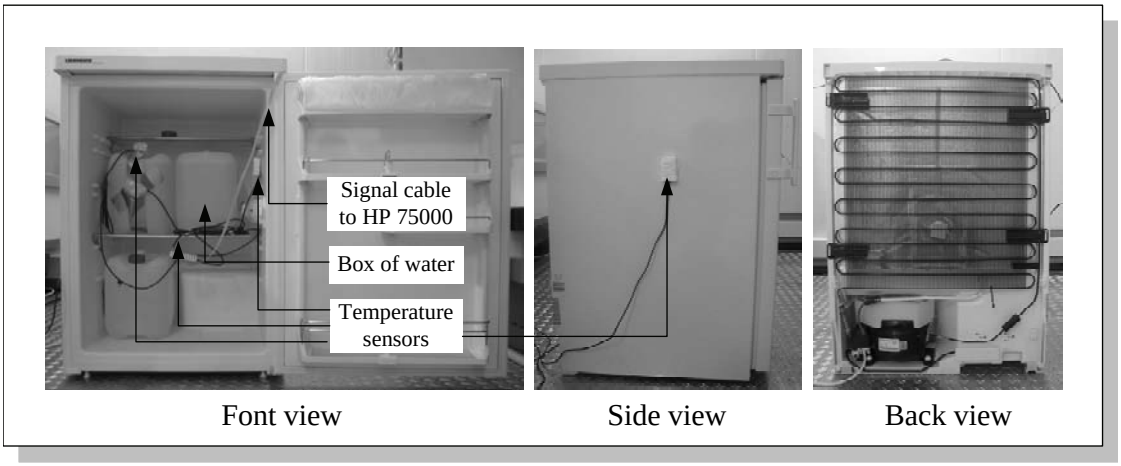

Figure 5.3: Measurement setup of household refrigerator

Figure 5.4: HP 75000 data logger

pulse width, time interval, totalize, gated totalize, and up/down count. In the measurement, the signals were transferred to the LabView program in a personal computer via the interface card PCI-GPIB IEEE-488.2. With this card, the user could do an instrument control and data acquisition with the data logger HP 7500 B. This card could connect up to 14 instruments using standard IEEE-488 cables such as the C488-2M interface cable. Version 6.2 of LabView program is a commercial program like C, Basic and Pascal. But it has a special purpose for scientific applications in laboratories. LabView program is not a text-based language, but is based on graphics. Graphic symbols are used in the programming processes. This language is called G. This program was interfaced with the HP E1031A to transfer data to the PC.

5.1.4 Refrigerator temperature profiles

This subsection presents a general descriptions of the refrigerator temperature curves of the refrigerator that were measured from the start-up point, at which the product temperature is nearly equal to the ambient temperature (25 ^oC). A continuous cooling down was done until the refrigerator temperature was in stability, i.e. temperature near to 0 ^oC. The temperature at the stability state was examined for one day (at least). Then, the refrigerator is turned off,

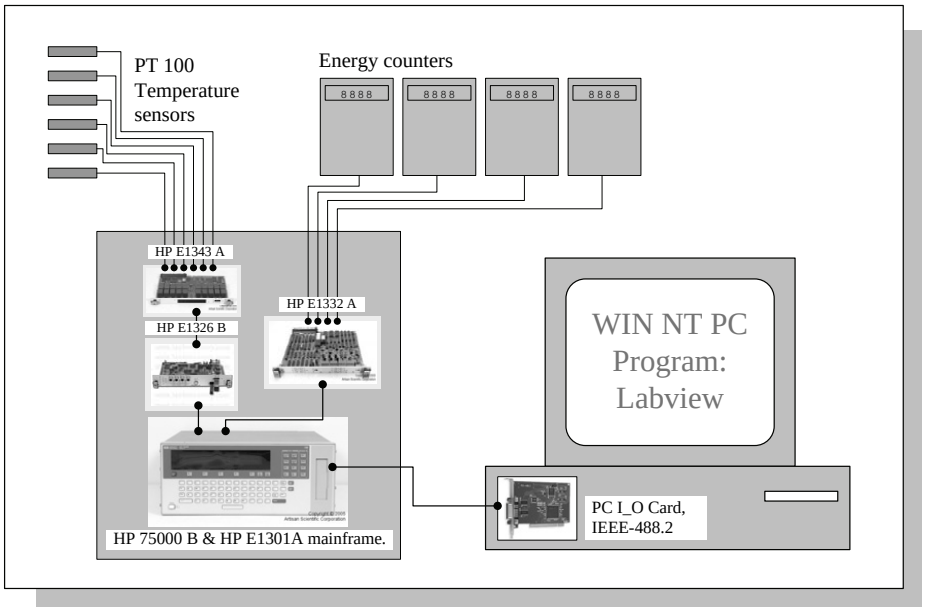

Figure 5.5: Measurement technique by HP 75000 B VXI series data logger

changing it to the heating up process. In the heating up process, the refrigerator temperature was raised up, as well as the goods temperature. The temperature data was measured until it reached 20 ^oC. The measurement results of the old model refrigerator are shown in Figure 5.6.

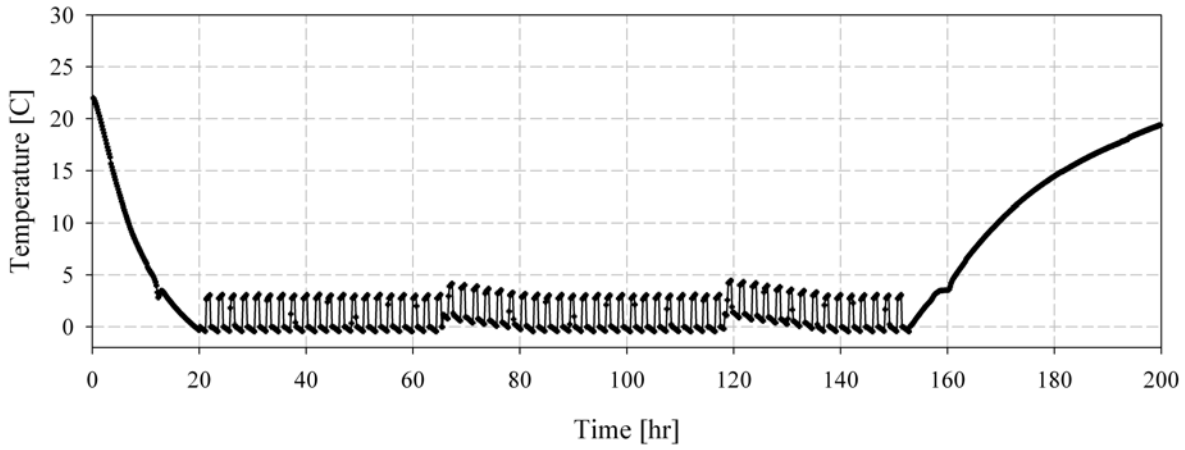

Figure 5.6: Temperature profile of 8 kg of water during one cycle operation at ambient temperature of 25 ^oC

The temperature profile in Fig. 5.6 shows the important sections which were used for the DSM activities in this work. These are the sections during the cooling down and that during the heating up. The in-depth analysis of these two sections is presented as follows.

5.1.5 Cool down method

The objective of the measurement here is to determine the duration that the cabinet temperature takes to cool down from the point at which its temperature has a small difference

with ambient temperature until it is in stabily (around 0 ^oC), and to determine the energy consumption and the compressor duty cycle during that cooling down period.

In first procedure of the test, the refrigerator temperature was set at +25 ^oC (with a load inside), the door opened and the power supply switched off. The second procedure involved closing the door, the refrigerator switched on, with the thermostat at its middle setting point, and left to stabilize. The temperature was recorded every 10 minutes during a 24 hour period. During such a period, the energy consumption was measured and the compressor duty cycle determined. The results are shown in Fig. 5.7. The number of hours that

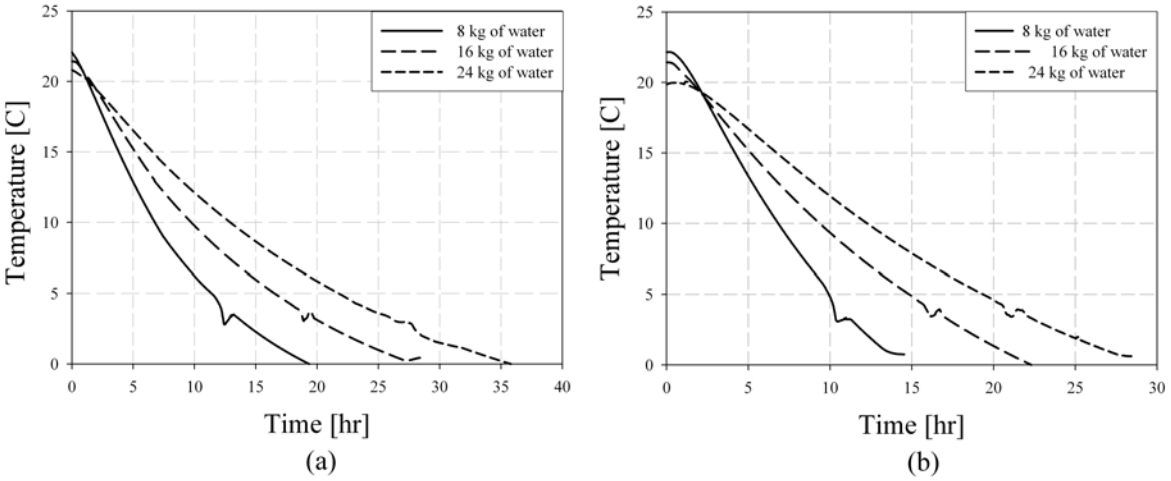

Figure 5.7: Water temperature during cooling down process at the ambient temperature of 25 ^oC: (a) Old type refrigerator (b) New type refrigerator

the refrigerators used during the cooling down of the product to stability (nearly to 0 ^oC) and the amount of electrical energy consumed during the cooling down process of the two refrigerator models are shown in Table 5.3.

	Old refrigerator model	New refrigerator model
Number of hours (hr)		
8 kg of water	19.35	15.10
16 kg of water	28.47	22.28
24 kg of water	35.78	28.66
Energy consumption (kWh)		
8 kg of water	1.65	1.18
16 kg of water	2.25	1.73
24 kg of water	3.17	2.24

Table 5.3: Duration that refrigerators used and the energy consumed during cool down process

5.1.6 Cold storage capability test method

The objective of this test method is to determine of how long refrigerators can maintain the product temperature below $+10^oC$ from the moment the electricity switched off.

In this test method, the refrigerator was allowed to stabilize with a load inside it. The electricity supply was then switched off at the moment the thermostat switched on the compressor. Internal temperature was monitored and recorded every ten minutes. The time recorded for the warmest point to exceed $+10^0C$ is reported. The experimental results are shown in Fig. 5.8.

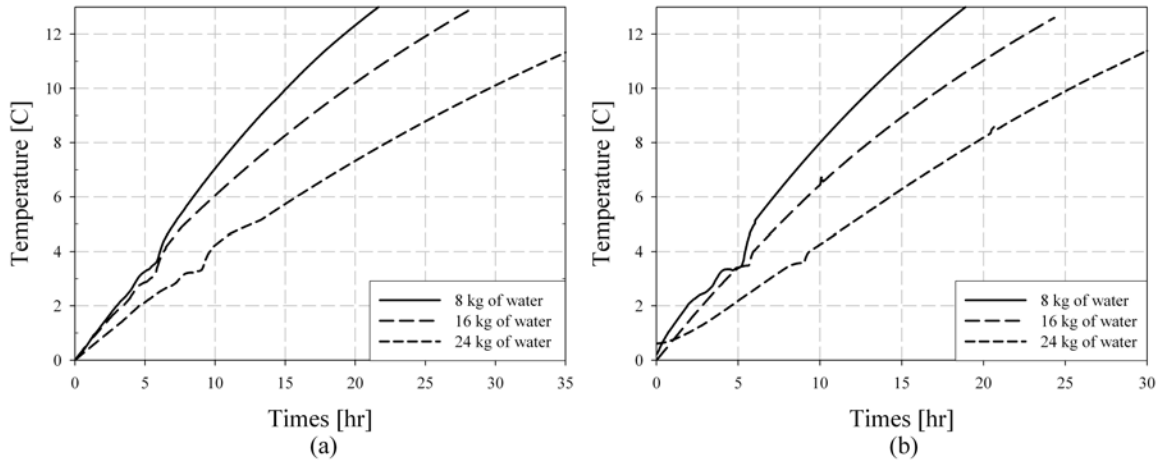

Figure 5.8: Water temperature during heat up process: (a) Old refrigerator model (b) New refrigerator model

	Old refrigerator model	New refrigerator model
Number of hours (hr)		
8 kg of water	15.08	13.20
16 kg of water	19.44	17.44
24 kg of water	29.57	25.33

Table 5.4: Duration that refrigerators used to heat up goods temperature to $+10^oC$

5.2 Refrigerator simulation results

5.2.1 Model outcome

The simulation of the refrigerator behaviour during operation with different amounts of products stored inside refrigerator has been performed. The simulation results during the cooling down process were compared with the measurement data, as shown in Fig. 5.9. Those during the heating up process compared with the measured data as shown in Fig. 5.10.

5.2.2 Simulation accuracy

Figure 5.9 and Figure 5.10 show that the simulated profiles of the goods temperature is very similar to the temperature profiles obtained from measurements. The accuracy of the simulation model for the old refrigerator model is 6.41 percent average error from the real

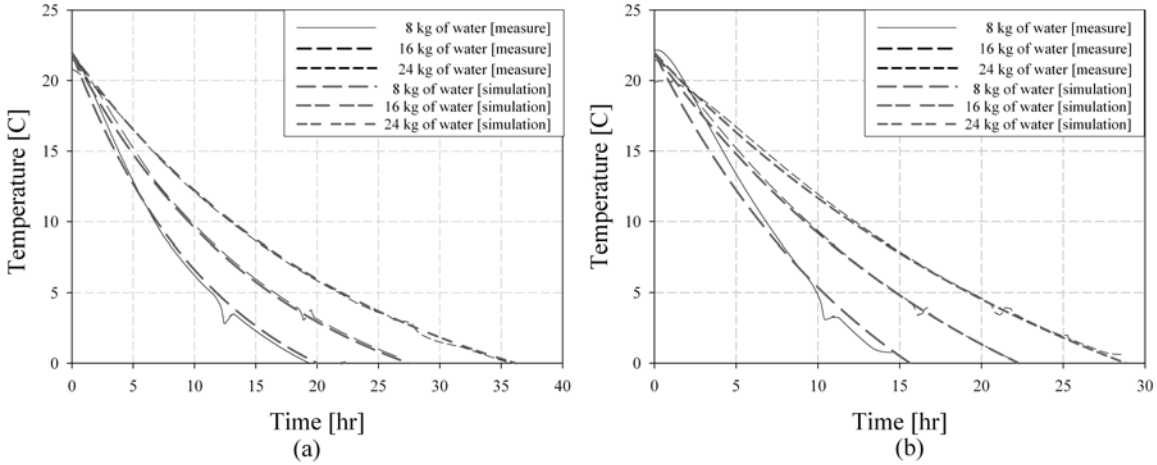

Figure 5.9: Simulation results of goods temperature during a cooling down process compared with the measurement results: (a) Old refrigerator model (b) New refrigerator model

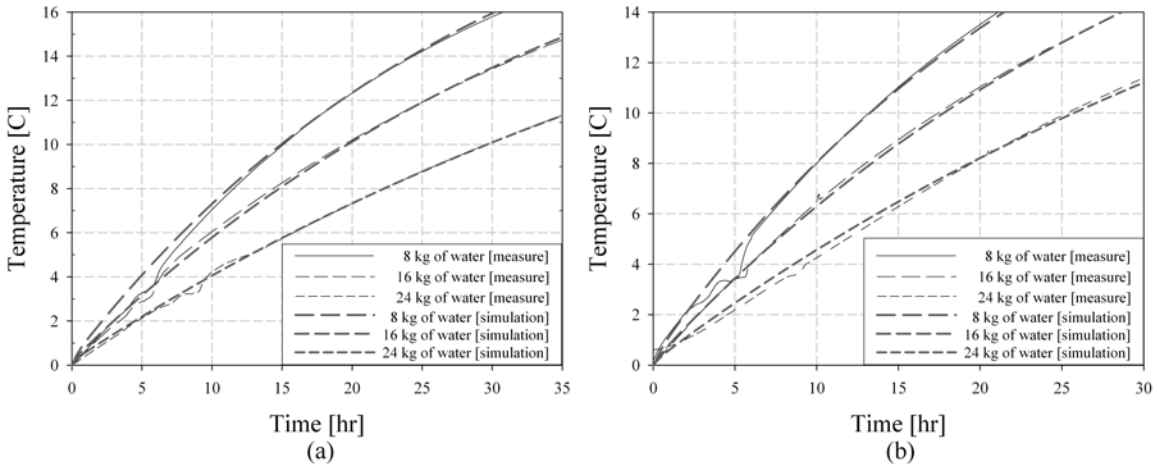

Figure 5.10: Simulation results of goods temperature during a heating up process compare with the measurement results: (a) Old refrigerator model (b) New refrigerator model

measurement. For the new refrigerator model, the error on average is 6.78 percent, as shown in Table 5.5. The error is less than 10 percent, it is in the acceptable range (medium precision) for the simulation modeling [64, 65]. This information confirmed the suitability of the model in estimating the refrigerator temperature profiles for this work.

5.2.3 Storage capability generated by the model

As described in the previous section, the model has a good accuracy in generation of the refrigerator temperature profiles. The model was the used to simulate the temperature profiles of differences sizes of products stored in the refrigerators. In practical use of refrigerators is often found that size of products stored in each household is different. To realize a more accurate model of daily use, variation of the amount of products stored in the refrigerator were provided in this study. Sizes of goods used in the simulation were 5, 10, 15, 20, 25

	Old refrigerator model	New refrigerator model
The error during cool down (%)		
8 kg of water	12.72	18.80
16 kg of water	7.28	2.90
24 kg of water	2.98	6.13
The error during heat up (%)		
8 kg of water	9.77	4.41
16 kg of water	2.61	2.62
24 kg of water	3.27	5.86
Average error (%)	6.41	6.78

Table 5.5: The error of the refrigerator simulation model

and 30 kg respectively. The indoor ambient used for the simulation was the standard ambient temperature of 25 ^oC. The simulation results are shown in Fig 5.11 and Fig. 5.12.

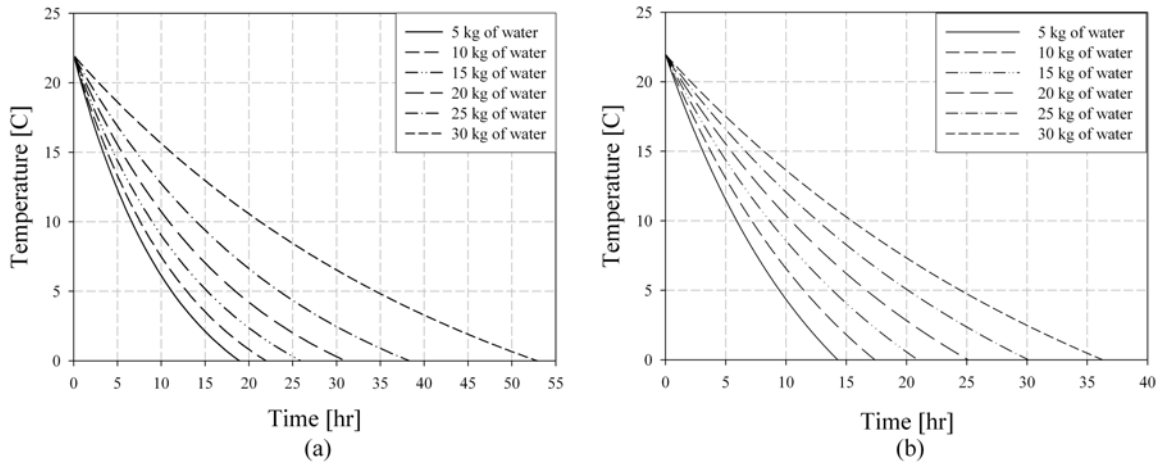

Figure 5.11: Simulation results of product temperature during a cooling down process at an ambient temperature of 25 ^oC: (a) Old refrigerator model (b) New refrigerator model

The experiment found that the time needed for cooling down goods temperature from 22 ^oC to 0 ^oC vary between 18 and 52 hours for the old refrigerator model, and between 14 and 36 hours for the new refrigerator model, as shown in Fig. 5.13 (a). The results are different owing to the product quantity stored in refrigerator in each test case. During the cooling down process, the old refrigerator model consumed electrical energy between 1.50 kWh and 4.22 kWh. In case of the new refrigerator model, the electrical energy between 1.11 kWh and 2.82 kWh was consumed. The energy consumption of refrigerators is in direct variation with size of products, as shown in Fig. 5.13 (b).

To select the most suitable range of goods temperature for both of DSM activity and food preservation purposes, the cabinet temperature during the heating up process were observed in three cases. The first case is when temperature is increased from 0 ^oC to 5 ^oC. The refrigerator can hold the temperature in this range for between 5.46 hours to 17.66 hours. The second case is when the temperature is increased from 0 ^oC to 8 ^oC (WHO standard). The refrigerator can hold the temperature in this range for between 9.64 hours to 31.0 hours. Finally, the third case is when the temperature is increased from 0 ^oC to 10 ^oC. The

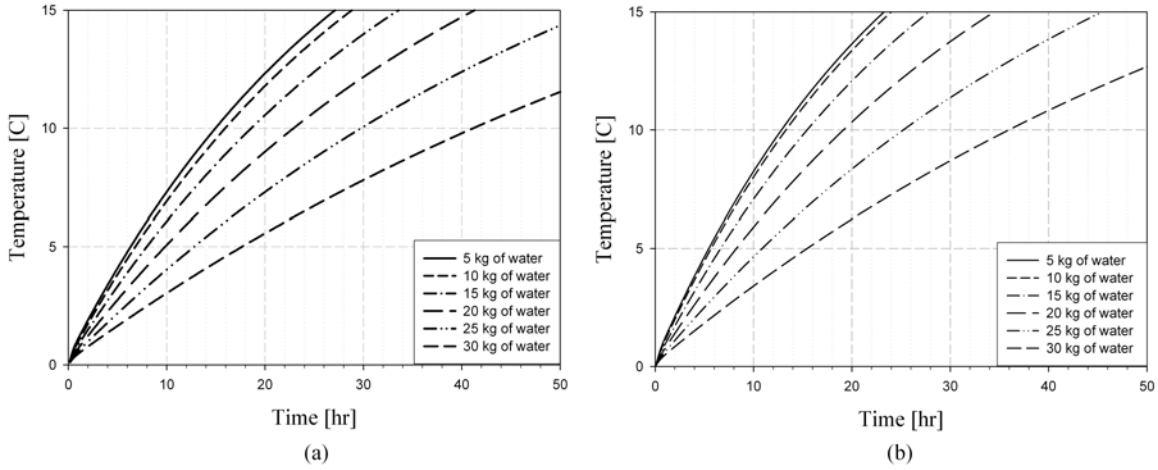

Figure 5.12: Simulation results of product temperature during a heating up process at ambient temperature of 25 ^oC: (a) Old refrigerator model (b) New refrigerator model

refrigerator can hold the temperature in this range for between 12.84 hours to 41.16 hours. The results above show that although temperature in the ranges 0 ^oC to 5 ^oC and 0 ^oC to 8 ^oC are more preferable for food preservation than the third range, the refrigerators give shorter durations to hold temperature within both these ranges. The temperature range of ^oC to 10 ^oC is within the ISO standard for food preservation, and is of more benefit to this study than both ranges above due to its provision of longer storage capability, as shown in Fig. 5.14 (c).

5.3 Cold storage capability of refrigerator for DSM activities

The storage capability information of refrigerator is very important to the concept of DSM activity via the cold storage of the refrigerator. If refrigerators can turned off throughout the night (peak clipping method, section 3.3, page 42), e.g. from 6 pm to 6 am of the next day for the low latitude locations, and operate only in the day time when a lot of surplus energy is produced by the PV generator (load shifting method, section 3.3, page 42) it would provide the most benefit to the reduction of the peak energy demand. The best temperature range for the DSM in this work should provide storage capability in refrigerator for over 12 hours. Figure 5.14 shows that the product temperature in the range 0 ^oC to 10 ^oC could hold for over 12 hours storage time, even though the minimum amount (5 kg of water) is stored inside refrigerator. The case (c) in Fig. 5.14 was therefore selected for the DSM activity.

Figure 5.15 and Figure 5.16 provide the simulated storage capabilities of refrigerators based on different sizes of products stored. The red line in y-axis which intersects temperature profiles demarcate the product temperature at 12 hours. As for the red-line in x-axis, its intersect with the temperature profiles demarcate the time duration that refrigerator can hold the temperature within the range of 0 ^oC to 10 ^oC. The information above shows that the storage capability of refrigerator is dependent on sizes of products stored inside the cabinet. The larger size of product has the advantage of holding longer temperature ranges than the smaller size; however it consumes higher energy during the cool down process.

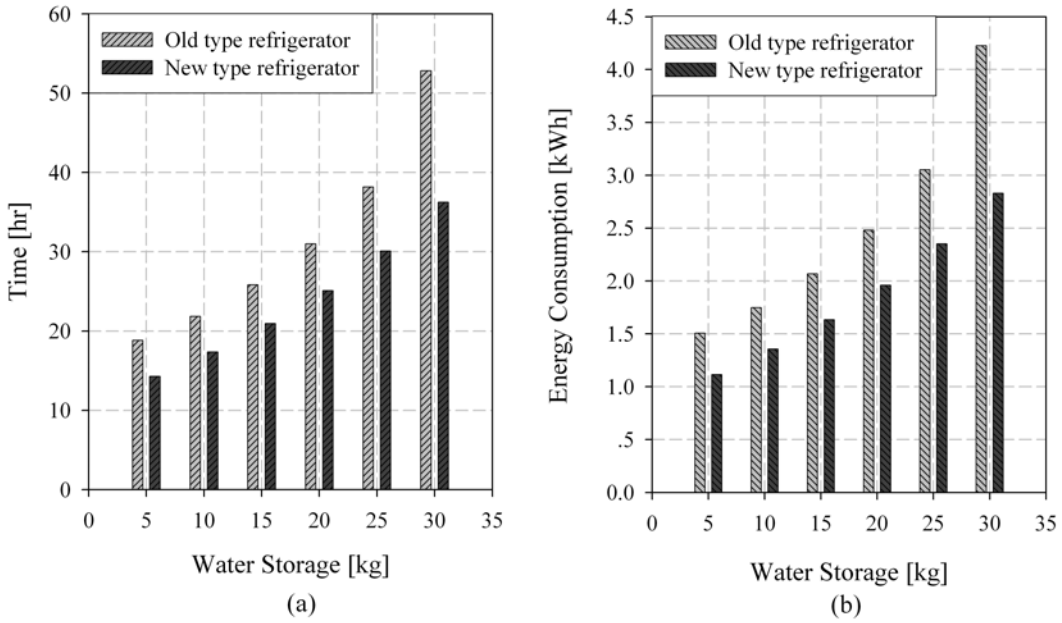

Figure 5.13: Cool down process at ambient temperature of 25 ^oC:(a) Time used for cooling the product from 22 ^oC to 0 ^oC (b) Energy consumed during the cooling process

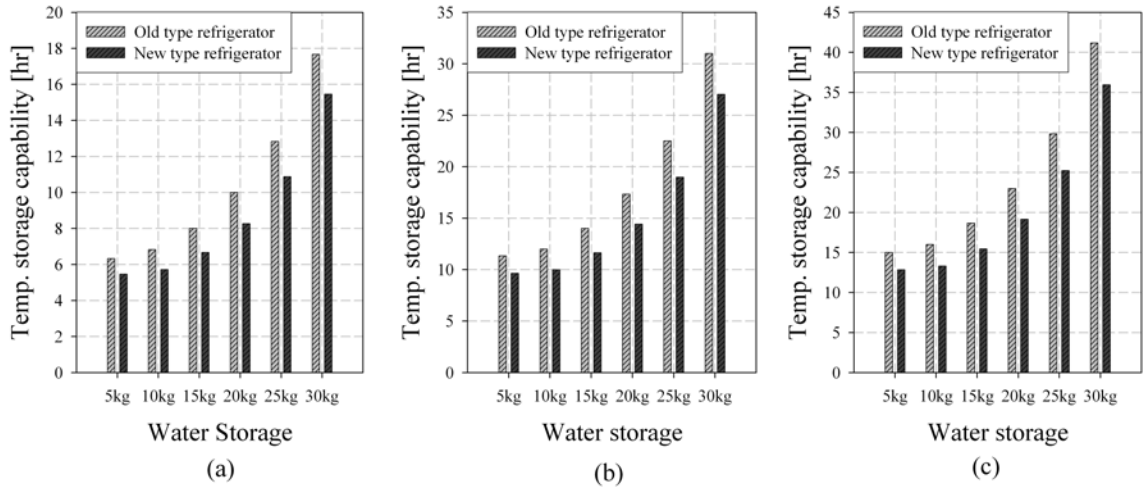

Figure 5.14: Temperature storage capability of refrigerators during the heating up process at ambient temperature of 25 ^oC: (a) from 0 ^oC to 5 ^oC (b) from 0 ^oC to 8 ^oC (c) from 0 ^oC to 10 ^oC

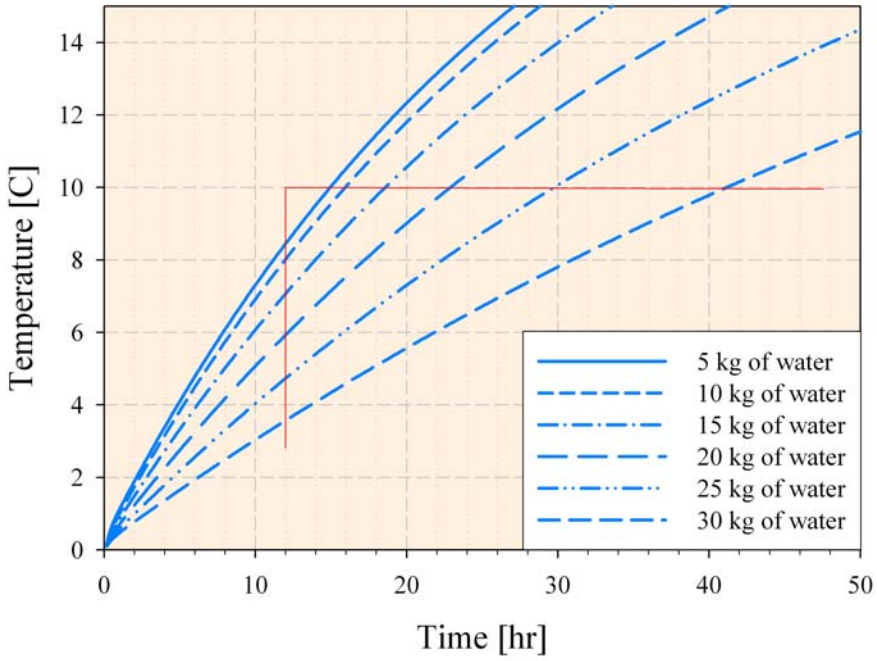

Figure 5.15: Simulation results of goods temperature during a heating up process at ambient temperature of 25 ^oC of old refrigerator model

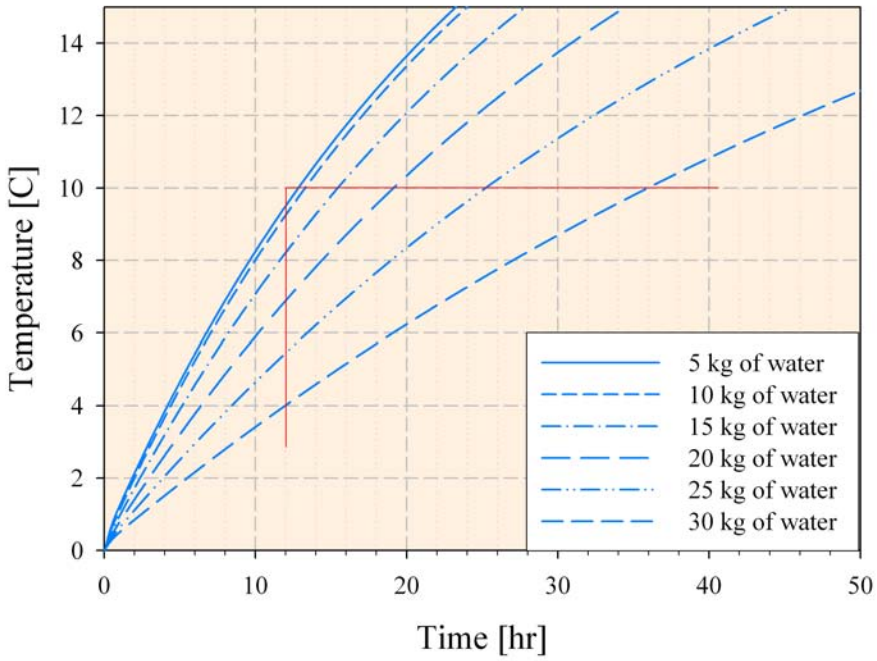

Figure 5.16: Simulation results of goods temperature during a heating up process at ambient temperature of 25 ^oC of new refrigerator model

Fig. 5.17 and Fig 5.18 show the simulated temperature and power profiles of refrigerators based on normal operation as well as during application of the cold storage concept. In the simulation, refrigerators were assigned to be turned off in the period 6 pm to 6 am of the next day, and to operate only in the day time. The load profiles were examined after the refrigerators were in the stability running mode, i.e. the product temperature is close to 0 ^oC. The simulation results show that the load profiles of refrigerators operated under the cold storage concept have changed. The power consumption of refrigerators exist only in the day time, as shown in Fig. 5.17 (b) and Fig. 5.18 (b). This makes the concept suitable for application in the small villages that electrify by PV-Diesel hybrid system, to reduced the evening peak energy demand.

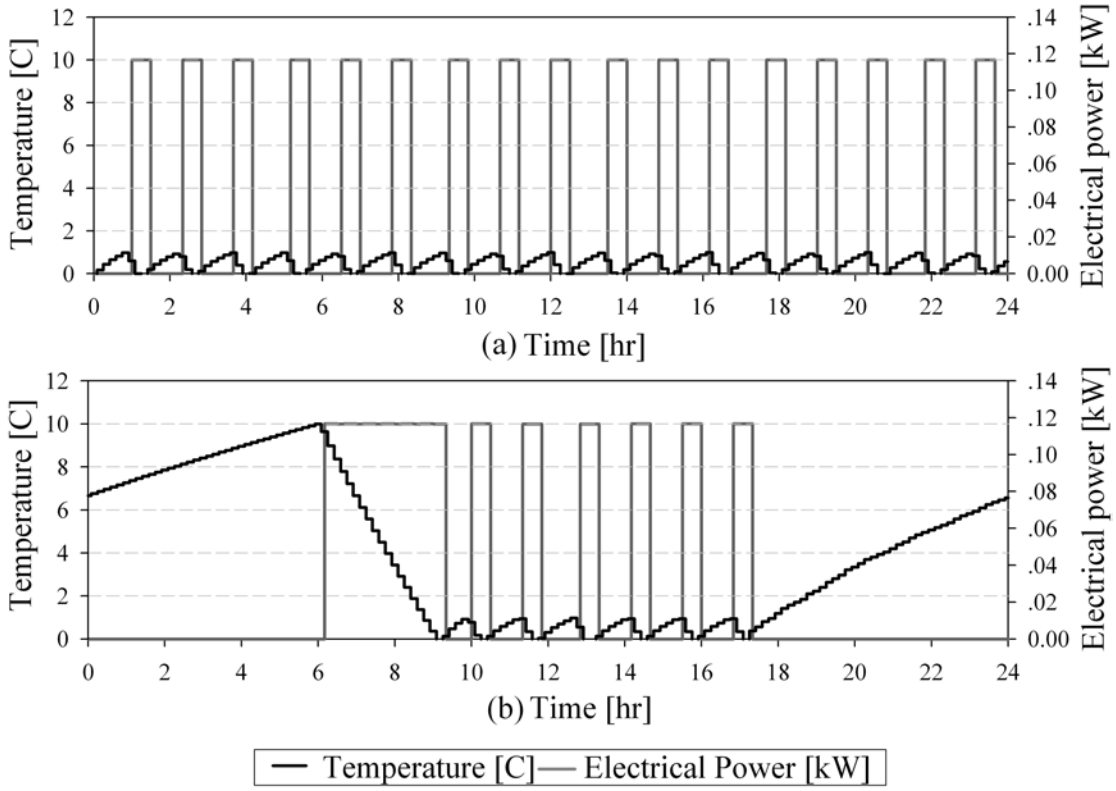

Figure 5.17: Load profiles of the old refrigerator model with 5 kg of water stored inside: (a) Normal operation (without cold storage concept) (b) Operation with cold storage concept

However, Figure 5.17 (b) and Figure 5.18 (b) show that, during the first two hours in the morning, the refrigerators need more energy to cool down the cabinet temperature to stability (0 ^oC) again (The energy supply to refrigerator during this period is described in chapter 6.4.4, page 82). The energy demand per day of the refrigerators is not significantly different either when operated normally or when cold storage concept is applied, as shown in Fig. 5.19.

The information above emphasized that the storage capability of refrigerator could be useful for the DSM activity in the small village electrification by PV-hybrid system. The investigation of DSM via the cold storage concept in the refrigerator, in the small village electrification, is described in the next chapter.

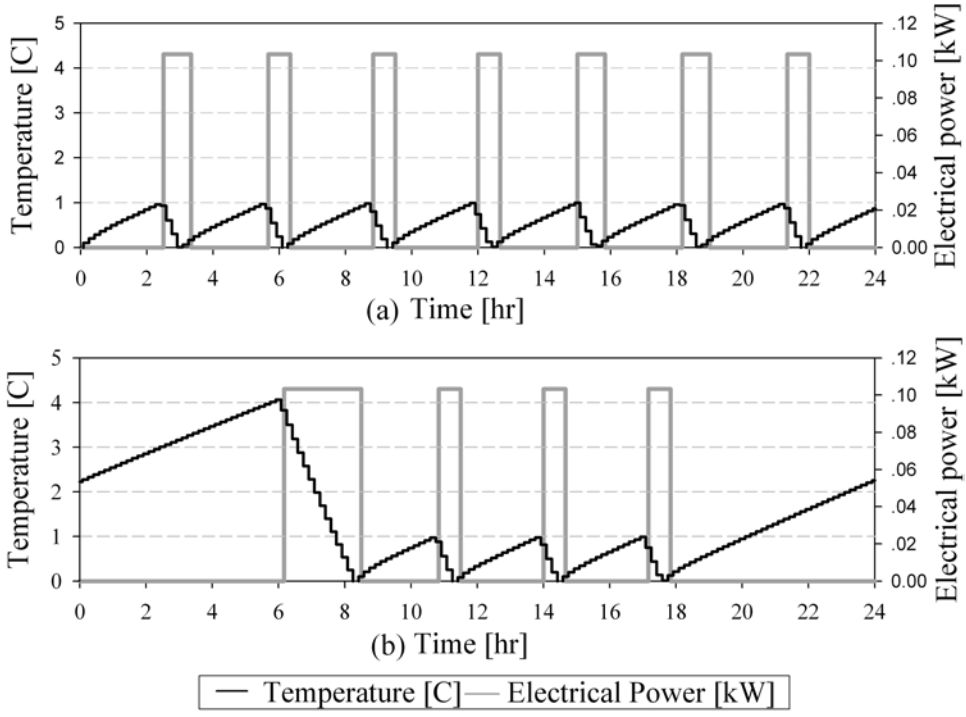

Figure 5.18: Load profiles of new refrigerator model with 30 kg of water stored inside: (a) Normal operation (without cold storage concept) (b) Operation with cold storage concept

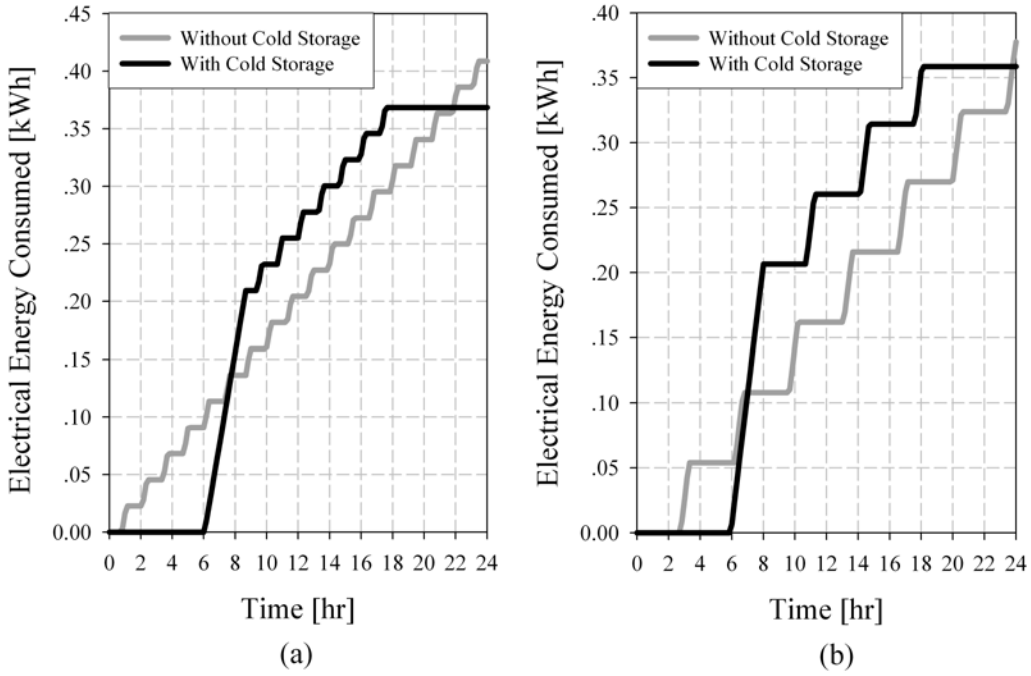

Figure 5.19: Electrical energy consumption per day of refrigerators operated with and without cold storage concept: (a) Old refrigerator model with 5 kg of water (b) New refrigerator model with 30 kg of water

Chapter 6

Case Study for Small Village Electrification Systems

This chapter describes the application of the cold storage capability of household refrigerators in a small village where refrigerators have been used for food preservation and health care purposes for the villagers. The objectives of the study in this part are:

- *To investigate the significant difference in the electrical generation system when refrigerator operates with and without DSM concept. The significant difference here means, in the amount of reduction of electricity demand per day of the village, the peak saving during the evening, the change in the SOC of the storage battery and diesel operation characteristics.*

- *To investigate the benefits of DSM on the generation side, i.e. the battery lifetime, diesel generator lifetime, the overall cost of the system and the system reliability.*

The Ban Pang Praratchatan village, in the North of Thailand, is the village selected to be a case study in this work. The overall energy consumption during the first installation of the system was 7.928 kWh/day, which is in the small scale category. However, the daily energy demand in the village increased after the system was installed. Details of this village are described in the following.

6.1 The case of the Ban Pang Praratchathan village, Thailand

6.1.1 Location and background

The Ban Pang Praratchatang is a hill-tribe village, as part of the Doi Tung Development Royal Project in Mae Fah Luang, a district of Chiang Rai province. It is located in the northern part of Thailand, as shown in Fig. 6.1. This area encompasses a total of 22 village communities of different ethnic minority groups and hill-tribes; Akha, Lahu, Tai Yai and ethnic Chinese immigrants. They continue to perform ancient rituals and celebrate traditional folk festivals throughout the year. With many aspects of their culture and way

Figure 6.1: Map of Thailand and location of the Ban Pang Praratchatan in Chiang Rai Province [67]

of life well preserved, these ethnic communities are of immense ethnographic interest and importance to the study and preservation of the rich cultural heritage of Asia. Access to education, vocational training and a range of employment opportunities enable the ethnic minority groups in the project area to preserve their heritage whilst progressing into modernity. They earn a steady income and have become self-sufficient. As a result, there has been a substantial improvement in their standard of living and quality of life. The village communities have managed to achieve a level of sustainable development that fosters the harmonious co-existence of indigenous culture and the surrounding natural environment. Renewable energy resources in BPP have been analyzed. The irradiation is quite high with an average value of 4.91 kWh/m2.d [66]. A typical house and typical electrical appliances in the village are shown in Fig. 6.3 and Fig. 6.4 respectively.

6.1.2 Potential of solar energy in the Ban Pang Praratchatan village

The potential of solar energy in the Ban Pang Praratchatan village is high, with the suitability to produce electricity by PV for the village through the year. The monthly average of solar irradiation is shown in Table. 6.1. The data in this table is very important to the study. It is used as an input variable for the simulation program to generate the hourly irradiation

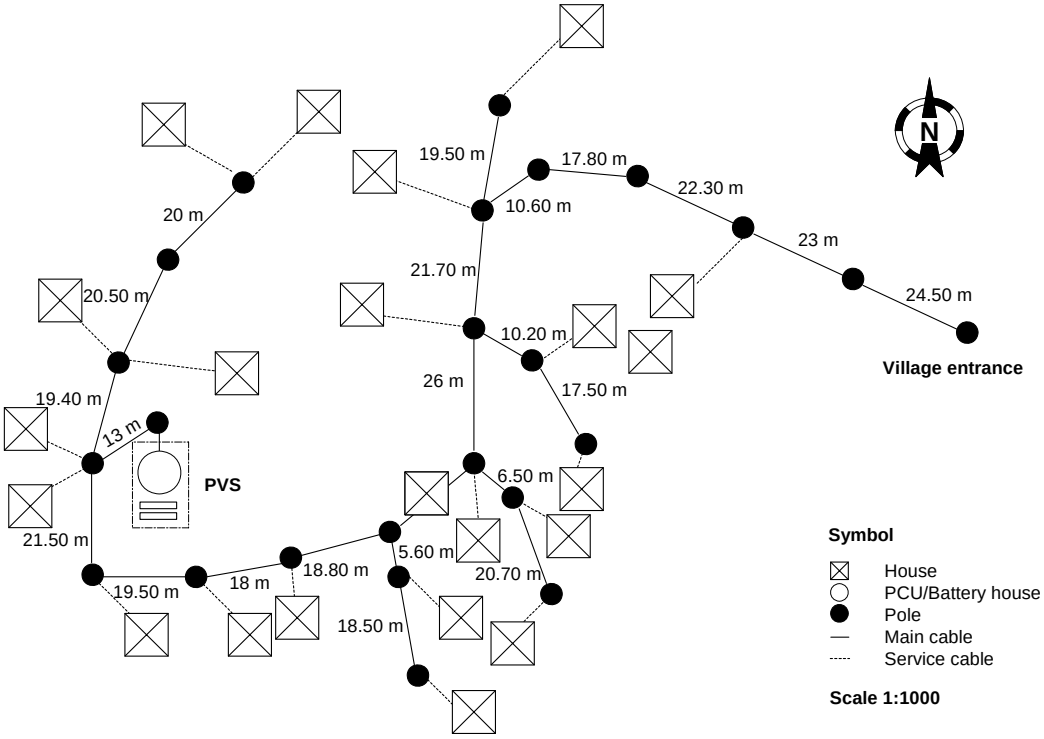

Figure 6.2: Map of the Ban Pang Praratchatan in Chiang Rai Province [66]

Figure 6.3: A typical house in the Ban Pang Praratchatan village

Figure 6.4: Electrical appliances which are used in the Ban Pang Praratchatan village

Month	Jan	Feb	Mar	Apr	May	Jun	Jul	Aug	Sep	Oct	Nov	Dec	Ave
Irradiation (kWh/m^2d)	4.24	4.79	5.25	5.86	6.19	5.46	4.85	5.46	4.58	4.58	4.32	4.18	4.91

Table 6.1: Solar irradiation at the Ban Pang Praratchatan village [66]

data at the Ban Pang Praratchatan village. The hourly irradiation profiles from January to December are shown in Fig. 6.5. These are obtained based on equations in section 2.1 (page 9), and on the numerical data in Table A.2 (page 102). Fig. 6.5 shows that the highest solar irradiation happens from the beginning of March to the middle of May, which is the summer season. Afterward, the irradiation climbs down when the summer changes to the rainy season, which usually occurs during the middle of May to the end of October [68].

6.1.3 Ambient temperature of the Ban Pang Praratchatan village

Due to the location of the village in the Northern part of Thailand, the average ambient temperature of 25.69 ^oC is lower than that of the other regions in Thailand. The maximum ambient temperature is 36^oC, in the summer season lasting from the middle of February to the end of May. Afterward, the temperature decreases as shown in Fig. 6.6 and Table. A.3.

6.1.4 Electrification system in the Ban Pang Praratchatan village

The Ban Pang Praratchatan is a case study that is especially suitable in showing the trend of electricity demand in small hill-tribe villages. It has the potential to expand to be a big village in the future. The Ban Pang Praratchatan has about 22 households with 140

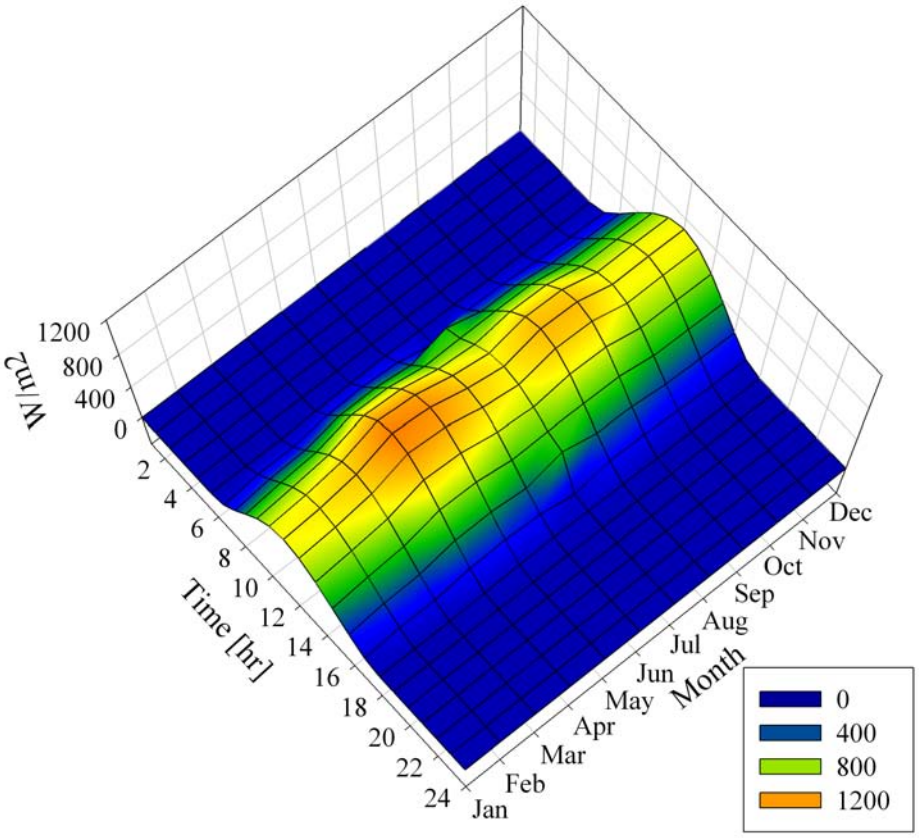

Figure 6.5: Hourly irradiation data at the Ban Pang Praratchatan village

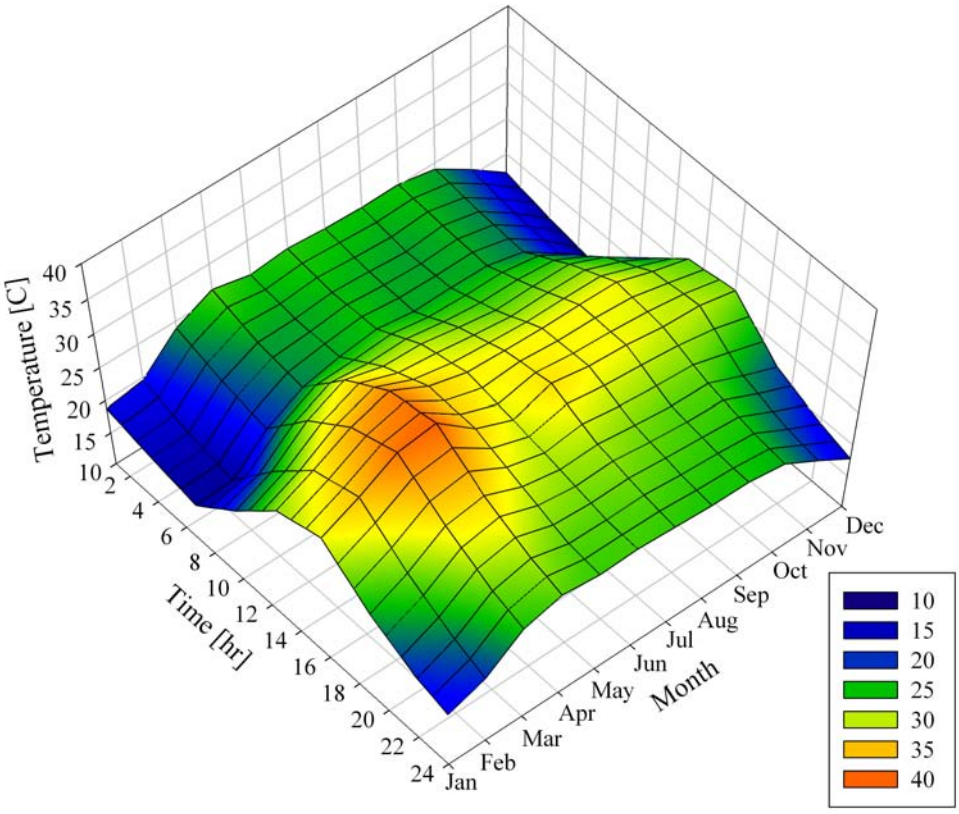

Figure 6.6: Ambient temperature at the Ban Pang Praratchatan village

inhabitants, as shown in Fig. 6.2. Income for inhabitants currently comes from work as employees under the Doi Tung Development Royal Project. In 1999, the village was electrified by the Public Work Division (PWD) with 5 strings of the Battery Charging System (BCS) with a total installed capacity of 750 Wp (150 Wp/string). In 2002, PWD installed 3,000 Wp of the photovoltaic stand-alone system. The villagers have a mutual agreement for the period of electricity usage. The electrical appliances in the village will turn off during the day time, except refrigerators, as shown in Table 6.2. The average electricity demand is calculated at 7,928 Wh/d [66].

6.2 DSM applied in the Ban Pang Praratchatan village

In this study, the refrigerator operation pattern characteristic has been modified by the DSM method. The other appliances, e.g. fluorescent lamp, TV, tape player and etc, as shown in Table 6.2, are scheduled to operate stictly in the evening from 18.00 - 22.00 hours, and only during when the villagers are in their houses. DSM is applied to refrigerators via its cold storage in order to manage the utilization of the refrigerators in the village. To demonstrate the benefits of DSM on electrification in the village, the load profile of the village has been divided into two cases. The first case is the existing load profile without DSM applied to refrigerators. This profile is obtained based on traditional use of the refrigerators. The other case is the new load profile which is obtained when the DSM concept is applied to refrigerators. Both the cases of load profiles are provided to the simulation program, to investigate the benefits of DSM on the electrification system.

6.2.1 Existing load profile

From survey, the load profile of the Ban Pang Praratchatan village is a continuous load owing to the traditional operation of refrigerators throughout the day. The peak load is often found in the evening, the period when the villagers stay in their homes. The existing load profile of the village is shown in Fig.6.7. Table 6.2 shows the existing electrical loads in the Ban Pang Praratchatan village. The peak is load of 2,222 W. The duration of peak energy demand is 4 hours in the evening.

6.2.2 New load profile with the DSM concept

The experimental results in the last chapter show that refrigerator can turned off for 12 hours without adverse effects on the goods stored inside. Hence the simple strategy which has been used to control the refrigerator in this study is to switch it off for 12 hours in order to reduce the peak energy demand during the evening. In the experiment, the refrigerators were programmed to be turned off for 12 hours during the evening and in the night. The new load profile which is obtained after the DSM is applied to the user side is shown in Fig. 6.7, and details of the duration of use of electrical appliances are shown in Table 6.3. The peak of a new load profile is 2,072 W; it is 150 W lower than before the application of the DSM to the refrigerators. However, the energy consumption per day is still the same.

The study shows that the peak energy demand per day of the village has been reduced by the DSM method via the cold storage concept of therefrigerator. The difference in the load profiles is shown in Fig. 6.7. This can be of benefit to the devices on the generation side,

Appliance	Power (W)	Quantity (Unit)	Total power (W)	Duration (Hr)	Consumption (Wh/d)
Fluorescent lamp	36	2	72	18.00-22.00	288
Fluorescent lamp	40	1	40	18.00-6.00	480
Fluorescent lamp	18	40	720	18.00-22.00	2,880
Color TV14¨	60	5	300	18.00-22.00	1,200
Color TV20¨	82	2	164	18.00-22.00	656
Black and white TV14¨	50	1	50	18.00-22.00	200
Refrigerator	100	4	400	1.00-24.00	1,600
Tape player	120	3	360	18.00-22.00	1,440
VCD player	48	2	96	18.00-22.00	384
Fan	40	3	120	18.00-22.00	480
Total			2,430		10,040
Peak Power (W)			2,222		

Table 6.2: Load profile without the DSM concept: load demand and the duration of use in the Ban Pang Praratchatan village

Appliance	Power (W)	Quantity (Unit)	Total power (W)	Duration (Hr)	consumption (Wh/d)
Fluorescent lamp	36	2	72	18.00-22.00	288
Fluorescent lamp	40	1	40	18.00-6.00	480
Fluorescent lamp	18	40	720	18.00-22.00	2,880
Color TV14¨	60	5	300	18.00-22.00	1,200
Color TV20¨	82	2	164	18.00-22.00	656
Black and white TV14¨	50	1	50	18.00-22.00	200
Refrigerator	100	4	400	**6.00-18.00**	1,600
Tap player	120	3	360	18.00-22.00	1,440
VCD player	48	2	96	18.00-22.00	384
Fan	40	3	120	18.00-22.00	480
Total			2,430		10,040
Peak Power (W)			2,035		

Table 6.3: Load profile with the DSM concept: Load demand and the duration of use in the Ban Pang Praratchatan

e.g. the battery, the diesel generator, e.t.c. However, in order to establish exactly how this method benefits the generation side, the load profiles with and without the DSM, as well as the characteristics of each system component are applied to the simulation program developed under the Labview program to investigate the benefits of the DSM method in the electrical generation system. The programming algorithm is shown in Appendix C, page 113. The existing and the new load profiles are applied to the simulation program in order to comparare the benefits of load profiles with and without the DSM on the generation system. Descriptions of system components are given in the following section.

6.3 System Device Descriptions

The main device descriptions for the generation system componentsused in the simulation consisted of the characteristics of the PV generator, diesel generator, battery storage, the power conditioning and the balance of system. The descriptions are given below:

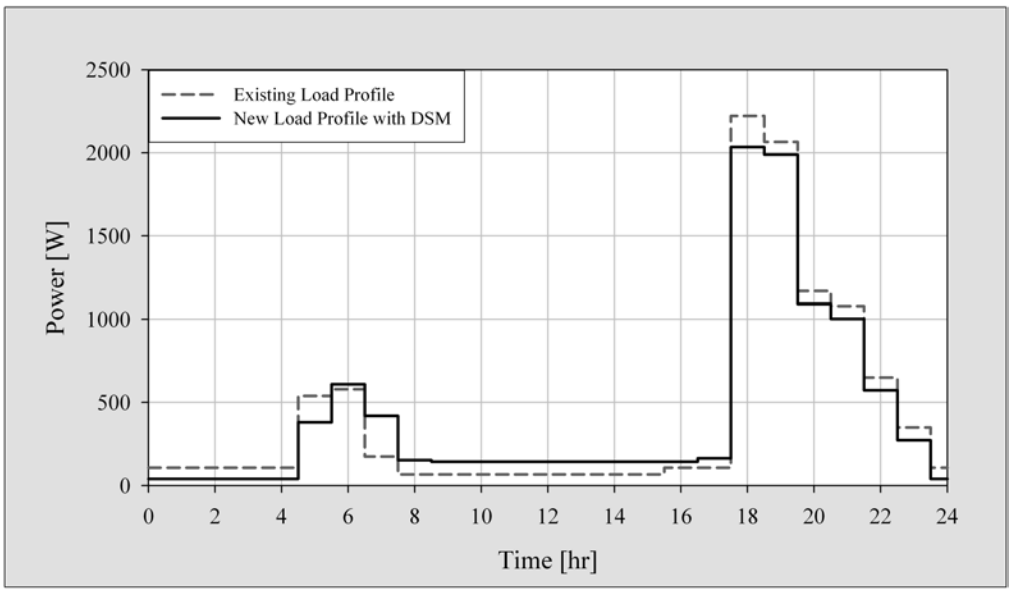

Figure 6.7: Comparison of the old load profile and the new load profile

PV Generator

Characteristics: SIEMENS module SP75 with module peak power = 75 (W), I_{SC}=4.8 (A), V_{OC}=21.7 (V), V_{MPP}=17.0 (V), I_{MPP}=4.4 (A) and β = -0.077 $V/^oC$ (75 Wx26 module)

Orientation: South facing modules with a tilt angle of 20^o

Costs: Investment cost is 3,000 Euro/kWp, O&M is 0.05 %/year of investment cost, operating lifetime 20 years.

Diesel Generator

Characteristics: Yanmar DG, 5 kW, lifetime is assumed to be 30,000 hours

Costs: For 5, 25, 50, 75 and 1,000 kW rated powers investment costs are equal to 533, 325, 220, 183 and 160 Euro/kW respectively, Overhaul 15,000 hours, overhoual cost 20% of invesment maintenance cost 3%/year of investment
Diesel fuel cost at BPP is 0.4 Euro/liter

Battery Storage

Characteristics: Exide batteries, Type: OPzS SOLAR 305, Part Number: NVSL020305WC0FA, $C_{10}@1.8V/C, 25^oC = 220$ Ah, Norminal Voltage = 2 V, ageing model parameters capacity (C_0) = 100 % of the nominal, DOD = 70 %, and the end of lifetime is at 80% of the nominal capacity and lifetime is taken to be 8 years,

Costs: investment cost = 160 Euro/kWh, O&M = 0.05%/year of investment

Power Conditioning

Characteristics: PV inverter, type Sunny Boy with MPP tracking, Bi-directional battery converter, type Sunny Island, Lifetime is taken to be 12 years.

Costs: Investment cost of the PV-inverter and battery converter are taken to be 720 Euro/kW and 1,155 Euro/kW respectively O&M is 1.0%/year of investment

Balance of System	
Characteristics:	AC power-line of 220 V (420 m), inter-bus for communication, control unit and control room
Costs:	Investment costs of 15% of the total system investment. Project lifetime of 20 years, discount rate of 5-10%

6.4 Simulation results

This part describes the simulation results of the PV-Diesel hybrid system after load profiles and information on system components were applied to the simulation program. The potential of electricity production from the PV generator is determined from the input of the solar energy data, the characteristics of PV generator and components to the simulation program. The simulation results are generated and saved in text files. In addition, the energy produce by diesel-generator and the state of charge of the battery are also obtained by assigning the old and new load profile to the simulation program. Both load profiles are assumed to have constant patterns throughout the year. Descriptions of the simulation results are presented below.

6.4.1 Electrical energy from the PV array

The irradiation data as described in section 6.1.2, page 70, is used in the simulation program which was developed under the LabView software. In the simulation, the Siemens SP75 PV generator was assigned to be made up of 26 modules, arranged 13 in series x 2 in parallel. The description of the Siemens SP75 is shown in Appendix B, page 103. The hourly simulation results of the energy produced by the PV generator from January to December are shown in Fig. 6.8. The best energy production is 1,437.28 W, it was found at noon of an April day, which is a month in summer. The worst energy production is 1,042.01 W, in January. Refering to table 2.1, page 10, the daily irradiation of the recommended average days for each month is obtained by simulation are shown in Fig. 6.9. The average daily irradiation in a year is 9.04 kWh/day. The correlation between the hourly energy demand and the energy produced by PV generator during the worst month (worst irradiation than the other months) are shown in Fig. 6.10, which describes that during 8 a.m. to 4 p.m.(16.00 hours) the energy from the PV generator is enough to supply the refrigerator whose operation is now modified by the DSM activity. However, the shortcommings of the cold storage concept occurred during the beginning of the day, i.e. from 6 to 8 a.m., and during in the end of the day, i.e. from 16 to 18 Hours. The study found that in such periods the electrical energy from PV generator was not enough to run the compressors. In this case, energy discharged by the battery bank was supplied to the grid. By this method, the battery is discharged twice a day and is re-charged again during daytime, from 9 a.m. to 3 p.m., at which time there is a large quantity of electricity produced by the PV generator. Moreover, during the night, batteries could be charged by the surplus energy from the diesel generator as well. Fig. 6.11 shows the distribution of weekly system availability of the PVHS in April. The comparison has been done between the load profile with and without the DSM of the Ban Phang Praratchatan village. It is quite clear that the operation characteristic of diesel generator has been changed as a consequence of the changing in characteristic of load profiles. With the load profile with the DSM concept, the diesel generator is operated twice a day. The simulation shows that the first operation is found

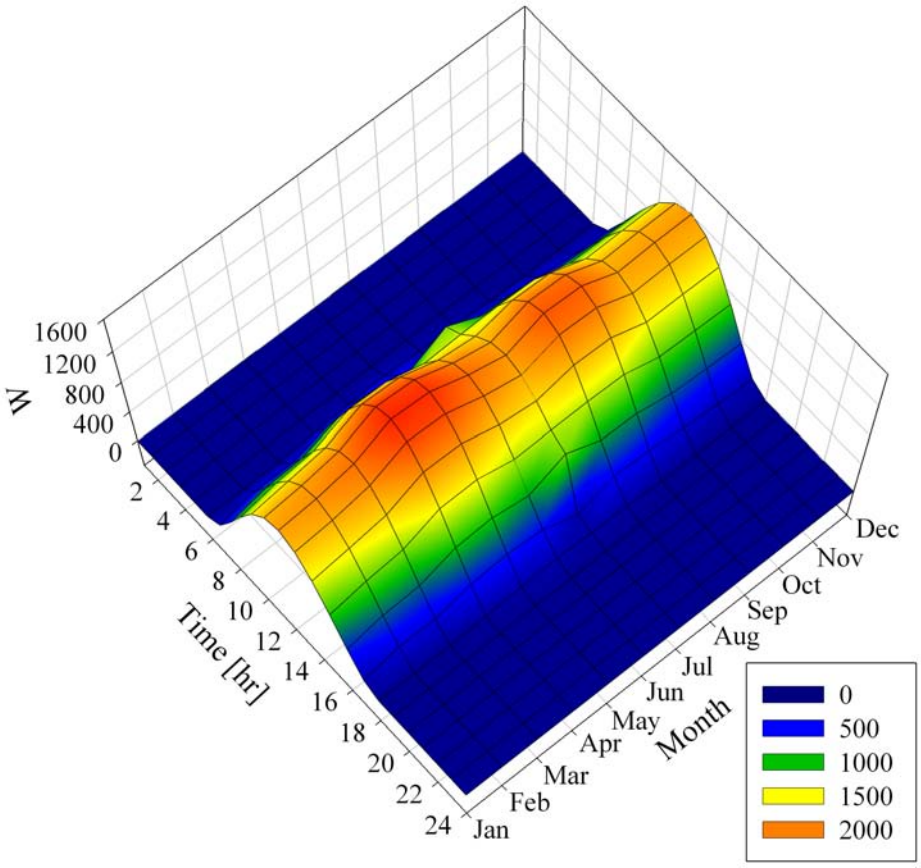

Figure 6.8: Norminal power from PV generator

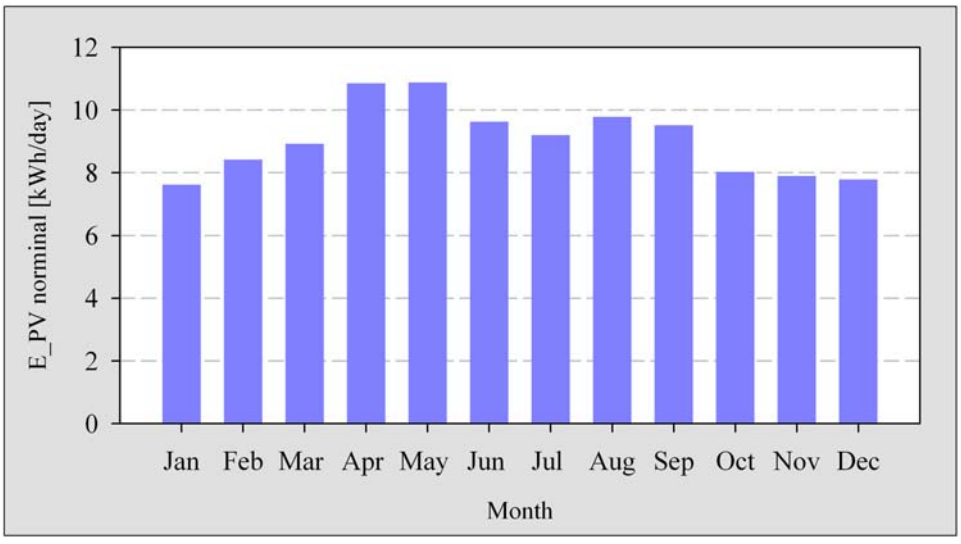

Figure 6.9: Daily nominal power of PV generator at the recommended days of each months

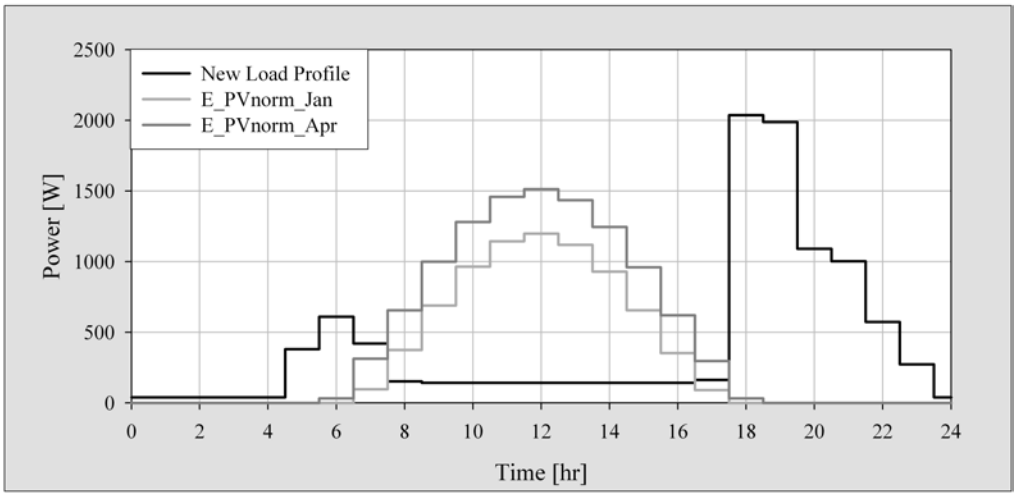

Figure 6.10: Comparison of the power produced by PV generator during January and April and the load profile with the DSM concept

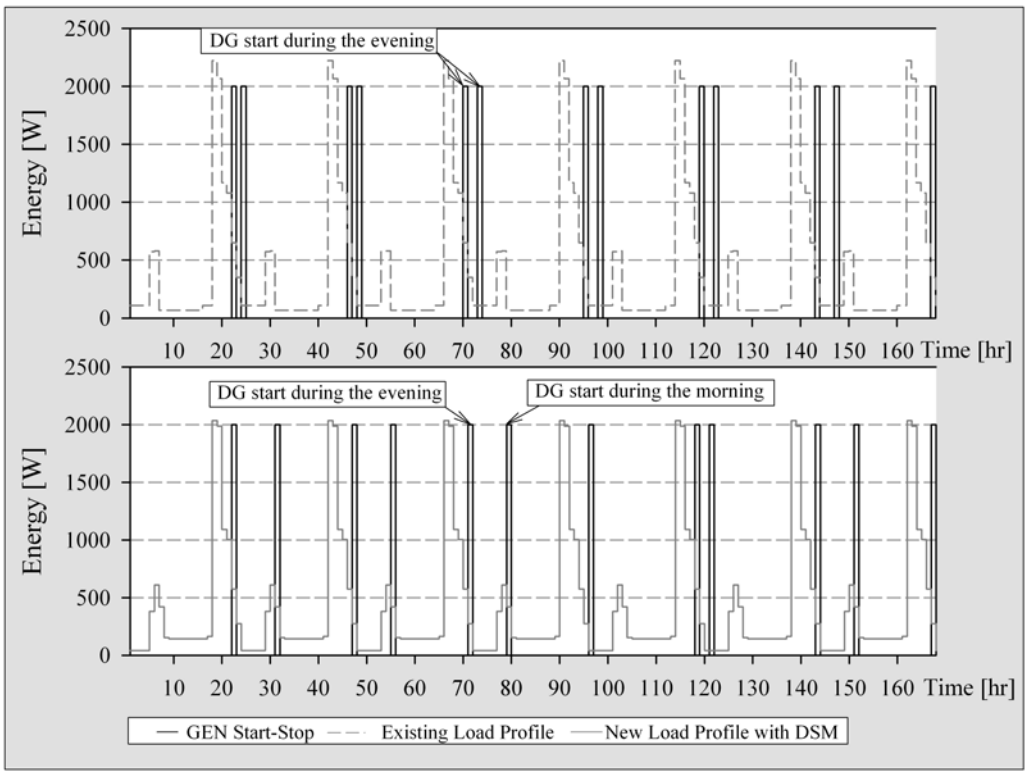

Figure 6.11: The changed operation characteristic of the diesel generator by the new load profile with the DSM

in the morning after the energy of the battery bank drops near to the minimum set point. The second operation was found during the evening. The operation of the diesel generator is reduced by 1 hour during the week. It has no significance on the reduction of diesel energy cost (the details are given in section 6.4.4, page 82). Although the energy demand during the day increased owing to the operation of refrigerator under the DSM concept, the electrical power produced by PV generator was plentifully available for the entire load during that period. This was 143 W, as shown in Fig. 6.10. The avalanche of energy drawn from battery to the load was often found in the evening, during which the peak demand occurred. In the evening, the batteries were continuously discharged until the SOC reached 30 percent, then the diesel generator started to operate. While the diesel generator was operating the battery was recharging again. Further clarification on the SOC of the battery is given below.

6.4.2 The weekly SOC of the battery

Fig. 6.12 shows the comparison of the weekly SOC of battery when the system is operated based on the load profile with and without the DSM in January and in April. The Blue line is the SOC of battery which is obtained based on the load profile with the DSM method, and the red line represents the SOC of the battery obtained by based on the load profile without the DSM method.

Moreover, the simulation results as shown in Fig. 6.12 show that the heavy discharge of battery bank happened in January, owing to the solar radiation in January being lower than in other months. Hence, the SOC of battery which is close to 20 percent is often found in January more than in the other months. But, after the DSM is applied to the PVHS, the heavy energy discharge from the battery bank during the evening is reduced due to the reduction of energy demand in the evening. The SOC of battery is observed to have improved, as represented by the blue line. Fig. 6.12 shows that the SOC of battery as represented by the blue lines is better than that represented by red lines. The SOC has therefore been improved by the DSM method. The percentage improvement of the SOC of the battery is described in the following section.

6.4.3 The yearly SOC of the battery

The yearly state of charge (SOC) of battery for the load profile with and without the DSM concept are shown in Fig. 6.13. There is a difference in the SOC of battery in each case. The clear difference was found in summer, the rainy season and the beginning of the winter season. The blue line in the graph represents the SOC of battery which is obtained based on the load profile with the DSM concept. It is on average further from the minimum discharge of battery than the red line, which means that the SOC of the battery has been improved. However, the details in Fig. 6.13 cannot define exactly difference between the SOC that Obtained from the load profile with and without the DSM concept.

In order to clearly discern the difference between these two graphs, the ranges of the SOC are used for this purpose. The frequency of SOC of battery bank in each range was deduced. The result of this procedure is shown in Fig. 6.14. The study found that the SOC of battery which is obtained based on the load profile with the DSM concept is better than that obtained based on the load profile without the DSM concept. The frequency distribution in Fig. 6.14 shows that the SOC of the battery with the system operated based on the

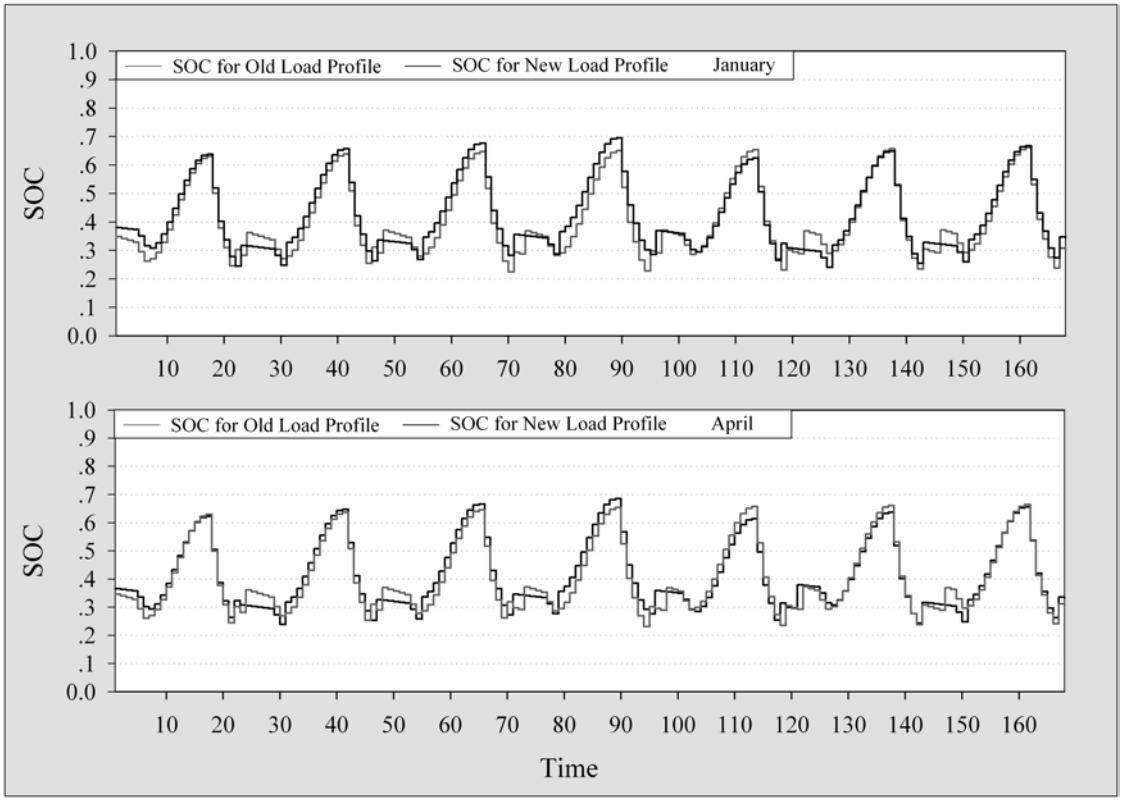

Figure 6.12: Comparison of weekly state of charge (SOC) of battery obtained based on the load profile with and without the DSM concept

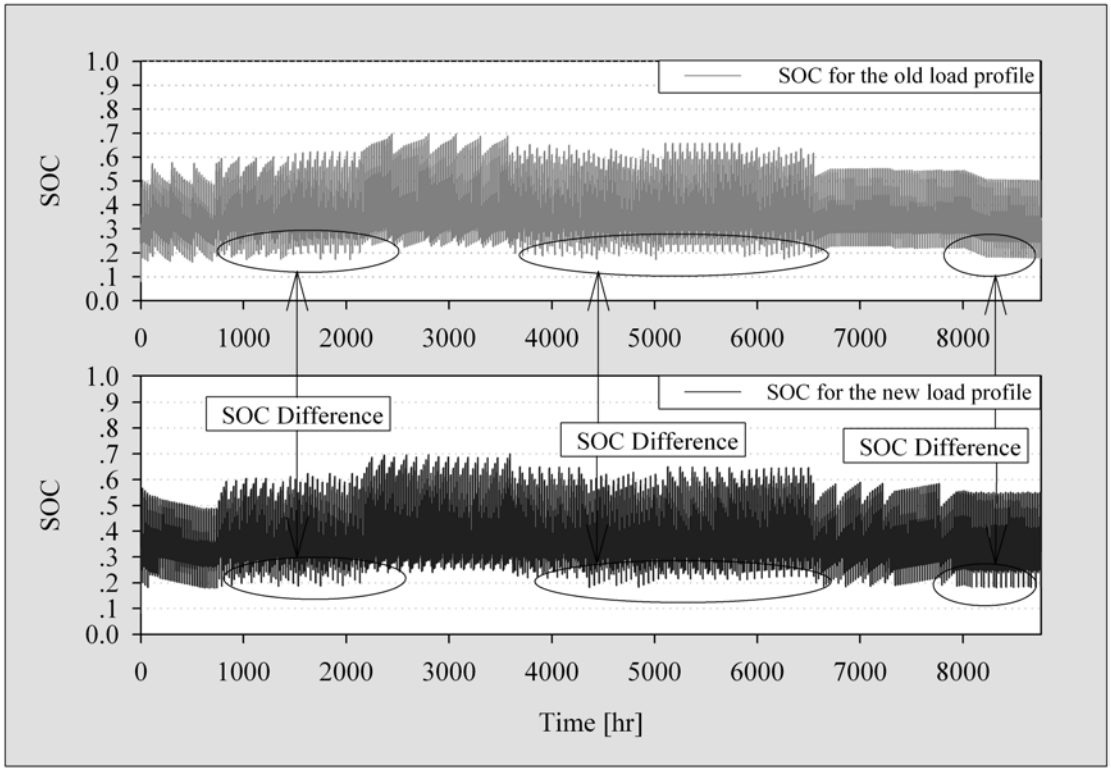

Figure 6.13: Hourly state of charge (SOC) of battery during one year, obtained based on the load profile with and without the DSM concept

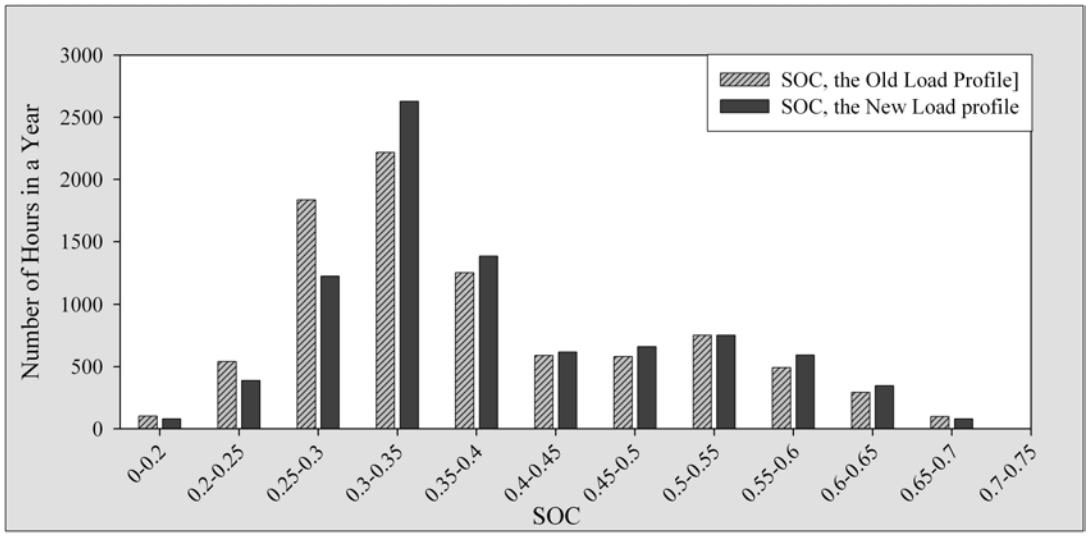

Figure 6.14: The frequency distribution of the SOC of battery during one year operation

load profile without the DSM concept is often found between 25 to 30 percent, which is a wide interval. But, when compared to the SOC of the battery obtained based on the load profile with the DSM concept, it was found that the SOC of battery mostly occurred at 30 to 35 percent. It has been shifted from the lower range to the higher range. The result of the study in this section clearly shows that the SOC of battery has been improved by the DSM method. The SOC of the battery is related to the DOD of the battery. The DOD of the battery is equal to one minus by the SOC. The DOD is the important factor used to define the lifetime of the battery. The lifetime of the battery in the case study could be defined by using the endurance cycles graph of the battery provided by the manufacturer, as shown in Appendix B., page 112. The comparison between the DOD obtained by the load profile with and without the DSM concept has been done in order to know by how much the lifetime of battery has been improved. After converting the SOC to be the DOD, it was found that the DOD of the load profile without the DSM concept is 65-75 percent, or 70 percent on average. And the DOD achieved by the load profile with the DSM concept is 65-70 percent, or 67.5 percent on average. The life cycles of the battery is obtained by a simple analytical method, via the graph in Fig. 6.15. By this method, the life cycles of battery when the system is operated based on the load profile with and without the DSM concept is 2,500 cycles and 2,300 cycles respectively. The study shows that lifetime of the battery is improved by 200 cycles.

6.4.4 Energy produced by the diesel generator

The peak energy demand during the evening has been reduced by operating of the generation system based on the load profile with the DSM concept. Consequent to the reduction of the peak energy demand, the diesel generator operation hours in the evening have been reduced as well. However, the simulation shows that refrigerator is operated continuously during two hours in the morning, hence the operation twice a day of the diesel generator, i.e. in the morning and during the evening to cover this demand. But when the system is operated based on the load profile without the DSM concept, the DG is operated only in the evening, as shown in Fig. 6.16. The amount of electrical energy produced by diesel generator depends on the seasonal and the daily energy demand. The small reduction of

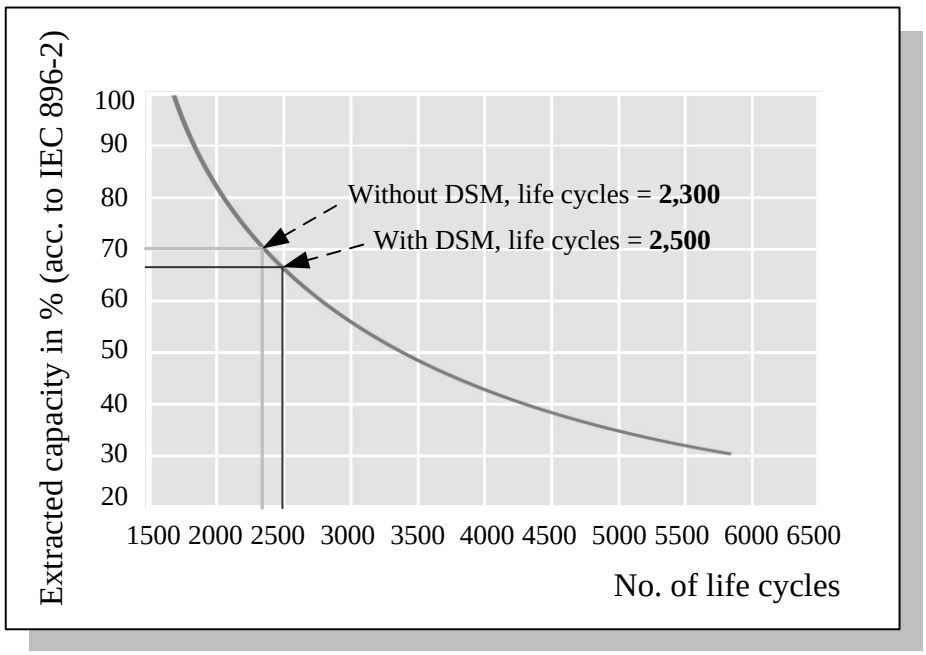

Figure 6.15: Illustration of the life cycles of battery. An improvement has been achieved by applying the DSM concept to the load

peak energy demand during the evening has a small significance on the reduction of the daily operation hours of diesel generator, as described below.

The comparison of daily energy produced by DG in each month is shown in Fig. 6.17. The figure shows that the daily energy produced by DG when it is operated based on the load profile with the DSM concept is lower than when it is operated based on the load profile without the DSM concept. The average daily energy output of the diesel generator which is operated based on load profile with and without the DSM concept is 4.97 and 5.17 kWh/day respectively, as shown in table 6.4 and table 6.5 in the next section. The operation hours of diesel generator based on the load profile without the DSM concept is 950 hrs/year, or 2.60 hrs/day on average. The operation hours of diesel generator based on the load profiles with the DSM concept is 914 hrs/year, or 2.50 hrs/day on average. The operation hours of diesel generator have been reduced. However, the reduction in the operation hours of diesel generator is very small. It has no major significant on the reduction of the energy cost of the electrification system. The study in this section shows that the DSM has more benefit to the battery section than to the diesel generator section.

6.5 System efficiency

This section describes the impact of the DSM method on system efficiency. The performance ratio (PR), Final yield (Y_f) and the solar fraction (F_{sol}) are indices that were used to describe the efficiency of the PV diesel hybrid system in this study. The energy balance of the electrification system, which comprises the energy demand, nominal power from PV generator, the used energy from PV generator and energy from diesel generator are investigated and shown in Table. 6.4 and 6.5 or in Fig. 6.18 and 6.19. This data has been used to calculate the PR, F_{sol} and Y_f of the system. The details are given as follows.

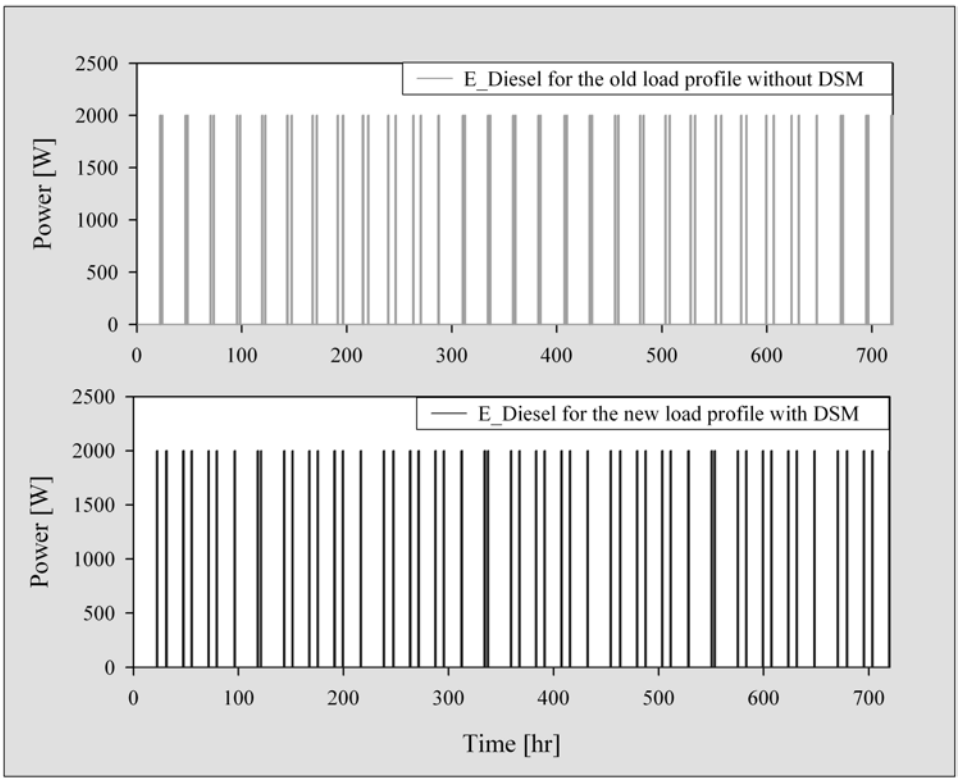

Figure 6.16: Comparison of the energy produced by diesel generator with and without the DSM applied to the load in April

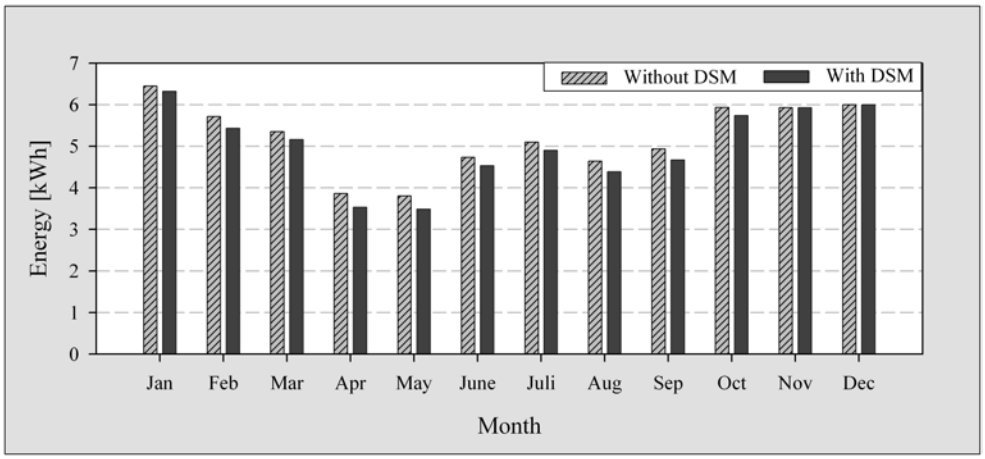

Figure 6.17: Daily energy generated by diesel generator in each month

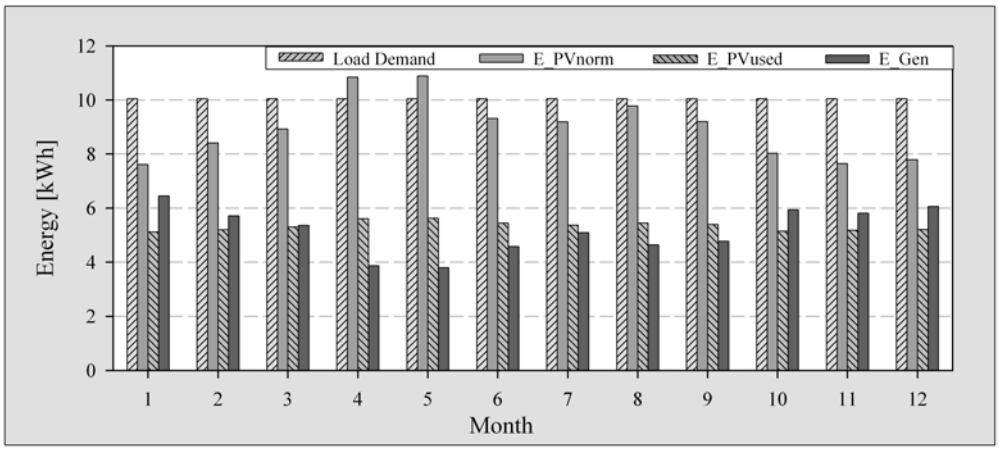

Figure 6.18: Energy balance of the PVHS with the old load profile

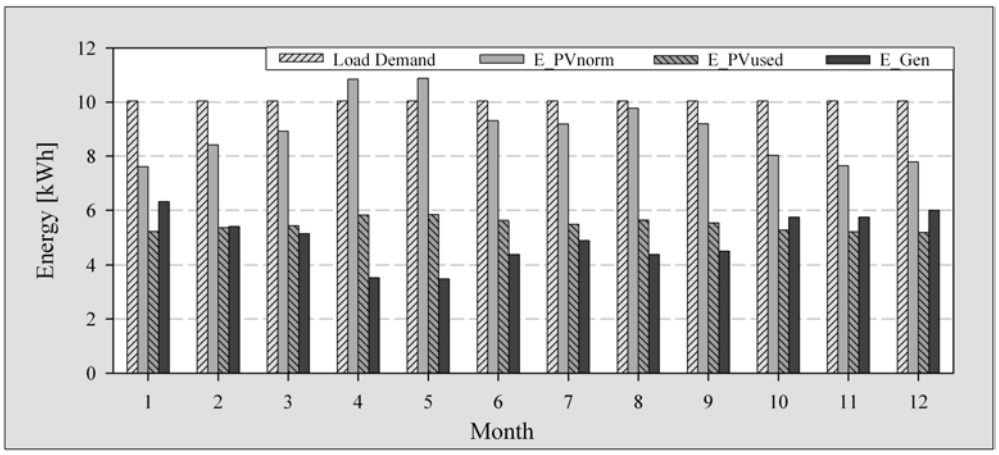

Figure 6.19: Energy balance of the PVHS with the new load profile

6.5.1 The performance ratio

The performance ratio (PR) characterizes the system losses and specifies how closely the system operation approaches the maximum power values provided by the solar generator. It is defined as the ratio of the used solar energy to the energy which nominally could be available, which theoretically would be generated if the solar generator always operated under the Standard Tests Conditions (STC), as shown in equation 6.1. The higher the PR is, the better the system uses its potential. A low PR value means production losses due to technical or design problems.

$$PR = \frac{E_{PVuse}}{E_{rat}} \tag{6.1}$$

where PR is the performance ratio, E_{PVuse} is the used solar energy and E_{rat} is theoretically energy available from PV generator at STC.

The study on PR of the generation system at the Ban Pang Praratchathan village found that the PR of system which is operated based on the DSM is better than when it is operated without the DSM. The PR averages of the system operated with and with out the DSM are 61.74 percent and 60.16 percent, respectively, as shown in Table. 6.4 and 6.5. The information shows that PR has increased by 2.6 percent. Which means that the energy losses of the system have been reduced and the real energy used from PV generator is

Month	Load Demand	E_PVnorm	E_PVused	E_Gen	PR(%)	FSol(%)	Yf
Jan	10.04	7.61	5.12	6.45	67.20	50.97	2.62
Feb	10.04	8.41	5.20	5.71	61.83	51.82	2.67
Mar	10.04	8.92	5.30	5.35	59.44	52.82	2.72
Apr	10.04	10.84	5.61	3.87	51.75	55.90	2.88
May	10.04	10.88	5.63	3.81	51.75	56.08	2.89
June	10.04	9.31	5.45	4.58	58.48	54.25	2.79
July	10.04	9.19	5.37	5.10	58.42	53.49	2.75
Aug	10.04	9.78	5.45	4.65	55.77	54.32	2.80
Sep	10.04	9.20	5.39	4.77	58.60	53.71	2.77
Oct	10.04	8.03	5.15	5.94	64.12	51.26	2.64
Nov	10.04	7.65	5.18	5.81	67.74	51.58	2.66
Dec	10.04	7.79	5.21	6.06	66.88	51.87	2.67
Average	10.04	8.97	5.34	5.17	60.16	53.17	2.74

Table 6.4: Energy balance of PVHS at the Ban Pang Praratchatan when the system was operated based on the old load profile

Month	Load Demand	E_PVnorm	E_PVused	E_Gen	PR (%)	FSol (%)	Yf
Jan	10.04	7.61	5.24	6.32	68.85	52.25	2.69
Feb	10.04	8.41	5.38	5.43	63.93	53.62	2.76
Mar	10.04	8.92	5.45	5.16	61.10	54.33	2.80
Apr	10.04	10.84	5.82	3.53	53.70	58.04	2.99
May	10.04	10.88	5.84	3.48	53.65	58.18	2.99
June	10.04	9.31	5.63	4.39	60.46	56.12	2.89
July	10.04	9.19	5.51	4.90	59.90	54.89	2.82
Aug	10.04	9.78	5.64	4.39	57.68	56.21	2.89
Sep	10.04	9.20	5.56	4.52	60.40	55.39	2.85
Oct	10.04	8.03	5.30	5.74	65.99	52.79	2.72
Nov	10.04	7.65	5.23	5.74	68.35	52.08	2.68
Dec	10.04	7.79	5.21	6.00	66.86	51.88	2.67
Average	10.04	8.97	**5.48**	**4.97**	**61.74**	**54.65**	**2.81**

Table 6.5: Energy balance of PVHS at the Ban Pang Praratchatan when the system was operated based on the new load profile

closer to the maximum energy produced by PV generator. The daily average of the PR in each month is shown in Fig. 6.20.

6.5.2 The solar fraction

The solar fraction is the ratio of the used solar energy to the total energy consumption, as shown in equation 6.2. The solar fraction has been used as a reference quantity for sizing the solar generator and the storage battery.

$$F_{sol} = \frac{E_{PVuse}}{E_{tot}} \tag{6.2}$$

where F_{sol} is solar fraction, E_{PVuse} is the used solar energy and E_{tot} is total energy consumption.

In this study, the solar fraction average for the system that operated without the DSM is 53.17 percent and the solar fraction average for the system operated with the DSM is 54.65 percent (as shown in Table. 6.4 and 6.5). This represents a 2.78 percent increase. The comparison of the solar fraction of PV diesel hybrid system when it is operated with and without the DSM is illustrated in Figure 6.21. The increase in the solar fraction of the

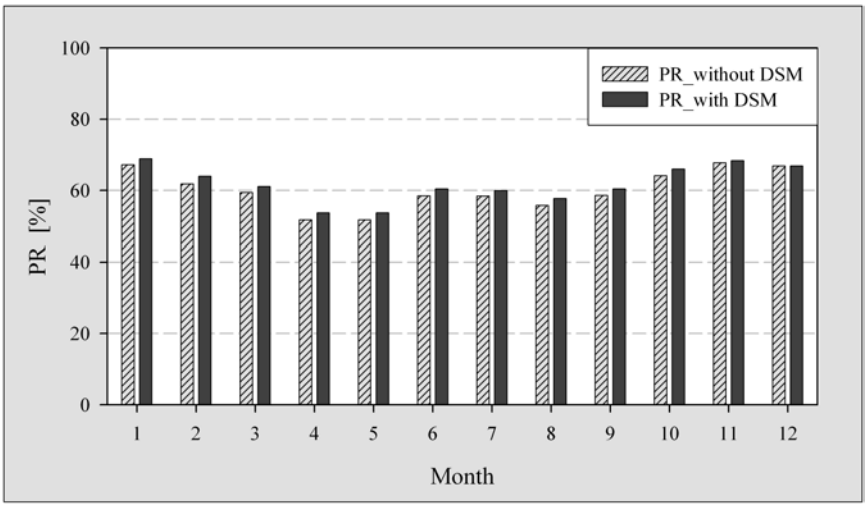

Figure 6.20: The comparison of the performance ratio of the system operated based on the load profile with and without the DSM

system operated based the DSM represents the increase in the electricity supplied to the load. The reason being that the refrigerator which is operated only during the day has effected the increase in energy demand during the day and, by implication, the amount of electrical energy produced by the PV array, which is supplied directly to the load. Hence, the losses in energy generated by PV array are reduced.

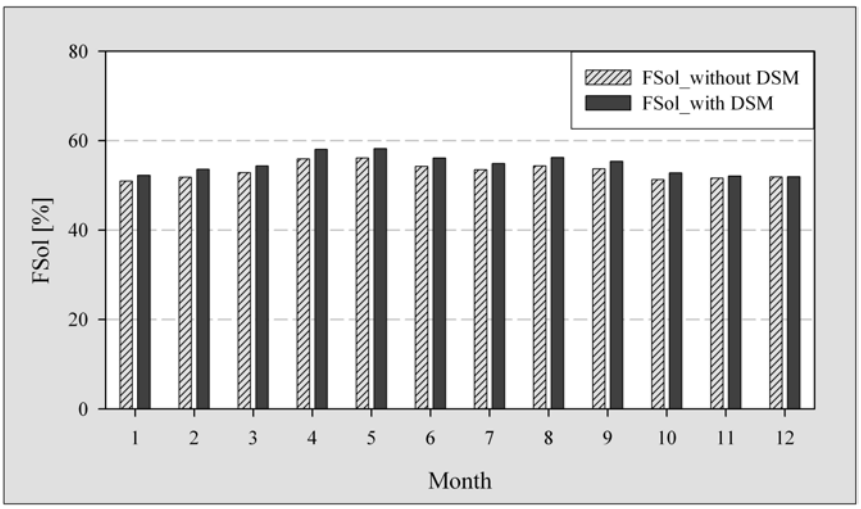

Figure 6.21: The comparison of the solar fraction of the system operated based on the load profile with and without the DSM

6.5.3 The final yield

The final yield (Y_f) is the average daily used solar energy per kilowatt of installed solar generator power, as shown in equation 6.3. It expresses the used solar energy as the number of equivalent daily full-load operating hours of the solar generator under standard test

conditions.

$$Y_f = \frac{E_{PVuse}/day}{P_{rat}} \tag{6.3}$$

where Y_f is final yield, E_{PVuse}/day is the average daily used solar energy and P_{rat}/day is the power (kilowatt) of installed PV generator.

Fig. 6.22 shows the final yield of the PV-Diesel hybrid system operated based on the DSM concept is higher than when it operated without the DSM concept. The final yield of the PV diesel hybrid system operated with and without the DSM is 2.81 and 2.74, respectively, as shown in Table. 6.4 and 6.5. The data in the tables show that the electricity generated by PV generator based on the DSM concept is used more comprehensively. The final yield of the system is increased by 2.55 percent.

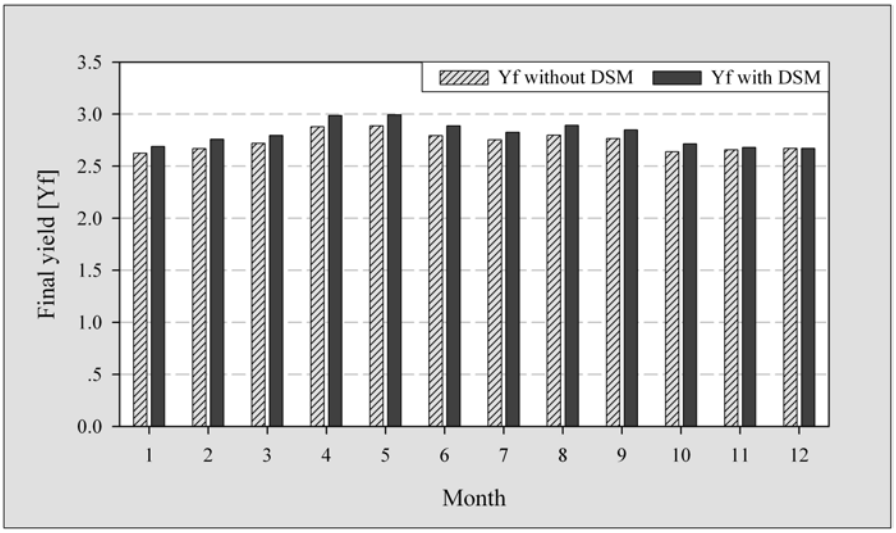

Figure 6.22: The comparison of the final yield of the system operated based on the load profile with and without the DSM

6.6 Energy cost reduction

The benefit of the longer lifetime of the battery used in the PV system is related to the reduction of the energy cost of the system. In this part is the presentation of the study results on the reduction of the energy cost of PVHS when the lifetime of the battery is improved. The comparison of the energy cost of the system when it is operated with and without the DSM concept has been done. The description of the lifetime, the capital cost and other factors of each component that is involved in the calculation of the energy cost are shown in tables 6.6 and 6.7. The capital cost of the whole system is 18,880.00 Euro. The interest rate is assigned to be 5 percent. In tables 6.6 and 6.7, the difference in the annuity cost and the specific energy cost was found in the battery part. When the PVHS is operated without the DSM concept the lifetime of the battery is 8 years. This means the annuity cost of battery is 467.38 Euro, and its specific energy cost is 0.128 Euro/kWh, as shown in table 6.6. However, when the system is operated with the DSM concept, the lifetime of battery is extended to 9 year, one year longer than when it is operated without the DSM concept. In this case, the annuity cost and specific energy cost of the battery changes to 425.00 Euro and 0.116 Euro/kWh respectively, as shown in table 6.7.

Description	Lifetime	Capital Cost	Interest rate	Annuity Factor	Annuity Cost	COE
PV	20	9062.40	5.00	0.0802	727.19	0.198
Inverter	10	1888.00	5.00	0.1295	244.50	0.067
DSG	11	2265.60	5.00	0.1204	272.75	0.074
Battery	8	3020.80	5.00	0.1547	467.38	0.128
BOS	10	944.00	5.00	0.1295	122.25	0.033
Installation	10	1699.20	5.00	0.1295	220.05	0.060
Total		18880.00			2054.14	0.560

Table 6.6: Annuity cost and the cost of energy of PVHS operated without the DSM at the Ban Pang Praratchatan

Description	Lifetime	Capital Cost	Interest rate	Annuity Factor	Annuity Cost	COE
PV	20	9062.40	5.00	0.0802	727.19	0.198
Inverter	10	1888.00	5.00	0.1295	244.50	0.067
DSG	11	2265.60	5.00	0.1204	272.75	0.074
Battery	**9**	3020.80	5.00	0.1407	**425.00**	**0.116**
BOS	10	944.00	5.00	0.1295	122.25	0.033
Installation	10	1699.20	5.00	0.1295	220.05	0.060
Total		18880.00			**2011.75**	**0.549**

Table 6.7: Annuity cost and the cost of energy of PVHS operated with the DSM at the Ban Pang Praratchatan

The graphical comparison of the annuity cost of each component in PVHS when it is operated with and without the DSM is shown in Fig. 6.23. The total annuity cost of the PVHS which operated with the DSM concept is lower than when it is operated without the DSM concept. The information in the graph shows that the reduction of the annual cost of battery part (green color) is a major reason for the reduction of the annuity cost for whole system.

The comparison of the specific cost of energy produced by the PVHS in the Ban Phang Praratchatan village is shown in Figure 6.24. The graph shows the DSM concept applied to the PVHS in the Ban Phang Praratchatan village is a reason for the reduction of the specific cost of energy from 0.560 Euro/kWh to 0.549 Euro/kWh, which is a 2 percent reduction. However, focusing only on the specific cost of energy for the battery, its energy cost is reduced by 9.37 percent.

6.7 Discussion

After the DSM concept, via the cold storage of refrigerator, is applied to the user side, it was found that the refrigerator operation pattern characteristic changed. The refrigerator is operated only in the day time. This change has a benefit to the stability of the system due to the fact that the peak energy demand during the evening has reduced after this method was applied. However, the daily energy consumption of the village did not change. Although the reduction in the evening energy demand caused a shorter operation duration of the diesel generator, in the morning, while the battery bank energy is lower than the minimum allowable, owing to refrigerator having drawn a lot of electricity to cool itself down, the diesel generator is operated again. The reduction of the peak energy demand caused the battery DOD to change from 70 percent to 67.5 percent. The new life cycle of battery is 2,500 cycles, an improvement of 200 cycles, as described in section 6.4.3 page 80. The reason that the daily energy demand of the village is still the same is owing to the fact that the DSM method has no major significance on the improvement of the diesel generator

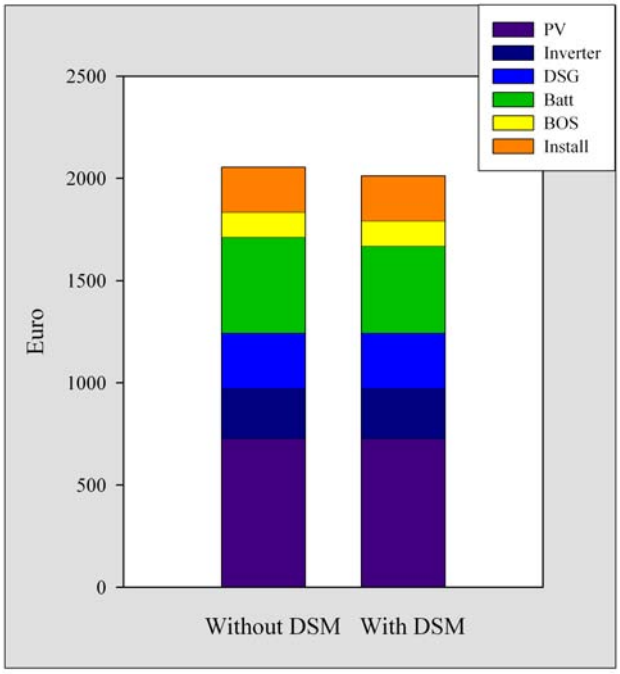

Figure 6.23: Comparison of annuity cost of PVHS in the Ban Phang Praratchatan village

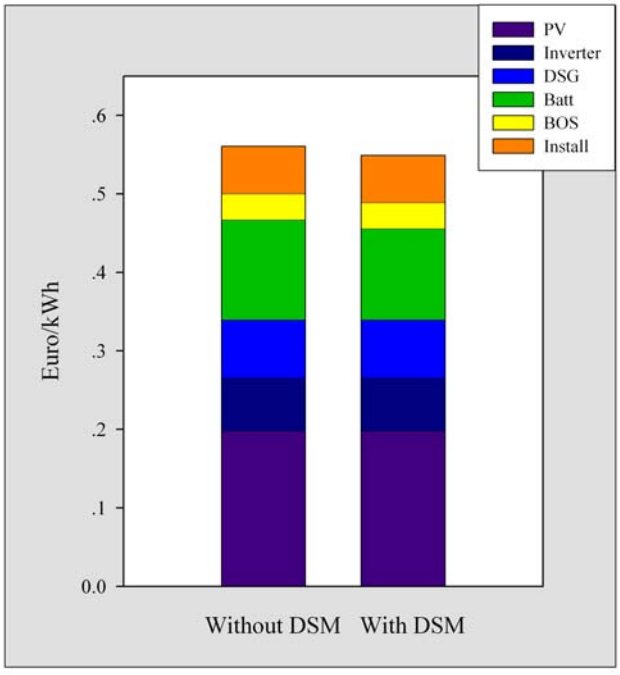

Figure 6.24: Comparison of the COE of PVHS in the Ban Phang Praratchatan village

working characteristics, as described in section 6.4.4 page 82.

The study in section 6.5 page 83 shows that the efficiency of the PV-Diesel hybrid system has been improved by the DSM method. The performance ratio, the solar fraction and the final yield of the system increased by 2.6 percent, 2.78 percent and 2.55 percent, respectively. Moreover the economic study results in section 6.6 page 88 show that the specific cost of energy of the battery is reduced by 9.37 percent. The information confirms that after the DSM concept was applied to the Ban Phang Praratchatam village, the villager has gained not only in the increase in the system reliability but also in the cheaper price of energy. The study above shown that the greatest benefit of the DSM via the cold storage method of the refrigerator mainly occurred for the battery bank, which is the second most expensive part in the PVHS. The DSM effected the reduction in the specific cost of energy of the battery, which caused the specific cost of energy of the whole system to reduce.

Chapter 7

Conclusion and Outlook

The study of the efficiency of the DSM on the small village electrification has been done in the two parts. In the first part, the electrical appliance (refrigerator) has been studied with the aim of reducing the energy used in the night time. For the second part, resulting from the first investigation, the study is focused on the small village and has estimated the benefits of the DSM on the component lifetime extension, the system stability and the energy cost of the PV-diesel hybrid system.

In the first study, the storage capability of the refrigerator has been researched in the Laboratory at IEE-RE, University of Kassel. The main point of the study was to investigate and to establish the storage capability of both the old and the new refrigerators which are commonly used in the rural villages. In the measurements, a variety of boxes of water (5 kg to 30 kg) were used as the product samples inside the refrigerators. The test of the storage capability was then carried out case by case. The study found that, with product samples from 5 to 30 kg, both the old and the new refrigerator models can hold the temperature in the range of 0 ^{o} to 10 ^oC (ISO standard temperature for preserving food) for 12 hours without powered operation.

In the second part of this research, the information on the cold storage capability of the refrigerator has been applied to the small village, which is electrified by the PV-diesel hybrid system. The Ban Phang Praratchatan village was selected as a case study for this work. It is a small village in the northern part of Thailand which has electrical energy utilization characteristics suitable for this study. After the system was installed, the villagers realised a problem in terms of the rising daily energy consumption. The survey found that the daily energy consumption of the village is 10.040 kWh, which is a 26.64 percent increase from that at the initial installation.

The benefits of the DSM on the reduction of daily energy demand, the improvement of the efficiency, stability of the system, the battery life time and the overall cost of energy have been investigated. The study found that, when the DSM concept, via the cold storage of refrigerator, were applied to the user side, the refrigerator operation characteristic changed. The refrigerator is operated only in the day time, which benefits the stability of the generation system due to the fact that the peak energy demand during the evening is reduced. The new daily peak energy demand is 2,035 kW, which is a reduction of 8.41 percent.

The reduction of peak energy demand during the evening resulted in the reduction of the energy supplied by the batteries to the load. The DSM brought benefits in the modification of the SOC and the DOD of battery. When the system was operated with the DSM, the DOD of battery changed from 70 percent to 67.5 percent. The new life cycle of battery

is 2,500 cycles, which is an improvement by 200 cycles. However, the study shows that the DSM method has no significance on the improvement of the diesel generator operation characteristic because the daily energy demand of the village does not change under this method.

Because the refrigerator is operated only in the day time, the energy produced by PV arrays does not supply only the battery bank but the refrigerator as well. With the actions above, the utilization of energy produced from PV generator has been improved and the loss via the storage and transmission part has been reduced. The study shows that the efficiency of PV-Diesel hybrid system has been improved by the DSM concept. The performance ratio, the solar fraction and the final yield of the system increased by 2.6 percent, 2.78 percent and 2.55 percent, respectively. Moreover, the economic study results show that the specific cost of energy of battery reduced by 9.37 percent. The information also confirmed that when the DSM concept was applied to Ban Phang Praratchatam village, the villagers gained both from the increase in the system reliability and the cheaper cost of energy compared to the previous system operation.

The study above showed that the benefits of the DSM through the cold storage method of refrigerator mainly occurred only with the battery bank, which is the second most expensive part of the PVHS. The specific cost of energy of the battery part was reduced by the DSM method, which also caused the specific cost of energy of the whole system to reduce too.

All in all, the results of the DSM application to the village electrification will be more interesting when the concept is applied to a larger size of village with a larger battery bank in the PVHS.

Bibliography

[1] Volker Quaschning: *Understanding Renewable Energy Systems*, Earth Scan Publishing, UK, London, 2005

[2] Solarbuzz: *Solar Photovoltaic, PV Module, Panel Prices*, Solarbuzz, 2005 [cited 2005]; 1(5): Available form: http://www.solarbuzz.com/moduleprices.htm 6/10/2005 10:20:05

[3] M. Schmela: *Market survey on global cell and module production in 2004*, PHOTON International, March 2005 [cited 2005 March]; 1(1): Available form: http://www.photon-magazine.com/news/news_05-03_ww_cells_and_modules_2004.htm 5/10/2548 12:58:07

[4] H. Partl et al.: *Generation and Transmission Prospects for Solar Electricity: UK and Global Markets*, Energy Conversion and Management Volume 44 (1988) 35-52

[5] M. Schmela: *High demand for PV in Japan: A dramatic cut in subsidies does not stop Japanese citizens from investing in solar*, PHOTON International, June 2004 [cited 2004 June 6]; 1(1): Available form: http://www.photon-magazine.com/news/news_2004-06_ap_sn_NEF.htm 27/9/2005 9:11:52

[6] M. Ibrahim: *Decentralized Structures and ModularSystems Technology for Electrification with Renewable Energies*, Sharjah Solar Energy Conference, Sharjah, UAE 2001

[7] K. Burges, B. van Hemert: *Market Introduction of Hybrid power Supply Systems*, PV Hybrid Power Systems Conference, Aix en Provence 2000

[8] Manwell, J. F., Stein, W. M., McGowan, J. G. and Baring-Gould, E. I.: *Hybrid 1 Operating Instructions Manual*, National Renewable Energy Laboratory, University of Massachusetts, January 1994.

[9] Andrew L. Rosenthal: *PV Hybrid System Performance*, PV Horizon: Workshop on Photovoltaic Hybrid System, Montreal, September 10, 2001.

[10] M. Ibrahim: *Decentralized Hybrid Renewable Energy System Control Optimization and Battery Aging Estimation Based on Fuzzy Logic*, Berlin: dissertation.de, Verlag im Internet GmbH, 2002.

[11] A. Hamzeh: *Experence With Stand-Alone Centralized and Individual House PV System in Syria*, Renewable Energy, Vol. 6, No. 5, pp 545-548, 1995

[12] U. Stuten bäumer et al.: *Performance of small-scale photovoltaic systems and their potential for rural electrification in Ethiopia*, Renewable Energy, Vol. 18, pp. 35-48, 1999

[13] W. Rakwichian et al: *A Study of Mini-Grid concept for the Villages without Electricity in Thailand*, Report submits to National Research Council of Thailand, 2004

[14] NREL: *Inner Mongolia Household PV-Wind Hybrid Systems Pilot Project*, Report form NREL, USA, 2000

[15] L. C. G. Valente and S. C. A. de Almeida: *Economic Analysis of a Diesel/Photovoltaic Hybrid System for Decentralized Power Generation in Northern Brazil*,Energy Vol. 23, No. 4, pp. 317323, 1998

[16] H. Gabler: *Autonomous Power Supply With Photovoltais: Photovoltaics for Rural Electrification-Real and Vision-*, Renewable Energy, Vol. 15, pp. 512-518 1998

[17] Elhadidy MA., Shaahid SM.: *Optimal sizing of battery storage for hybrid (wind + diesel) power systems*, Int. J. Renew Energy, Vol. 18(1), pp. 7786 1999

[18] Gajanana K. Hegde, Remeche Madomercandy, Binu Parthan: *Solar hybrid power system: An overview*, Renewable Energy for Sustainable Development, Der Carl von Ossietzky University Oldenburg, 2002

[19] Valente, Luiz Carlos Guedes; de Almeida, Silvio Carlos Aníbal *Economic analysis of a diesel/photovoltaic hybrid system for decentralized power generation in northern Brazil*, Energy Volume: 23, Issue: 4, April, 1998, pp. 317-323

[20] Andrew L. Rosenthal: *Evaluation of Hybrid Power System Alternatives:A Case Study*, Progress in Photovoltaics Research and Applications 7, 1999, 183-190

[21] S.M. Shaahid., M.A. Elhadidy: *Prospects of autonomous/stand-alone hybrid (photo-voltaic + diesel + battery) power systems in commercial applications in hot regions*, Renewable Energy Vol. 29, 2004, 165177

[22] Duffie, J.A. And Beckman, W.W.: *Solar Engineering of Thermal Process*, 2^{nd}edition, New York, John Wiley&Sons, 1991.

[23] RETScreen International: *Clean Energy Project Analysis*, RETScreen Engineering&Cases Textbook, 2003.

[24] D. Linden and T. B. Reddy: *Handbook of Batteries*, McGraw Hill, New York, 2002.

[25] M. Muselli, G. Notton, P. Poggi, A. Louche: *PV-Hybrid Power Systems Sizing Incorporating Battery Storage: An Analysis Via Simulation Calculations*, Renewable Energy Volume: 20, Issue: 1, May, 2000, pp. 1-7

[26] C.V. Nayar, S. J. Phillips, W. L. James, T. L. Prior and D. Remmer: *Novel Wind/Diesel/Battery Hybrid Energy Systems*, Solar Energy, 1993, Vol. 51, No. 1, pp 65-78

[27] M. Ashari and C.V. Nayar: *An Optimum Dispatch Strategy Using Set Point for A Photovoltaic (PV)-Diesel-Battery Hybrid System*, Solar Energy, Vol. 66, No. 1, 1999, pp 1-9

[28] W. Kleinkauf and J. Sachau: *Components for Modular Expandable and Adaptable PV Systems*, 12th EPVSEC, Amsterdam, the Netherlands, 1994

[29] G. Seeling-Hochmuth: *Optimisation of Hybrid Energy Systems Sizing and Operation Control*, PhD. Thesis, Kassel University, Kassel Germany 1998

[30] Matthew J. Parry-Hill, Robert T. Sutter and Michael W. Davidson *Molecular Expressions Microscopy Primer: Physics of Light and Color - Solar Cell Operation: Interactive Java Tutorial*, National High Magnetic Field Laboratory, The Florida State University, Tallahassee, Florida, [cited August 2];2(3): Available from: URL: http://micro.magnet.fsu.edu/primer/java/solarcell/

[31] J. Schmid: *Photovoltaic systems Technology*, Teaching Script, IEE-RE, University of Kassel, Germany, 2002

[32] BP Solar: *90 Watt Photovoltaic Module Saturn Technology: BP 790*, BP Solar, 3012E-2 05/04 [cited 2005 July 12]; 1(2): Available form: htttp://www.bpsolar.com

[33] Shell Solar: *Production Information Sheet: Shell SQ80 Photovoltaic Solar Module*, Shell Solar Custom Service Center, [cited 2005 July 15]; 2(2): Available form: http://www.sinetech.co.za/printdocs/sq80.pdf

[34] B. Buchholz: *Smart Web Index and data exchange options*, A Dissertation at University of Kassel, Germany, 2001

[35] Wikimedia The Free Encyclopedia: *PV Module Efficiency*, Wikimedia Foundation, [cite 2005 August 8]: Available form: http://en.wikipedia.org/

[36] B.H. Chowdhury, S. Rahman: *Analysis of Interrelationships Between Photovoltaic Power and Battery Storage for Electric Utility Load Management*, IEEE Trans. Power Systems, Vol. 3, No. 3. 1988

[37] Hansen, A. D. et al: *Models for a Stand-Alone PV System*, Risϕ-R-1219(EN)/SEC-R-12, Risϕ National Laboratory, Roskilde, 2000.

[38] Castañer, L. and Sivestre, S.: *Modelling Photovoltaic System using Pspice*, John Wiley&Sons, 2002.

[39] Roger A. Messenger, Jerry Ventre: *Photovoltaic Systems Engineering*2^{nded}, CRC Press LLC, the United States of America, 2004.

[40] T. Jimenez: *Hybrid Design Handbook*, NREL/EDRC Production, Chapter 6 Components, Draft Copy 1998

[41] John B. Heywood: *Internal Combustion Engine Fundamentals*, McGraw-Hill Inc., 1988, pp 823-398

[42] Michael Sigler: *Zur Optimierung des Einsatzes von Dieselgeneratoren in einem mit einem Speicher und mit Regenerativen Energiewandlungssystemen untersttzten Inselenergiesystem*, Studienarbeit, Stuttgart University, Stuttgart, Germany, 1990

[43] Berkines: *Data Sheets for Diesel Fuel Consumption*, 1992.

[44] Albrecht Schöttle: *Potential Dezentraler Stromversorgung mit Dieselmotoren in Entwicklungsländern*, Studienarbeit IER der Universität Stuttgart, 1992, Stuttgart, Germany.

[45] J.A.M. Bleijs, C.J.E. Nightingale and D.G. Infield: *Wear Implications of Intermittent Diesel Operation in Wind/Diesel Systems*. Wind Engineering, 1993, Vol. 17, No. 4, pp 206-219.

[46] Manwell, J. F. et al: *Hybrid2-A Hybrid System Simulation Model Theory Manual*, National Renewable Energy Laboratory, Subcontract No. XL-1-11126-1-1, 1998.

[47] IEA International Energy Agency: *Power System Programme:Lead-Acid Battery Guide for Stand-Alone Photovoltaic Systems*, IEA Task III Report IEA-PVPS 3-06:1999, December 1999

[48] W. Kleinkauf, Mohamed I. A. Ibrahim: *Decentralized Hybrid Renewable Energy Systems*, a dissertation at University of Kassel, Germany, 2002.

[49] CSB BATTERY CO., LTD: *Data Sheet of CSB Battery: Model GP645*, CSB BATTERY CO., LTD, [cited 2005 August 3]; 2(2): Available form: http://www.sinetech.co.za

[50] Stoecker, W. F.: *Design of Thermal Systems*, 3^{rd} edition, McGraw-Hill, 1989.

[51] Yaron, G. et al: *Solar Energy for Rural Communities: The case of Namibia*, Intermediate Technology Publications, 1994.

[52] Cogeneration Technologies^{TM}: *Demand Side Management*, Cogeneration Technologies^{TM}, [cited 2005 August 29]; 1(14): Available form: http://www.cogeneration.net/Demand_Side_Management.htm

[53] Anton Eberhard et al: *Electricity Supply and Demand Side Management Options:The History of Demand Side Management in the Power Sector*, World Commission on Dams, Option Issues Series IV.1, pp. 64, 2000.

[54] J. Byrn, S. Letendre, C. Govindarajalu and W. Young-Doo: *Evaluating the Economics of Photovoltaics in a Demand-Side Management Role*, Energy Policy, Vol. 24 No. 2. pp. 177-185, 1996.

[55] Ali Al-Alawi, S.M Islam: *Demand side management for remote area power supply systems incorporating solar irradiance model*, Renewable Energy, Vol. 29 pp. 2027-2036, 2004.

[56] IEADSM: *Strategic Plan 2004-2009*, International Energy Agency Demand-Side Management Program, [cited 2005 August 11]: Available form: http://dsm.iea.org

[57] Olof Björkqvist: *Perspectives on Demand-Side Energy Efficiency*, Ph.D. Thesis, Chalmers University of Technology, 1996, [cited 2005 August 29]; 2(7): Available form: http://www.bjorkqvist.nu/thesis/dsm.htm

[58] Look Dwight C., I. Sauer, Harry J.: *Engineering Thermodynamics*, PWS Publishers, 1986.

[59] EMBRACO: *Compressor Application Manual*, EMBRACO, [cited 2005 October 17]; 5(79): Available form: http://www.embraco.com.br/portugue/produtos/00007.pdf

[60] Dipl.-Ing Claus Ihle: *Klimatechnik mit Kaeltechnik*, Schriftenreihe Der Heizungsinenieur, Band 4, 3. Auflage, Werner-Verlag Duesseldorf.

[61] Michael J. Moran, Howard N. Shapiro, Bruce R. Munson and David P. Dewitt: *Introduction to Thermal Systems Engineering*, John Wiley & Sons, 2003.

[62] Lindon C. Thomas: *Fundamentals of Heat Transfer*, Prentice-Hall, INC. Englewood Cliffs, New Jersey, 1980, P.655

[63] International Standards Organization: *Household Refrigerator-Freezers-Characteristics and test methods*, ISO 8187, Geneva, Switzerland, p. 152, 1991.

[64] Burch Jay D., Huggins Jim C., Wood Byard D. Thornton Jeff W.: *Simulation-Based Ratings for Solar Hot Water Systems*, Proceedings of Solar'93, The 1993 American solar Energy Society Annual Conference, Washington DC, April 22-28, 1993.

[65] Industrial Research&Development Foundation: *Technical Note for 1975*, The National Science Foundation, [cited 2006 June 14], Available from: URL: http://www.nsf.gov/statistics/iris/excel-files/NSF%2089-323/tn.doc

[66] N. Ketjoy: *Photovoltaic Hybrid Systems for Rural Electrification in the Mekong Countries*, PhD. Thesis, Kassel University, Kassel Germany 2005

[67] Maps-Thailand.com: *Map of Thailand*, Maps-Thailand.com, [cited 2006 March 14]; 2(2): Available form: http://www.maps-thailand.com

[68] The Meteorological Department: *Climate of Thailand*, Thai Meteorological Department, [cited 2006 Feb 9]; 1(30: Available from: http://www.tmd.go.th/climate/climate_02.html

[69] Energy Research Institute, Chulalongkorn University: *Solar Energy Potential of Thailand*, Energy Research Institute, Chulalongkorn University, Bangkok, Thailand, 1998, [cited 2006 Dec 12]; 1(1): Available form: http://www.teenet.chula.ac.th/solar/

Appendix A

Climate Data

A.1 Sunshine hours at Ban Pang Praratchatan village

h												
DAY	Jan	Feb	Mar	Apr	May	Jun	Jul	Aug	Sep	Oct	Nov	Dec
1	7.92	9.00	8.67	10.00	8.08	6.00	3.17	2.00	5.08	9.50	6.75	6.50
2	7.58	8.83	7.92	7.33	8.00	8.00	1.75	N/A	3.33	9.50	1.92	7.42
3	6.83	9.08	9.50	2.42	8.00	6.33	N/A	N/A	9.08	9.80	N/A	8.00
4	7.92	9.25	9.25	6.33	9.00	8.00	N/A	N/A	9.00	9.50	6.67	7.17
5	5.50	9.17	8.42	7.25	7.83	6.25	N/A	6.92	4.67	9.25	9.50	6.75
6	7.25	9.17	8.67	7.92	8.25	4.17	0.17	8.25	4.00	0.50	9.50	5.92
7	7.83	9.17	9.00	6.92	4.92	5.00	2.00	6.00	1.92	4.33	9.42	7.33
8	7.83	9.42	8.67	9.67	7.58	5.33	5.92	1.08	3.42	6.58	9.25	N/A
9	8.00	8.83	9.17	9.58	8.33	5.58	5.00	4.83	1.50	6.00	9.08	N/A
10	7.92	9.42	9.50	8.42	6.75	4.08	N/A	2.83	8.92	6.08	8.83	8.00
11	7.92	9.42	9.42	8.92	7.25	3.42	N/A	1.67	9.08	8.92	8.50	4.17
12	7.92	9.08	8.25	9.33	7.50	2.75	17.00	1.08	9.25	7.25	6.00	7.92
13	8.58	9.25	9.50	9.83	2.00	8.08	1.25	2.17	9.50	5.17	7.58	7.50
14	7.67	8.83	6.08	9.08	8.25	8.00	2.83	4.75	8.42	1.83	7.50	7.08
15	8.00	9.33	7.67	8.17	7.67	6.75	5.00	6.00	N/A	6.92	8.00	2.42
16	8.00	9.25	9.42	9.50	7.58	6.50	N/A	4.25	8.25	7.25	8.17	4.75
17	8.00	9.50	9.08	4.25	6.17	5.75	2.08	5.25	6.00	8.33	8.00	8.30
18	8.17	9.42	6.50	42.00	1.08	3.00	5.50	3.75	9.75	3.00	7.42	5.50
19	8.00	8.75	7.08	3.08	N/A	5.00	6.58	5.17	9.92	17.00	8.08	7.00
20	8.00	9.33	7.00	9.00	1.92	5.00	6.50	6.50	5.58	9.25	8.00	8.00
21	7.83	8.17	7.08	7.25	1.58	2.83	7.67	1.25	8.33	9.50	4.92	7.92
22	7.33	8.50	9.33	6.17	7.75	5.50	75.00	6.08	7.92	9.42	N/A	7.92
23	8.00	8.75	9.58	7.42	5.67	1.17	3.25	4.33	9.08	8.75	2.00	7.92
24	8.00	8.42	8.00	10.00	8.17	1.58	1.42	N/A	7.83	9.67	6.25	7.92
25	7.83	9.58	6.00	9.50	5.42	92.00	8.00	1.00	7.00	8.75	8.00	7.50
26	3.75	5.92	7.08	8.00	1.92	N/A	N/A	6.50	8.42	9.67	8.00	7.00
27	7.58	9.00	9.25	8.08	4.75	8.00	6.67	6.75	4.00	5.08	7.92	7.00
28	7.83	8.67	9.08	8.25	6.08	1.58	8.42	1.75	9.50	7.17	25.00	6.75
29	4.42	N/A	6.00	8.33	7.00	3.00	8.25	1.58	9.50	6.08	92.00	5.25
30	7.67	N/A	7.58	9.33	4.08	3.42	6.50	8.30	9.42	6.00	3.50	6.58
31	8.00	N/A	7.83	N/A	5.83	N/A	6.00	3.00	N/A	6.83	N/A	6.50

Table A.1: Sunshine hours at Ban Pang Praratchatan village [69]

A.2 Hourly irradiation data in Ban Pang Praratchatan village

W/m^2

Time	Jan	Feb	Mar	Apr	May	Jun	Jul	Aug	Sep	Oct	Nov	Dec
6.00	0.00	0.00	0.00	17.01	29.75	40.09	27.75	23.96	4.80	0.00	0.00	0.00
7.00	47.86	99.87	102.55	163.74	181.44	150.76	46.75	138.44	125.59	87.38	62.48	48.19
8.00	190.80	246.34	265.45	356.87	362.69	306.29	426.25	303.74	293.96	233.62	213.85	199.91
9.00	363.67	416.52	453.05	570.66	561.78	481.22	489.91	490.91	481.49	398.56	386.56	374.71
10.00	527.91	572.92	626.76	764.74	741.60	641.60	602.35	662.88	652.31	549.79	546.08	536.72
11.00	645.23	682.62	749.17	900.09	866.64	754.09	685.17	783.59	771.66	655.81	658.37	650.96
12.00	687.73	722.04	793.24	948.61	911.41	794.53	715.21	826.99	814.47	693.91	698.79	692.11
13.00	645.23	682.62	749.17	900.09	866.64	754.09	685.17	783.59	771.66	655.81	658.37	650.96
14.00	527.91	572.92	626.76	764.74	741.60	641.60	602.35	662.88	652.31	549.79	546.08	536.72
15.00	363.67	416.52	453.05	570.66	561.78	481.22	489.91	490.91	481.49	398.56	386.56	374.71
16.00	190.80	246.34	265.45	356.87	362.69	306.29	426.25	303.74	293.96	233.62	213.85	199.91
17.00	47.86	99.87	102.55	163.74	181.44	150.76	46.75	138.44	125.59	87.38	62.48	48.19
18.00	0.00	0.00	0.00	17.01	29.75	40.09	27.75	23.96	4.80	0.00	0.00	0.00

Table A.2: Hourly irradiation at Ban Pang Praratchatan village

A.3 Ambient temperature at Ban Pang Praratchatan village

^oC

TIME	Jan	Feb	Mar	Apr	May	Jun	Jul	Aug	Sep	Oct	Nov	Dec
	17	16	16	15	15	11	17	16	15	15	14	10
1.00	18.80	19.60	24.00	26.30	25.10	25.60	25.20	25.00	25.10	24.10	20.90	17.30
2.00	18.30	18.90	23.30	25.60	24.80	25.30	25.00	24.70	24.90	23.90	20.60	16.80
3.00	17.70	18.20	22.60	24.90	24.60	25.10	24.70	24.40	24.80	23.60	20.20	16.40
4.00	17.20	17.50	21.90	24.20	24.30	24.80	24.50	24.10	24.60	23.40	19.90	15.90
5.00	16.70	17.00	21.50	23.90	24.30	24.90	24.40	24.20	24.50	23.30	19.80	15.60
6.00	16.30	16.60	21.00	23.60	24.40	25.00	24.40	24.30	24.40	23.10	19.60	15.20
7.00	15.80	16.10	20.60	23.30	24.40	25.10	24.30	24.40	24.30	23.00	19.50	14.90
8.00	17.60	18.70	23.10	25.70	25.90	26.30	25.40	25.20	25.20	24.30	21.20	17.00
9.00	19.50	21.20	25.50	28.00	27.40	27.50	26.60	26.00	26.00	25.50	22.80	19.00
10.00	21.30	23.80	28.00	30.40	28.90	28.70	27.70	26.80	26.90	26.80	24.50	21.10
11.00	23.50	26.00	29.70	31.90	29.90	29.30	28.50	27.80	27.90	27.80	25.70	22.90
12.00	25.60	28.10	31.40	33.30	30.90	29.80	29.30	28.90	28.90	28.80	26.80	24.70
13.00	27.80	30.30	33.10	34.80	31.90	30.40	30.10	29.90	29.90	29.80	28.00	26.50
14.00	28.50	31.00	33.90	35.30	31.80	30.10	30.50	30.00	29.90	29.50	28.20	26.80
15.00	29.30	31.80	34.70	35.70	31.80	29.70	30.80	30.10	29.80	29.30	28.50	27.20
16.00	30.00	32.50	35.50	36.20	31.70	29.40	31.20	30.20	29.80	29.00	28.70	27.50
17.00	28.10	30.70	33.90	34.60	30.80	28.90	30.20	29.30	28.80	28.20	27.20	25.60
18.00	26.30	28.90	32.30	33.10	30.00	28.50	29.20	28.30	27.70	27.30	25.60	23.80
19.00	24.40	27.10	30.70	31.50	29.10	28.00	28.20	27.40	26.70	26.50	24.10	21.90
20.00	23.10	25.70	29.40	30.40	28.30	27.50	27.70	26.90	26.30	26.00	23.40	21.00
21.00	21.80	24.40	28.20	29.30	27.40	27.00	27.10	26.50	26.00	25.50	22.70	20.10
22.00	20.50	23.00	26.90	28.20	26.60	26.50	26.60	26.00	25.60	25.00	22.00	19.20
23.00	19.80	22.00	26.10	27.50	26.30	26.30	26.20	25.70	25.40	24.70	21.60	18.50
24.00	19.00	21.00	25.20	26.70	26.00	26.20	25.80	25.40	25.30	24.40	21.20	17.80

Table A.3: Ambient temperature at Ban Pang Praratchatan village [69]

Appendix B

PV-Hybrid System Components

B.1 PV generator

SIEMENS

Solar module SP75

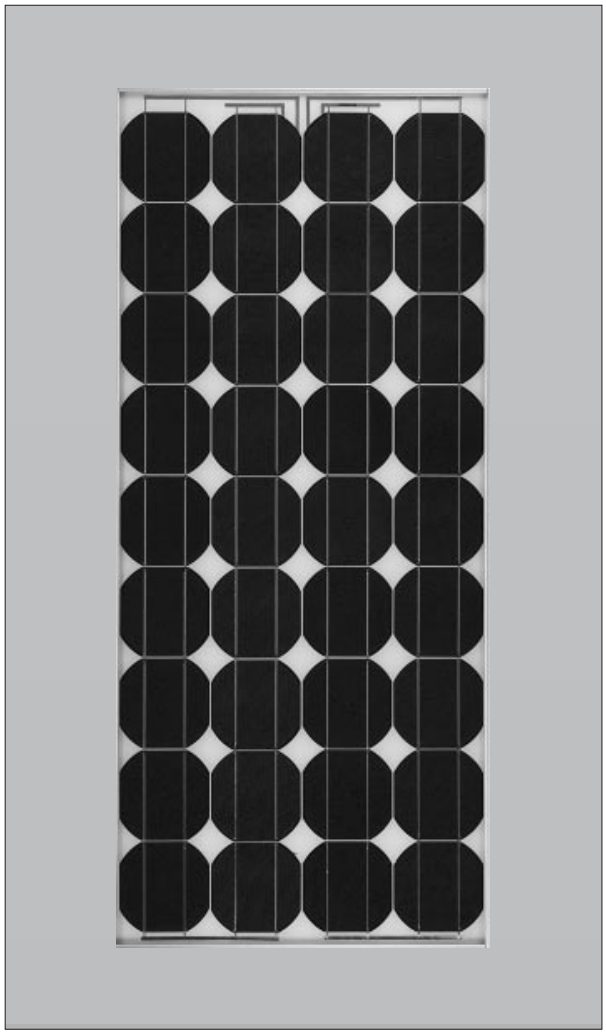

When it comes to reliable and environmentally-friendly generation of electricity from sunlight, solar modules from Siemens provide the perfect solution. Manufactured in compliance with the most stringent quality standards, Siemens Solar modules are designed to withstand the toughest environmental conditions and are characterized by their long service life. Siemens Solar modules are covered by a 25-year limited warranty on power output – your guarantee of trouble-free solar power generation.

PowerMax® technology
Siemens' proprietary PowerMax® technology optimizes the energy production of individual cells and solar modules for all types of environmental conditions. PowerMax® process optimization includes a special refining technique for ingots, a clean room semiconductor grade production process, and a multistage proprietary TOPS™ (Texture Optimized Pyramidal Surface) process. The TOPS process incorporates the formation of textured pyramids on the surface of the solar cell. These pyramids are then specially treated to passivate the surface. The cell's optical properties are optimized for maximum absorption of photons from the sun's light. TOPS also maximizes photon absorption from direct and diffused light (typical under cloudy conditions). This means that light absorption is especially high, even at low light levels. Siemens PowerMax® solar cells deliver maximum energy throughout the day.

Solar module	
Model:	**SP75**
Rated power:	**75 Watts**
Limited warranty:	**25 Years**

Certifications and Qualifications
- UL-Listing 1703
- TÜV safety class II
- JPL Specification No. 5101-161
- ESTI-IEC 1215/CEC503
- CE mark
- FM Certification

Intelligent module design

- All cells are electrically matched to assure the greatest power output possible.
- Ultra-clear tempered glass provides excellent light transmission and protects from wind, hail, and impact.
- Torsion and corrosion-resistant anodized aluminum module frame ensures dependable performance, even through harsh weather conditions and in marine environments.
- Built-in bypass diodes (12V configuration) help system performance during partial shadowing.

High quality

- Every module is subject to final factory review, inspection, and testing to assure compliance with electrical, mechanical, and visual criteria.
- 36 PowerMax® single-crystalline solar cells deliver excellent performance even in reduced light or poor weather conditions.
- Cell surfaces are treated with the Texture Optimized Pyramidal Surface (TOPS™) process to generate more energy from available light.
- Fault tolerant multi-redundant contacts on the front and back of each cell provide superior reliability.
- Solar cells are laminated between a multi-layered polymer backsheet and layers of ethylene vinyl acetate (EVA) for environmental protection, moisture resistance, and electrical isolation.
- Durable back sheet provides the module underside with protection from scratching, cuts, breakage, and most environmental conditions.
- Laboratory tested and certified for a wide range of operating conditions.
- Ground continuity of less than 1 ohm for all metallic surfaces.
- Manufactured in ISO 9001 certified facilities to exacting Siemens quality standards.

Easy installation

- ProCharger™-CR junction box accepts conduit, cable or wire and is designed for easy field wiring.
- Lightweight aluminum frame and pre-drilled mounting holes for easy installation.
- Factory configured for 12V operation and may be reconfigured in the field for 6V operation.
- Modules may be wired together in series or parallel to attain required power levels.

Performance warranty

- 25 Year limited warranty on power output.

Further information on solar products, systems, principles, and applications is available in the Siemens Solar product catalog.

Siemens modules are recyclable.

Solar module SP75

Electrical parameters		12 V / 6 V
Maximum power rating P_{max}	[W_p][1)]	75
Rated current I_{MPP}	[A]	4.4 / 8.8
Rated voltage V_{MPP}	[V]	17.0 / 8.5
Short circuit current I_{SC}	[A]	4.8 / 9.6
Open circuit voltage V_{OC}	[V]	21.7 / 10.9
Thermal parameters		
NOCT[2)]	[°C]	45±2
Temp. coefficient : short-circuit current		2.06 mA / °C
Temp. coefficient: open-circuit voltage		-.077 V / °C
Qualification test parameters [4)]		
Temperature cycling range	[°C]	-40 to +85
Humidity freeze, Damp heat	[% RH]	85
Maximum system voltage	[V]	600 (1000 V per ISPRA)
Wind Loading	PSF [N/m²]	50 [2400]
Maximum distortion[3)]	[°]	1.2
Hailstone impact	Inches[mm]	1.0 [25]
	MPH [m/s]	52 [v=23]
Weight	Pounds [kg]	16.7 [7.6]

1) W_p (Watt peak) = Peak power (Minimum W_p = 70 Watts)
Air Mass AM = 1.5
Irradiance E = 1000 W/m²
Cell temperature T_C = 25 °C

2) Normal Operating Cell Temperature at:
Irradiance E = 800 W/m²
Ambient temperature T_U = 20 °C
Wind speed v_W = 1 m/s

3) Diagonal lifting of the module plane

4) Per EIC 1215 test requirements

5) 12 Volt configuration

Voltage-current characteristic [5)]

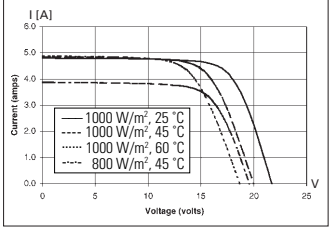

Module dimensions

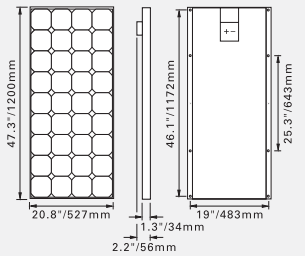

Hole diameter 0.26 inch (6.6 mm)
Mounting hole dimensions are center to center

ProCharger™-CR Junction-box

Maximum cable diameter: 4 mm²

System of protection: IP44

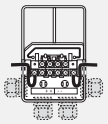

Your address for photovoltaics from Siemens Solar

JOINT RESEARCH CENTRE ESTI - Ispra

Status 3/98 – Subject to modification.

Siemens Solar GmbH
A joint venture of
Siemens AG and Bayernwerk AG
Postfach 46 07 05
D-80915 München
Germany

Siemens Solar Industries
P.O. Box 6032
Camarillo, CA 93011, U.S.A.
Tel: 805-482-6800
Fax: 805-388-6395
Web site: www.siemenssolar.com
E-mail: sunpower@solarpv.com

Printed in U.S.A.

Siemens Showa Solar Pte. Ltd.
Blk. 164 Kallang Way
#05-14/15 Kolam Ayer Industrial Park
Singapore 349248
Tel: 65-842-3886
Fax: 65-842-3887

Order No. 019897, Rev. B

B.2 Diesel generator

YDG Diesel Generator (Open Frame Type) **EPA Certified**

Air Cooled Diesel Generator Performance

Model			Open Frame Type		
			YDG2700EE-6EH	YDG3700EE-6EI	YDG5500EE-6EI
Oil supply interval	Fuel oil	hrs	6.5	8	5.5
	Lube oil		58	65	70
Lubricating oil temperature			less than or equal 110 degree C		
Revolution	No Load max.		3750 + or - 50 rpm		
Speed regulation	Transient Speed	%	less than or equal to 10		
	Speed Drop	%	less than or equal to 6		
	Setting Time	seconds	less than or equal to 5		
Stability	Frequency Change	Hz	less than, + or - 1		
Inclination (continuous)		degrees	less than or equal to 10		
Noise at Continuous Rated Output (Average in 4 Directions)	db(A)	at 1 m distance	92	93	96
		at 7 m distance	80	82	85
Lowest Starting Temperature (electric)		degree C	less than or equal to minus 10		
Voltage Regulation		%	10		

Note: the power rating standrads of Ynmar diesel engines conform to JIS B8013. JIS ratings are based on normal atmospherc conditions, which are defined as follows:

Standard Atmospheric Conditions:	JIS B8013-1977	Reference:
Intake Air Temperature	293 K (20 degree C)	ISO 3046/1-1986
Barometric Pressure	101.5 kPA (760 mm Hg)	198 K (25 degree C)
Relative Humidity	65%	100 kPA (750 mm Hg)

Fuel: Diesel fuel oil (BS 2869 class A1)
Lubricating oil: API grade CC, SAE 10W-30
Exhaust muffler: With exhaust silencer per std. spec.
Air intake: with air cleaner as per std. spec.

YDG Diesel Generator (Open frame type)

Air Cooled Diesel Generator Specification (EPA Certified)

Generator Spec. \ Model			Open Frame Type		
			YDG2700EE-6EH	YDG3700EE-6EI	YDG550EE-6EI
Type			Revolving field type AC generator		
Excitation System			Self-Excitation		
Frequency		Hertz	60		
Output	AC	Max. (kVA)	2.7	3.7	5.5
		Rated (kVA)	2.5	3.5	5.0
	DC	V-A (W)	12 - 8.3 (100)		
Rated Voltage		V	120	120 / 240	
Rated Current		A	20.8	29.2 / 14.6	41.7 / 20.8
Voltage Control System			AVR		
Rotation Speed		rpm	3600		
Number of Phases			Single Phase		
Number of Poles			2		
Power Factor			1.0		
Insulation Class			Class E		
Bearing Type			Ball bearing (seal type)		
Output receptacle	AC	V-A	250-15 (2 pcs.)	125-30 (Twist Lock, 1 pc.)	
				125 / 250-20 (Twist Lock, 1 pc.)	
	DC		250-10		
Breaker		AC	NFB-21A	NFB-15A (tandem)	NFB-21A (tandem)
		DC	Thermal Switch		
Voltmeter		V	150		
Pilot Lamp			none		
Grounding Terminal			1		
Protective Device			With stop device for when oil drops below the safety limit		
Generator Size (L X W X H)		mm	649 X 416 X 500	650 X 496 X 530	720 X 480 x 578
Dry Weight		kg	63	79	108

B.3 Inverter

Sunny Boy 1100/1700

The compact class

- Easy plant design and reduced installation costs
- SMA grid guard® (MSD)
- Diagnosis and communication via Powerline Communication, radio transmission or via data cable (RS232 or RS485)
- Extended temperature range –25 °C to +60 °C
- For outdoor and indoor installation
- Connection on the AC- and DC-side with connectors
- Surge voltage protection with integrated thermally monitored varistors

When configuring any solar power installation, the aim is to get the optimum match between the solar generator's output power and the inverter's input power. This includes having the widest possible selection of different inverter types. The compact SB 1100 and SB 1700 inverters have proven particularly successful with more than 30,000 units sold worldwide.
Packed full of innovative technologies, these "smaller" Sunny Boys also feature the international SMA grid guard interface. This ensures maximum reliability when operating the solar power system and enables electricity to be fed into mains grids anywhere in the world.

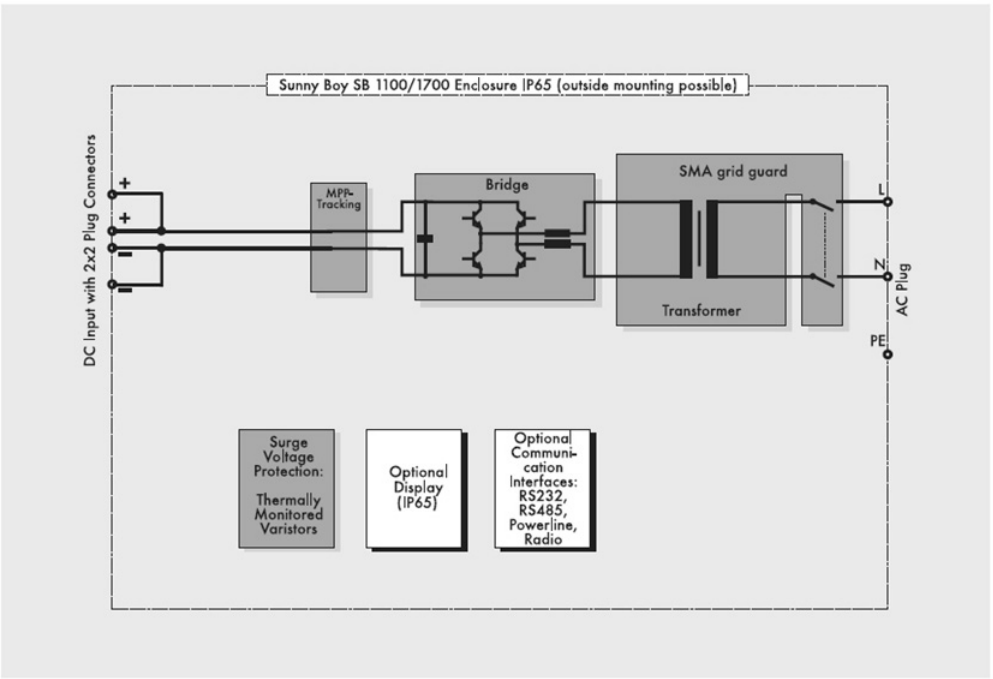

Schematic diagram of the Sunny Boy 1100/1700

Technical Data

	SB 1100	SB 1700
Input		
Recc. maximum PV-power (P_{PV})	approx. 1350 Wp *)	approx. 2050 Wp *)
Max. DC power ($P_{DC, max}$)	1210 W	1850 W
Max. DC voltage ($U_{DC, max}$)	400 V	400 V
PV-voltage range, MPPT (U_{PV})	139 V - 400 V	139 V - 400 V
Max. input current ($I_{PV, max}$)	10 A	12.6 A
DC voltage ripple (U_{pp})	< 10 %	< 10 %
Max. number of strings (parallel)	2	2
DC disconnection	Snap cable connectors	Snap cable connectors
Thermally monitored varistors	yes	yes
Ground fault monitoring	yes	yes
Pole confusion protection	Short circuit diode	Short circuit diode
Output		
Max. AC power ($P_{AC, max}$)	1100 W	1700 W
Nominal AC power ($P_{AC, nom}$)	1000 W	1550 W
THD of grid current	< 4 %	< 4 %
Default range of AC voltage (U_{AC})	198 V - 260 V	198 V - 260 V
Possible range of AC voltage	180 V - 265 V	180 V - 265 V
AC frequency (f_{AC})	49.8 Hz - 50.2 Hz	49.8 Hz - 50.2 Hz
Possible range of AC frequency	45.5 Hz - 54.5 Hz	45.5 Hz - 54.5 Hz
Phase shift (cos φ)	1	1
Short circuit proof	yes, current control	yes, current control
Connection to utility	AC Plug	AC Plug
Efficiency		
Max. Efficiency	93 %	93.5 %
Euro-eta	91.6 %	91.8 %
Enclosure		
accord. to DIN EN 60529	IP65	IP65
Mechanical Data		
Width / height / depth in mm	322 / 320 / 180	434 / 295 / 214
Weight	approx . 21 kg	approx . 25 kg

*) for PV-Plants in Germany

Sunny Island 3324

New off-grid inverter - A technology leap into the future

- Optimized for high ambient temperatures
- Very high overload capability
- Very high efficiency
- Integrated DC breaker and user interface
- Output load shedding
- DC and AC coupling of energy sources
- Easy start of a generator
- Battery and insect protection
- Easy installation and commissioning of 1-phase island system
- Non volatile parameter settings
- Compatible to Sunny Family products
- 24 V Battery voltage

The new Sunny Island 3324 battery inverter is the first addition of battery off-grid inverter since Sunny Island 4500. Perfectly sine wave off-grid electricity is now available with highest efficiency, robust power and outstanding reliability. Simple to run & use, yet loaded with powerful and advanced features. The Sunny Island 3324 is designed to meet nearly all needs for off-grid applications as well as back-up power systems.

Whatever & wherever electric power is needed, this new Sunny Island will perform!

Technical Data

Electrical / Mechanical data

Nom. battery voltage:	VDC,nom	24 V
Battery voltage range:	VDC	21 V ... 32 V
Nom. AC voltage:	VAC,nom	230 V
AC voltage range:	VAC	202 ... 253 V
AC frequency:	fAC	50 Hz
AC input charge current:	IAC chrg	14.5 A @ 25 °C
	10 A @ 45 °C	
Max AC pass through current (transfer relay):		56 A
Consumption (no load operation):		approx. 22 W
Consumption (standby):		<4 W
Total harmonic distortion:		<3 %

Enclosure: IP30
Weight: approx. 39 kg
Size: width 390 mm x length 590 mm x height 245 mm

Temperature range
-25 °C ... +50 °C

Cooling concept:
Electronics encapsulated in separate compartment;
low noise temperature controlled fan cooling;
exchangeable fan module; air / insect filter easy to clean

Interfaces:
- 2 LEDs; 2-line-LCD; 4 push buttons
- 1 dry contact output for load shedding
- 1 interface RS232 / RS485 galvanic isolated (optional)

Accessories:
- Remote battery temperature sensor (included)
- Generator Management "GenMan" (optional)

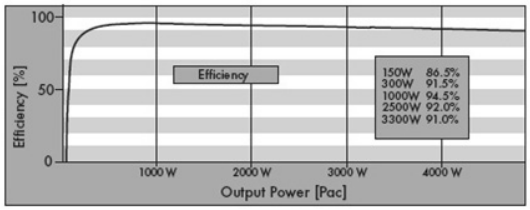

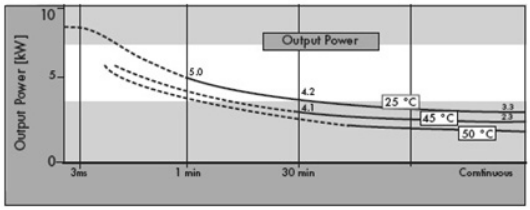

www.SMA.de
Freecall +800 SUNNYBOY
Freecall +800 78669269

Innovation in Systems Technology
for the Success of Photovoltaics

SMA

B.4 Battery

Classic™

Energy storage for outstanding power applications.

The Classic OPzS Solar range has been well proven for decades in medium and large power requirements. This energy storage battery is a low maintenance lead acid battery with liquid electrolyte. Due to their robustness, long design life and high operational safety they are ideally suitable for use in solar and wind power stations, telecommunications, power distribution companies, railways and many other safety equipment power supplies.

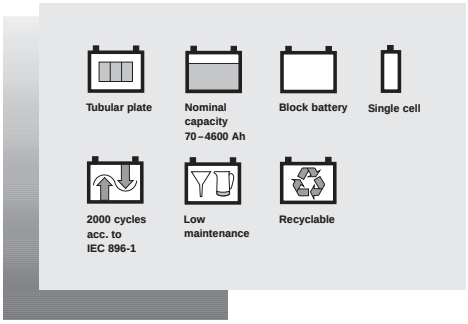

Drawings with terminal position, terminal and torque

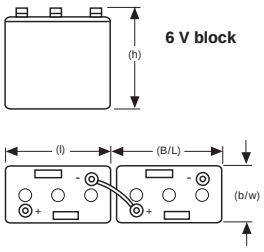

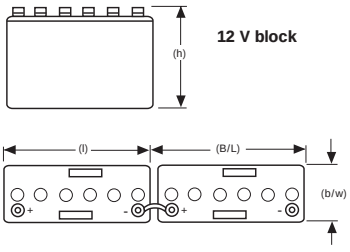

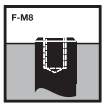

20 Nm

Not to scale!

OPzS Solar series

Classic™

Technical characteristics and data

Type	Part number	Nominal voltage V	Nominal capacity C_{120} 1.85 V/C 25°C Ah	Length (l) max. mm	Width (b/w) max. mm	Height* (h) max. mm	Installed length (B/L) mm	Weight including acid approx. kg	Weight acid** approx. kg	Internal resistance mΩ	Short circuit current A	Terminal	Pole pairs	Capacities in Ah (C_6 - C_{240} at 25°C) C_6 1.75 V/C	C_{10} 1.80 V/C	C_{12} 1.80 V/C	C_{24} 1.80 V/C	C_{48} 1.80 V/C	C_{72} 1.80 V/C	C_{100} 1.85 V/C	C_{120} 1.85 V/C	C_{240} 1.85 V/C
Block																						
OPzS Solar 70	NVSL120070WC0FA	12	70	275	208	385	285	35	15	18.18	688	F-M8	1	55.0	51.5	63.7	69.4	78.4	79.8	81.0	82.7	92.9
OPzS Solar 140	NVSL120140WC0FA	12	140	275	208	385	285	45	14	9.26	1314	F-M8	1	95.4	103.0	108.2	118.7	141.6	145.2	136.0	139.9	162.3
OPzS Solar 210	NVSL120210WC0FA	12	210	383	208	385	393	64	19	6.46	1884	F-M8	1	131.4	154.5	162.0	177.7	206.0	217.8	203.9	210.1	234.1
OPzS Solar 280	NVSL060280WC0FA	6	280	275	208	385	285	41	13	2.68	2283	F-M8	1	203.4	206.0	229.3	250.8	296.2	304.9	287.0	294.0	338.3
OPzS Solar 350	NVSL060350WC0FA	6	350	383	208	385	393	56	20	2.39	2800	F-M8	1	245.5	257.5	284.0	311.5	374.2	383.7	355.0	364.1	424.5
OPzS Solar 420	NVSL060420WC0FA	6	420	383	208	385	393	63	20	1.96	3106	F-M8	1	284.3	309.0	322.9	354.6	420.8	432.6	408.0	417.7	482.9
Cell																						
OPzS Solar 190	NVSL020190WC0FA	2	190	105	208	405	115	13.7	5.2	1.45	1400	F-M8	1	122	132	134	145	165	175	185	190	200
OPzS Solar 245	NVSL020245WC0FA	2	245	105	208	405	115	15.2	5.0	1.05	1950	F-M8	1	159	173	176	190	215	230	240	245	260
OPzS Solar 305	NVSL020305WC0FA	2	305	105	208	405	115	16.6	4.6	0.83	2450	F-M8	1	203	220	224	240	270	285	300	305	320
OPzS Solar 380	NVSL020380WC0FA	2	380	126	208	405	136	20.0	5.8	0.72	2850	F-M8	1	250	273	277	300	330	350	370	380	400
OPzS Solar 450	NVSL020450WC0FA	2	450	147	208	405	157	23.3	6.9	0.63	3250	F-M8	1	296	325	330	355	395	420	440	450	470
OPzS Solar 550	NVSL020550WC0FA	2	550	126	208	520	136	26.7	8.1	0.63	3250	F-M8	1	353	391	398	430	480	515	540	550	580
OPzS Solar 660	NVSL020660WC0FA	2	660	147	208	520	157	31.0	9.3	0.56	3650	F-M8	1	422	469	477	515	575	615	645	660	695
OPzS Solar 765	NVSL020765WC0FA	2	765	168	208	520	178	35.4	10.8	0.50	4100	F-M8	1	492	546	555	600	670	710	750	765	805
OPzS Solar 985	NVSL020985WC0FA	2	985	147	208	695	157	43.9	13.0	0.47	4350	F-M8	1	606	700	710	770	860	920	970	985	1035
OPzS Solar 1080	NVSL021080WC0FA	2	1080	147	208	695	157	47.2	12.8	0.43	4800	F-M8	1	669	773	784	845	940	1000	1055	1080	1100
OPzS Solar 1320	NVSL021320WC0FA	2	1320	215	193	695	225	59.9	17.1	0.30	6800	F-M8	2	820	937	950	1030	1150	1230	1295	1320	1385
OPzS Solar 1410	NVSL021410WC0FA	2	1410	215	193	695	225	63.4	16.8	0.27	7500	F-M8	2	888	1009	1024	1105	1225	1305	1380	1410	1440
OPzS Solar 1650	NVSL021650WC0FA	2	1650	215	235	695	225	73.2	21.7	0.26	7900	F-M8	2	1024	1174	1190	1290	1440	1540	1620	1650	1730
OPzS Solar 1990	NVSL021990WC0FA	2	1990	215	277	695	225	86.4	26.1	0.23	8900	F-M8	2	1218	1411	1430	1550	1730	1850	1950	1990	2090
OPzS Solar 2350	NVSL022350WC0FA	2	2350	215	277	845	225	108.0	33.7	0.24	8500	F-M8	2	1573	1751	1770	1910	2090	2200	2300	2350	2470
OPzS Solar 2500	NVSL022500WC0FA	2	2500	215	277	845	225	114.0	32.7	0.22	9300	F-M8	2	1667	1854	1875	2015	2215	2335	2445	2500	2600
OPzS Solar 3100	NVSL023100WC0FA	2	3100	215	400	815	225	151.0	50.0	0.16	12800	F-M8	3	2080	2318	2343	2520	2755	2910	3040	3100	3250
OPzS Solar 3350	NVSL023350WC0FA	2	3350	215	400	815	225	158.0	48.0	0.14	14600	F-M8	3	2268	2524	2550	2740	2985	3135	3280	3350	3520
OPzS Solar 3850	NVSL023850WC0FA	2	3850	215	490	815	225	184.0	60.0	0.12	17000	F-M8	4	2592	2884	2915	3135	3430	3615	3765	3850	4040
OPzS Solar 4100	NVSL024100WC0FA	2	4100	215	490	815	225	191.0	58.0	0.11	17800	F-M8	4	2775	3090	3125	3355	3650	3840	4000	4100	4300
OPzS Solar 4600	NVSL024600WC0FA	2	4600	215	580	815	225	217.0	71.0	0.11	18600	F-M8	4	3099	3451	3490	3765	4100	4300	4500	4600	4850

**The above mentioned height can differ depending on the used vent(s).* ***Acid density d_N = 1.24 kg/l*

Data are also valid for dry charged version.
Change „W" (Wet) to „D" (Dry)
in the part number.
E.g.:
filled and charged NVSL120070 W C0FA
dry charged NVSL120070 D C0FA

Drawings with terminal position, terminal and torque

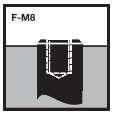

20 Nm

OPzS Solar 190 up to OPzS Solar 1080

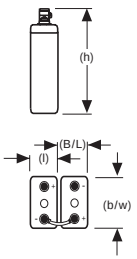

OPzS Solar 1320 up to OPzS Solar 2500

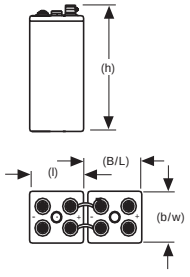

OPzS Solar 3100 OPzS Solar 3350

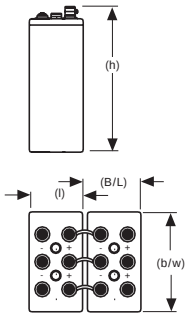

OPzS Solar 3850 up to OPzS Solar 4600

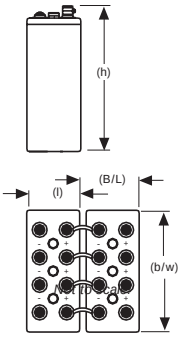

Not to scale!

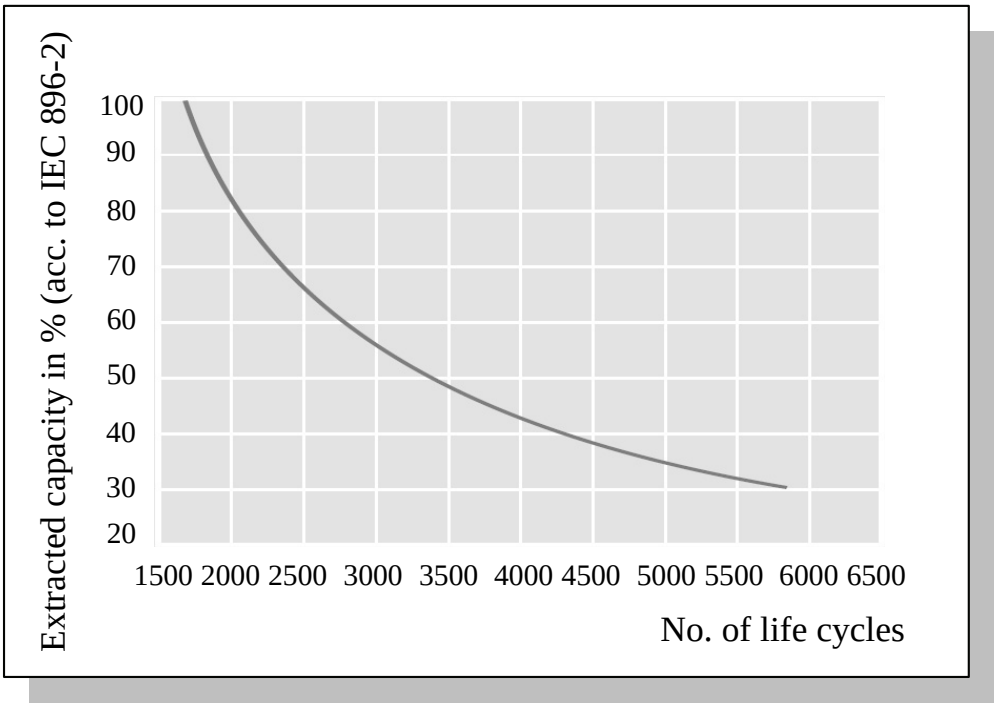

Figure B.1: Endurance in cycles according to IEC 896-2 for the OPzS battery

Appendix C

Simulation Algorithm

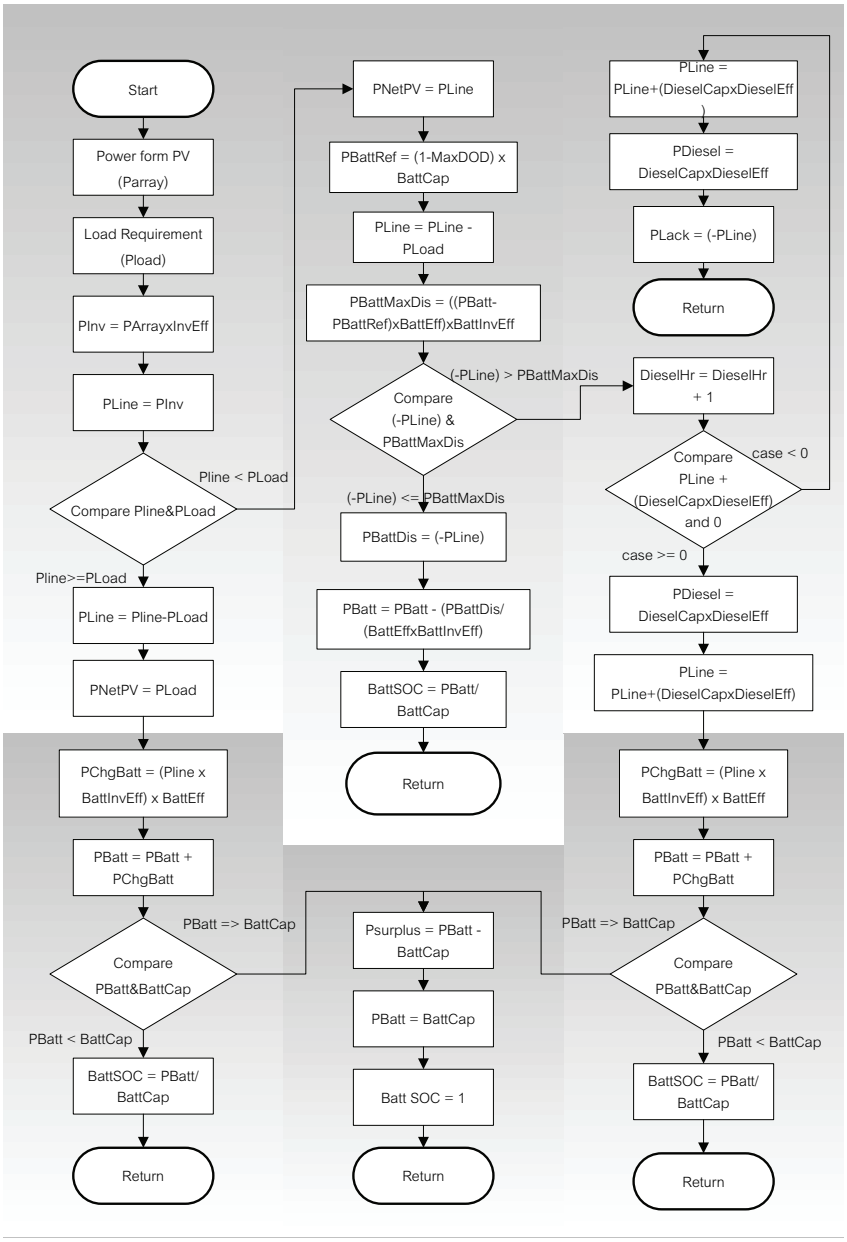

Figure C.1: PVHS grid tired algorithm